

Master Thesis



Czech
Technical
University
in Prague

F3

Faculty of Electrical Engineering
Department of Measurement

Altitude control system for trajectory control of stratospheric balloon

David Hofman

Supervisor: prof. RNDr. René Hudec, CSc.

Field of study: Aerospace Engineering

Subfield: Avionics

May 2024

I. Personal and study details

Student's name: **Hofman David** Personal ID number: **476085**
Faculty / Institute: **Faculty of Electrical Engineering**
Department / Institute: **Department of Measurement**
Study program: **Aerospace Engineering**
Branch of study: **Avionics**

II. Master's thesis details

Master's thesis title in English:

Altitude control system for trajectory control of stratospheric balloon

Master's thesis title in Czech:

System řízení letové výšky stratosférického balónu pro kontrolu trajektorie

Guidelines:

Stratospheric balloons have no flight control capabilities of their own. However, by changing the flight altitude, different wind directions can be found which affect the flight trajectory. This expands the range of applications, including payload testing for space missions and research of energetic phenomena in the atmosphere, e.g. X-ray emissions of auroras and ground-based gamma rays.

At the beginning of the thesis, different methods of changing the flight level will be presented and compared in terms of energy requirements, balloon life and carrier gas leakage through the balloon envelope and the ratio of operating empty weight to payload, while also comparing other limitations of the given arrangements. Focus primarily on physical ballast, changing the volume of the carrier gas by compressing it, changing the weight by compressing the gases from the surrounding atmosphere, and this during the use of zero-pressure and super-pressure balloons and their combinations. Compare the different layouts of photovoltaic panels in terms of efficiency, power-to-weight ratio and drag effect.

Furthermore, evaluate the behavior of the stratosphere in terms of the optimal atmospheric conditions for the possibility of controlling the trajectory by change of the flight altitude and indicate the limits of operation in the given conditions.

Describe the ECMWF or NOAA forecast model in the stratosphere and select and describe the parameters that affect balloon flight and the physics of the balloon's thermal environment.

Design, implement and describe a software tool in Matlab and/or Python to optimize the system design of the controlled stratospheric balloon and to simulate the flight trajectory of the designed balloon.

The software must meet the following requirements:

A) Design of an optimal stratospheric balloon system:

- Must include the following inputs: payload, flight mission characteristics, material properties (strength, density, the thickness of the envelope material) and the technology used (different types of solar panels and their arrangement, different battery technologies)
- Designs the layout of the entire flight system
- Determines the shape and volume of the balloon at different flight altitudes and defines the tension in the envelope for zero and super-pressure balloons
- Includes sizing of altitude control devices, solar panel and battery capacity

B) Simulation Environment:

- Used to simulate the behavior of the balloon and predict the trajectory
- Calculation based on drag and heat exchange between the balloon and the environment using real meteorological data from ECMWF or NOAA
- It will include the calculation of the available energy in the batteries and the potential energy, gas leakage simulation through the balloon envelope, the possibility to control the balloon manually by command or by connecting a control algorithm

C) User interface:

- The program will have a user-friendly graphical interface for entering parameters and visualizing results
- Allows saving and loading of projects
- If the input parameters are incorrectly entered outside the limits, it will cancel the calculation and display warning or error messages, the possibility of changing calculation parameters in the settings window with a description of their meaning

D) Software testing

- Functionality testing of the proposed program will be done with the help of Ad-hoc and limit testing

In the conclusion, the next steps in development of the created software tools will be presented, along with the possible control algorithms. At the same time indicate the potential applications of controlled stratospheric balloons in various fields with an emphasis on low-cost solutions for small payloads.

Bibliography / sources:

1. BAGINSKI, Frank; WILLIAMS, Tami; COLLIER, William. A parallel shooting method for determining the natural shape of a large scientific balloon. SIAM Journal on Applied Mathematics, 1998, 58.3: 961-974.
2. BELLEMARE, Marc G., et al. Autonomous navigation of stratospheric balloons using reinforcement learning. Nature, 2020, 588.7836: 77-82.
3. DU, Huafei, et al. Energy management strategy design and station-keeping strategy optimization for high altitude balloon with altitude control system. Aerospace Science and Technology, 2019, 93: 105342.
4. DAI, Qiumin, et al. Performance simulation of high altitude scientific balloons. Advances in Space Research, 2012, 49.6: 1045-1052.
5. CARLSON, Leland A.; HORN, Walter J. New thermal and trajectory model for high-altitude balloons. Journal of Aircraft, 1983, 20.6: 500-507.
6. The Loon Library [online]. Loon LLC., 2021 [viewed 8 February 2023]. Available from: <https://x.company/projects/loon/the-loon-collection/>

Name and workplace of master's thesis supervisor:

prof. RNDr. René Hudec, CSc. Department of Radioelectronics FEE

Name and workplace of second master's thesis supervisor or consultant:

Date of master's thesis assignment: **10.02.2023** Deadline for master's thesis submission: **24.05.2024**

Assignment valid until:
by the end of summer semester 2024/2025

prof. RNDr. René Hudec, CSc.
Supervisor's signature

Head of department's signature

prof. Mgr. Petr Páta, Ph.D.
Dean's signature

III. Assignment receipt

The student acknowledges that the master's thesis is an individual work. The student must produce his thesis without the assistance of others, with the exception of provided consultations. Within the master's thesis, the author must state the names of consultants and include a list of references.

Date of assignment receipt

Student's signature

Acknowledgements

I would like to express my gratitude to my thesis supervisor, Prof. René Hudec, PhD, CSc., whose guidance, support and encouragement have been very important throughout this thesis. I am especially grateful for his feedback, dedication and general insight and assistance.

Deep gratitude goes to my family for their support during my studies and constant encouragement. A particular appreciation goes to my partner Mylene Garin for her endless love, understanding, patience, and unwavering support, and to my two cats, Nessie and Nancy, for cheering me on during difficult moments while writing this thesis.

Last but not least, I would like to thank all the previous researchers who worked on stratospheric balloons and were able to lay the foundation on which this thesis could build. Thanks also to the tools DeepL, which helped me with language correction and difficult translations, and to ChatGPT for fast and efficient code debugging.

Declaration

I declare that I have written the submitted thesis independently and that I have listed all sources used in accordance with the Methodological Guideline on the Observance of Ethical Principles in the Preparation of University Thesis. In Prague, 24. May 2024

Abstract

Stratospheric balloons are lighter-than-air bodies filled with a lifting gas that can carry payloads above the troposphere. As such, they are uncontrollable and their flight path is determined primarily by atmospheric conditions, making their use very limited. With the ability to change flight altitude, winds of varying directions can be found at different altitudes and thus the flight path can be controlled, offering many potential future applications including payload testing for space missions and research into energetic phenomena in the atmosphere e.g. X-ray emission from aurora and terrestrial gamma-ray bursts.

Keywords: High-Altitude Balloons, trajectory control, stratosphere, altitude control

Supervisor: prof. RNDr. René Hudec, CSc.
katedra radioelektroniky,
Technická 1902/2,
Praha

Abstrakt

Stratosférické balóny jsou tělesa lehčí než vzduch naplněná nosným plynem, která mohou dopravit náklad nad troposféru. Jako taková jsou neovladatelná a jejich dráha letu je dána především atmosférickými podmínkami, čímž je jejich využití velmi omezené. S možností změny letové hladiny lze nacházet v různých výškách větry různých směrů a tím lze řídit trajektorii letu, což nabízí mnoho potenciálních budoucích využití včetně testování payloadů pro kosmické mise a výzkum energetických jevů v atmosféře např. rentgenové emise polárních září a pozemních gama záblesků.

Klíčová slova: Stratosférické balóny, řízení trajektorie, stratosféra, řízení výšky

Překlad názvu: Systém řízení letové výšky stratosférického balónu pro kontrolu trajektorie

Contents

Part I	
Introduction	
1 General Introduction	3
1.1 Introduction to High-Altitude Balloons	3
1.2 Current Uses and Limitations . . .	5
1.2.1 Advantages of High Altitude Balloons	5
1.2.2 Limitations of High-Altitude Balloons	7
1.2.3 Examples of Scientific Missions	8
1.2.4 Examples of Commercial Missions	9
1.3 Objectives and Scope of the Thesis	12
Part II	
Theoretical Foundations and Design Aspects	
2 Overview of Altitude and Trajectory Control Methods	17
2.1 Day and Night Cycle	17
2.2 Options for Controlling Altitude and Trajectory	18
2.3 Role of Super-Pressure balloon .	19
2.3.1 Differences in energy demand	19
2.3.2 Balloon Stability	20
3 Atmospheric Behavior and Flight Conditions	23
3.1 Characteristics of the Atmosphere	23
3.1.1 Stratosphere	23
3.2 Optimal Flight Conditions	25
3.3 Forecast Models	26
3.3.1 Important Parameters for Flight Simulation	26
3.3.2 ECMWF Model	26
3.3.3 GFS Model	26
3.3.4 Selection and Use of Forecast Model	27
4 Balloon Shape and Structure	29
4.1 Shape of Balloon	29
4.2 Balloon Elements	31

4.2.1 Gores	31	6.2 Batteries	45
4.2.2 Tapes and Tendons.....	33	6.3 Solar Panels.....	46
4.2.3 Caps	34	6.4 Compressor	48
5 Balloon Aerodynamics and Thermodynamics	35	6.5 Payload	49
5.1 Aerodynamics	35	6.6 Thermal Management Systems .	49
5.1.1 Introduction.....	35		
5.1.2 Zero and Super pressure balloons differences	36	Part III	
5.1.3 Simplification.....	37	Flight Control System Design	
5.1.4 Estimation of Drag Coefficient	37	7 Selection of Design Approach and Configuration	53
5.2 Heat Environment	38	7.1 Reasons for the choice of control methods	53
5.2.1 Introduction.....	38	7.2 Selected methods	54
5.2.2 Heat Transfer Mechanisms ..	39	8 Stratospheric Balloon	57
5.2.3 Modelling Thermal Environment	40	8.1 Derivation of the Equations	58
5.2.4 Standard Atmosphere	42	8.2 Simplified numerical calculation algorithm	61
6 Energy Systems	45	9 System for Changing Flight Levels	67
6.1 Introduction	45	9.1 Tandem pumped helium balloon	67
		9.2 Super pressure balloon with air ballast.....	75

10 Energy Systems	81		
10.1 Energy Requirements	81		
10.1.1 Energy for altitude change	81		
10.1.2 Energy for Payload	83		
10.1.3 Other Energy Requirements	84		
10.2 Solar Panels	85		
10.2.1 Introduction	85		
10.2.2 Theoretical Background	85		
10.2.3 Calculation of Solar Panel Design Parameters	90		
10.3 Batteries	92		
11 Simulation Environment Setup	95		
11.1 GFS Forecast Parameters Retrieval	95		
11.1.1 GFS Data Structure	95		
11.1.2 Data compression	96		
11.1.3 Positional indices	97		
11.1.4 Pressure levels	97		
11.2 Simulation Modeling	98		
		11.2.1 Data interpolation	98
		11.2.2 Kinematic model	99
		11.2.3 Thermal model	101
		11.3 Gas Leakage	101
		11.3.1 Introduction	101
		11.3.2 Mechanisms	102
		11.3.3 Calculations	102
		Part IV	
		Software Tool Development and Testing	
		12 Development of Software Tool	107
		12.1 Requirement Specifications	107
		12.2 Design of the Optimal Stratospheric Balloon System	109
		12.3 Design of Simulation Environment	110
		12.4 User Interface and Software Usability	111
		12.4.1 Model-View-Presenter architecture	112
		12.4.2 Implementation of PyQt6	113

12.4.3 Saving and Loading Functionality.....	114	14.2.1 Objectives	134
12.4.4 Plots	115	14.2.2 Summary of the Study....	134
13 Testing and Validation	117	14.2.3 Summary and Evaluation of the Software	135
13.1 Testing	117	15 Recommendations and Future Perspectives	137
13.1.1 Selection of Test Methods .	117	15.1 Further Software Development	137
13.1.2 Ad-Hoc Testing	118	15.2 Expansion of Possible Applications and Uses	140
13.1.3 Limit Testing	119	15.2.1 Contribution of Controllable Balloons to Research and Commercial Applications	140
13.1.4 Unit Testing.....	120	15.2.2 Scientific Research Applications	141
13.2 Validation	123	15.2.3 Commercial Applications .	142
13.2.1 Balloons Envelope	123	15.2.4 Security and military applications	143
Part V Conclusion			
14 Summary of Findings and Evaluation	129	16 General Conclusion	145
14.1 Examples of Balloon Systems	129	Appendices	
14.1.1 Budget Example Mission ..	129	A Bibliography	149
14.1.2 Scientific Example Mission	131	B Input tables for Example Missions	155
14.2 Evaluation of the Proposed System and Results	134		

C Validation tables	159
D Acronyms	161
E Attachment Contents	163

Figures

1.1 Types of High-Altitude Balloons .	5	4.1 Cylindrical-shaped Balloons designed by Project Loon[2]	31
1.2 Artistic rendering of ASTHROS observatory with super-pressure balloon	9	4.2 The production of the Big 60 balloon	32
1.3 Flight trajectories of Loon balloons over Puerto Rico [1]	10	4.3 Lobed Gore Geometry [7]	33
1.4 Pressure differential locations in reverse ballonet as used in Loon Balloons [2]	11	4.4 Diamond shaped gore of project Loon Super-pressure Balloon	33
1.5 Stratollite balloon with stratocraft gondola including 1 zero-pressure and 2 superpressure balloons [3]	11	4.5 Braided Dyneema tendon attached to the apex assembly load ring on Loon super-pressure Balloon [2]	34
1.6 >24-hour loitering of Stratollite balloon[4]	12	5.1 Estimated Drag Coefficient of a Balloon as a Function of Reynolds Number	38
2.1 Altitude control methods[5]	19	5.2 Thermal Environment of High Altitude Balloon [2]	39
2.2 Passive stability of tandem ZP and SP helium balloons lifting 1000 N payload	21	6.1 GUSTO observatory at the NASA Columbia Scientific Balloon Facility[8]	47
3.1 Atmospheric pressure and temperature in relation to altitude with highlighted stratosphere based on the US Standard Atmosphere 1976 model [6]	24	6.2 Altitude Control Compressor of Project Loon [2]	48
3.2 Wind cone illustrating the winds over the entire altitude range [2]	25	8.1 Small section of balloons envelope for derivation of the equations[9]	59
		8.2 Shape optimization of zero-pressure balloon	64
		8.3 Graph showing behaviour of Δs_{new} parametrization function for $\Delta s = 1$	66

9.1 Variation of tandem helium system parameters across the entire altitude range.....	71	12.3 Simulation environment with loaded balloon data and input parameters.....	112
9.2 Variation of BinB air ballast system parameters across the entire altitude range	78	12.4 Interactive Error Highlighting: Tooltip for Input Correction Upon Mouse Hover	114
10.1 Equation of Time [10]	87	12.5 Optimize Tab Plot Layout Showing Solar Panel Power Output on the Least Sunny Day	115
10.2 Solar angles[11].....	88	13.1 Validation of Envelope Shape for two specific buoyancy values	124
10.3 Solar Irradiance Over the Day for Different Altitudes in Prague on March 26, 2024	89	13.2 Validation of Envelope Stress for two specific buoyancy values	125
11.1 Temperature forecast data for area near south pole at 10 Pa pressure altitude visualised in Panoply[12] and downloaded using developed software from GFS GrADS Data Server[13].....	97	14.1 Outer Balloon Shape of Budget Example Mission	130
11.2 Pressure Levels of GFS model with indicated range of altitudes for high-altitude balloons	98	14.2 3days Energy Balance of Budget Example Mission	130
11.3 Comparison of gas leak in SP and ZP balloons over 60 days period .	104	14.3 Stress in Outer Balloon of Budget Example Mission	131
12.1 Original Software in Matlab ..	108	14.4 Gas Weight and Volume of Balloons over altitude range of Budget Example Mission	131
12.2 Optimization environment with input and output date.....	111	14.5 Shapes of ZP and SP Balloons of Scientific Example Mission	132
		14.6 3days Energy Balance of Scientific Example Mission	133

14.7 Stresses in Balloons of Scientific Example Mission	133
14.8 Gas Weight and Volume of Balloons over altitude range of Scientific Example Mission	134

Tables

9.1 Optimization Outcomes for Tandem Helium System Across Temperature and Updraft Variations	74
13.1 Inputs for Validation of Balloon Calculation	123
B.1 Flight and Balloon Specifications for Budget Example Mission	156
B.2 Flight and Balloon Specifications for Scientific Example Mission	157
C.1 Limits of Flight Input Fields	159
C.2 Limits of Optimization Input Fields	160



Part I

Introduction



Chapter 1

General Introduction



1.1 Introduction to High-Altitude Balloons

Ballooning has a rich history dating back to its invention in 1783 with its first untethered manned flight demonstration before King Louis XVI of France.[1] This pioneering occasion provided a perfect ground for the development of ballooning and the expansion of its applications and realisations. Balloons found their first military use by 1794 when they served as observation platforms during enemy bombardment. Moving on into the latter part of the 19th century, the scientific community began using balloons to study atmosphere. This was a very important development which led in particular to the discovery of atmospheric stratification of the atmosphere, an important discovery for meteorology. [1]

Not long after, it became clear that studies of the atmosphere at higher altitudes were too challenging for a manned flight, leading man to use unmanned flights to get better data from higher altitudes. Tactical and strategic use of balloons became wide-spread during World War II with Japan's use of balloon bombs against the United States. Military use further developed in the Cold War era to spy on Soviet territories and even to conduct atmospheric nuclear tests. [1]

Today, balloons are used in a wide range of fields, including atmospheric and meteorological research, communications technology, space exploration, earth observation and military applications. Developments in balloon technology

have expanded the range of balloon types from recreational hot air balloons to sophisticated stratospheric balloons that are capable of conducting large-scale research operations in the stratosphere over extended periods of time, from days to months. [1]

This thesis focuses on high altitude balloons. They are characterized by crossing the troposphere, ascending into the stratosphere and occasionally even reaching the lower mesosphere. These balloons float high above storm clouds and above most of the total mass of the atmosphere. They operate at altitudes well above all civil aviation and below all satellites orbiting the Earth. Different types of high-altitude balloons are designed, each adapted to specific mission and environmental conditions in the upper atmosphere:

Weather balloons Designed primarily for meteorological observations, these balloons are cost-effective for short-term missions. Known for their predictable performance and simple deployment procedures, they are usually made of latex, which expands as it rises. At a certain altitude, internal overpressure causes the balloon to burst, initiating its descent. They do not last long at maximum flight altitude and are therefore mainly used to collect data as they pass through different layers of the atmosphere. [1]

Zero-pressure balloons These balloons are designed to operate without maintaining an internal pressure higher than the ambient atmospheric pressure. They compensate for the gas expansion between day and night by allowing the excess gas to be release. Their mission does not end with the balloon bursting due to overpressure, as is the case with weather balloons. This makes them suitable for longer-duration flights at stable altitudes. However, their flight level gradually decreases due to the continuous release of lifting gas and must therefore be compensated for, for example, by discarding ballast. As their envelope is not subject to any overpressure, very thin and light films can be used for the envelope, making them the most buoyant type of balloon. This type of balloon is destined for research and observation missions lasting several days at very high altitudes. [1]

Super-pressure balloons These balloons are designed to maintain a higher internal pressure than the ambient atmospheric pressure, allowing them to float at a constant altitude for extended periods without the need to release ballast. However, the overpressure of the lifting gas requires the use of stronger films for balloon envelope. This results in a buoyant balloon compared to a zero-pressure one. Therefore, they are mainly intended for long-duration, low altitude flights where continuous data collection and observation are necessary. [1]

Each balloon is designed to meet a specific function and the requirements of a particular mission. While this division into three basic types provides a

basic idea, it is important to note that there are many other variations and combinations of these variations. As shown in Figure 1.1, these three basic types serve as the most common and therefore basic types of balloons, and also represent different approaches to balloon design: flexible, unpressurised and pressurised envelope.



(a) : Weather Balloon [14]



(b) : Zero-pressure Balloon [15]



(c) : Super-pressure Balloon [16]

Figure 1.1: Types of High-Altitude Balloons

1.2 Current Uses and Limitations

High-altitude balloons have contributed significantly to the development of knowledge of the Earth and its atmosphere, space and other areas. They have evolved from a simple curiosity to defy gravity into sophisticated platforms for scientific research and commercial applications. Technological advances have gradually led to the development of more durable materials, navigation and observation techniques, but at the same time new means of overcoming the earth's gravity have been developed, such as aircraft and later satellites. And so it would seem that the time and importance of balloons and other lighter-than-air bodies has gradually faded. However, even though other aerospace platforms offer many unsurpassed advantages, balloons are still, for the time being, irreplaceable in some areas, primarily because of their obvious advantages.

1.2.1 Advantages of High Altitude Balloons

Flight Altitude: High-Altitude Balloons ascend above the normal flight level of air traffic, reaching height unattainable by any air-breathing aircraft. At the same time, they are closer to the Earth's surface than satellites, which must fly at much higher altitudes to maintain their orbits

around the globe. This flight altitude allows balloons to float above most of the Earth's weather systems and atmosphere and puts them in a unique position. [1] This location is optimal for atmospheric research, environmental monitoring and astronomical observations, mainly due to the reduced influence of the atmosphere on observations. At the same time, it combines the close and detailed observation capabilities of aircraft with the wide coverage of satellites. If well equipped, balloon platforms can provide continuous imagery of a single location with superior resolution to satellites due to their closer distances from the ground, making them suitable for applications such as disaster monitoring and assessment, agricultural surveys and mapping. [1]

Low Cost and Accessibility: High-altitude balloons are much cheaper to build and operate than satellites or other airborne vehicles. Balloons do not require highly sophisticated and complex systems like satellites or aircraft. And the launch itself does not require the complex infrastructure required for satellites; high-altitude balloons can be launched from virtually anywhere with minimal infrastructure. They require no fuel for propulsion and use only atmospheric currents for control. They do not require the expensive fuel supplies and complex propulsion systems used in other types of aerial vehicles. [1] Above all, the low cost of balloon missions allows for scalability and customisation of projects, offering flexibility to researchers and commercial users alike. All of this has important implications for democratisation, allowing educational institutions, small businesses and developing countries to participate in high-altitude experiments and telecommunications projects that were previously the domain of well-funded government agencies and large corporations.

Rapid Deployment and Flexibility: They can be deployed in a reasonably short time-frame and with a relatively simple infrastructure [2], a critical aspect that significantly increases their usability for a wide range of applications. They are particularly suited to scenarios requiring immediate or early response, such as natural disasters, where temporary communication relays need to be established or damage needs to be analysed. [1] No runway or rocket is required to launch the balloon. Only suitable wind conditions are required, as strong winds could damage the balloon's envelope.

Possibility to recover the deployed equipment: Unlike space-based platforms, balloons offer the capability to recover a launched device. At the end of the mission, the balloon envelope bursts and the payload lands safely on the ground using recovery systems, if the balloon is equipped with recovery systems. This allows very expensive equipment to be sent repeatedly, while at the same time enabling an iterative development process for experimental technologies. Engineers and scientists can refine their designs based on real-world data and performance feedback, a cycle that is often cost prohibitive with satellite-based equipment. [1]

Low Environmental Impact: From an environmental perspective, payload recovery reduces the risk of contributing to space debris, which is an increasing problem in low Earth orbit. In addition, a large part of the balloon systems (gondola and payload) can be reused for the next mission. Compared to rockets or aircraft, balloons do not need hydrocarbon fuel to operate. They only need lifting gas. The only large part that cannot be reused is the plastic envelope of the balloon, which can, however, be recycled. Balloons thus have a very low environmental footprint compared to other mainly space platforms [1].

1.2.2 Limitations of High-Altitude Balloons

It should not be forgotten, however, that there are some disadvantages that can limit the balloons applicability and suitability compared to other platforms. These limitations arise from the nature of their design and the environment in which they operate.

Limited Durability: One of the main disadvantages of balloons is their limited service life (few hours for weather balloons up to more than 300 days for super-pressure balloons [2])[1]. Their flight altitude is subject to extreme conditions, in particular extremely low temperatures and increased radiation, which often leads to material degradation. In addition, pressurised balloons are subject to gas leaks, which gradually reduce their altitude and lifetime, and zero-pressure balloons can only carry limited ballast to balance night and day temperatures, which limits their ability to stay aloft for long periods of time. Therefore, the longest recorded mission life so far belongs to a balloon from Project Loon, which managed to stay in operation for a full 336 days [2], which is still a very short time compared to satellites, where the record is held by Landsat 5, which stayed in orbit for 29 years [17], but very long compared to sounding rockets, that stay in space typically between 5 to 20 minutes[18].

Operational Limits: Balloons by their very nature lack any trajectory control. They are at the mercy of the winds and their trajectory is hard to predict. Even with some level of control, achieving a precise trajectory or stable position is often impossible. As a result, high-altitude balloons are often launched at the poles where the polar stratospheric vortex effect can be used to keep the balloon on a circular, predictable trajectory. [1]However, launching balloons in polar regions significantly increases the cost and limits their ability to capture specific areas on Earth, so these balloons are mainly used for large and expensive scientific instruments. [19][20]

Airspace Navigation Issues: Operation of high-altitude balloons also involves passage through controlled airspace and may require contact with air traffic control, which can present a significant logistical challenge. The difficulty of controlling their trajectory means that balloons can inadvertently cross international borders, requiring negotiations with various aviation authorities to avoid diplomatic incidents. In the worst case, balloons can be perceived as a threat and shot down, as was the case with the Chinese balloon over the US [21], highlighting the possibility of international tensions.

Weather sensitivity: The performance and trajectories of high-altitude balloons are very sensitive to weather and atmospheric conditions. The lack of accurate forecast models for the stratosphere increases operational problems and makes reliable mission planning difficult. Adverse conditions can also compromise payloads, with the risk of unexpected balloon envelope rupture posing a constant threat to mission success. [2]

One would think that the disadvantages would be so great that balloon missions would cease to exist and balloons would be consigned to history as the first means of human lift-off. That this is not the case is shown by the following examples of missions, both commercial and scientific, which prove that they will be with us for some time to come.

■ 1.2.3 Examples of Scientific Missions

ASTHROS is a planned mission to provide new information about stellar feedback in the Milky Way and other galaxies. Originally scheduled for launch in December 2023, this mission has been postponed until December 2024 or 2025 due to delays in other Antarctic missions caused by the Covid-19 pandemic and logistical constraints by NASA's Balloon Program Office to allow more than two Antarctic missions per year. [22] It will perform detailed 3D mapping of ionized gas in star-forming regions using 122 μm and 205 μm fine structure line [NII] observations. The mission seeks to circumvent the limitations imposed by the Earth's atmosphere, which obscures the wavelengths of the 122 μm line, limiting their observations to high-altitude or space-based platforms. It will therefore be the first high-spectral resolution images in this spectrum.[22] The mission features the deployment of a 2,500 kg observatory, including a 2.5-meter telescope, on a high-altitude balloon that floats approximately 40 km above the sea to reach its science targets during a 21 to 28-day flight from Antarctica. To understand the size of the mission. the balloon will be about 150 meters wide, which is approximately size of football stadium.[19] Artistic rendering of the observatory is shown in Figure1.2.

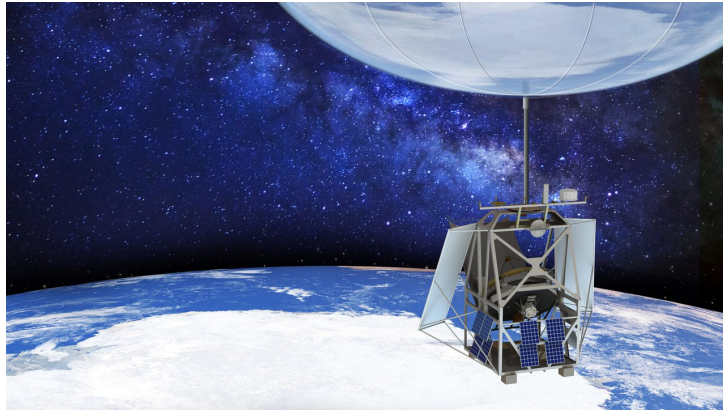


Figure 1.2: Artistic rendering of ASTHROS observatory with super-pressure balloon

BEXUS is a collaboration between ESA's Education Office, the SNSA and the DLR. BEXUS allows university students from all over Europe to design, build, test and launch real balloon experiments into the upper atmosphere. The aim of this programme is to enrich students' technical and personal development through direct knowledge transfer, networking opportunities and multicultural experiences in the space industry. BEXUS is zero-pressure balloon able to lift payload up to 100 kg up to float altitude up to 30 km and spend 2 to 5 hours in the stratosphere. [1]

Gusto mission, launched on 31 December 2023 from McMurdo Station in Antarctica, uses a 39 million cubic foot, helium-filled, zero-pressure balloon equipped with advanced detectors to measure emissions from the interstellar environment. The GUSTO project, led by the Johns Hopkins University Applied Physics Laboratory with significant contributions from the University of Arizona and other major institutions, aims to study the life cycle of interstellar gas in the Milky Way and Large Magellanic Cloud. The GUSTO project, which holds the NASA record for the longest scientific balloon flight with a large payload and long duration, exemplifies the effectiveness of using high-altitude balloons for cost-effective, high-quality astrophysical research that provides clear observations without the atmospheric distortions typical of ground-based telescopes. [20]. The observatory is shown in Figure 6.1.

■ 1.2.4 Examples of Commercial Missions

Project Loon was a very innovative project founded under Google (Alphabet) to provide internet access in remote and rural areas around the world. The project used stratospheric balloons at altitudes between 18-25km to create a

wireless network with speeds comparable to LTE connections. The balloons were designed to navigate by harnessing stratified layers of wind at different altitudes, allowing them to maintain position or move as needed, enabling internet coverage in specific areas. Although the project was terminated due to commercialization issues, it is one of the most advanced examples of a steerable balloon. Figure 1.3 shows the balloon flights over Puerto Rico to re-establish telecommunications services after the devastating hurricane in 2017.[1]

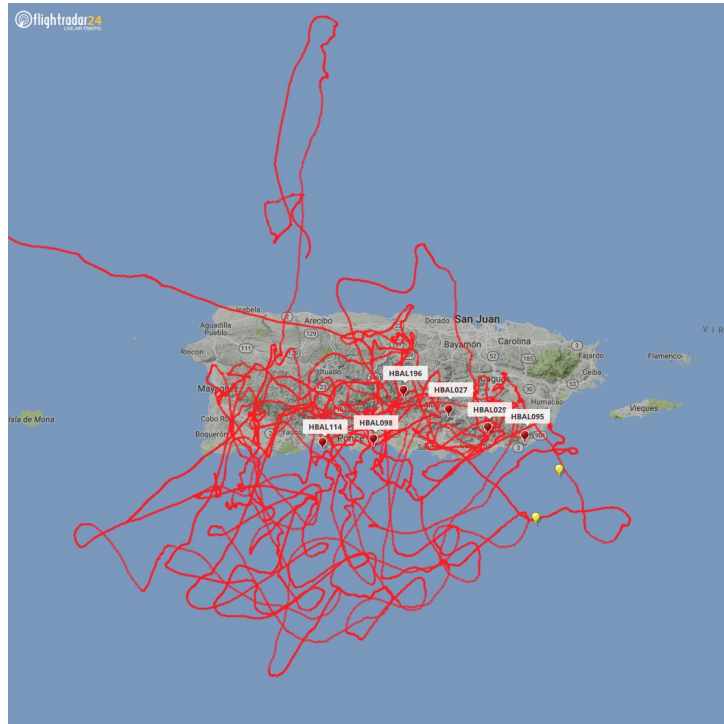


Figure 1.3: Flight trajectories of Loon balloons over Puerto Rico [1]

The latest iteration of the balloon uses a reverse balloon-in-balloon architecture of a super-pressure balloon. The outer balloon contains compressed ambient air as ballast and the inner balloon contains the lift gas. As a result, there is no overpressure between the lift gas and the ambient gas and leakage is limited. The disadvantage of this arrangement is the complexity of filling the ballonnet with lift gas. This architecture is shown in Figure 1.4.[2]

World View Enterprises is a privately held American company that was founded to develop new controllable balloons to offer unique scientific, commercial and even tourist applications.

One of World View's key offerings is the Stratollite balloon and Stratocraft gondola, for applications such as weather observation, disaster response, environmental monitoring and communications. The balloon can ascend to

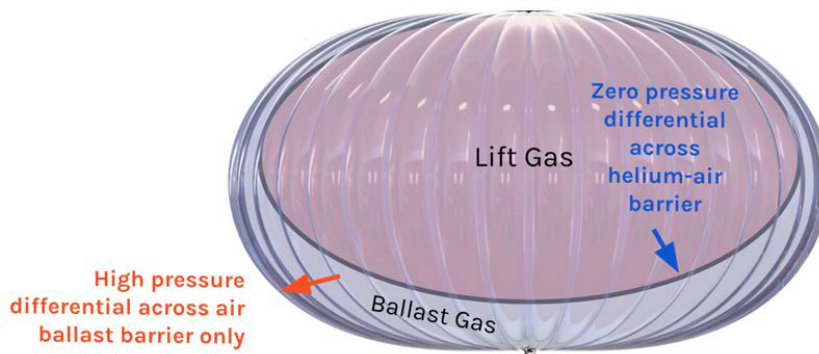


Figure 1.4: Pressure differential locations in reverse ballonnet as used in Loon Balloons [2]

an altitude of 23.5km above sea level and carry a payload of up to 50kg, while delivering 250W of continuous power.[4] The flight control system consists of one zero-pressure balloon that serves as a carrier balloon and then one or more super-pressure balloons into which ambient air is pressurized and serves as a variable ballast. This setup is shown in Figure1.5 At the end of the flight gondola can fly to selected ground location under powered parafoil.

In addition to Stratollite, World View is also exploring the concept of



Figure 1.5: Stratollite balloon with stratocraft gondola including 1 zero-pressure and 2 superpressure balloons [3]

space tourism, using its high-altitude balloons to transport passengers closer to space. This experience would allow passengers to see the curvature of the Earth against the backdrop of space, giving them a unique perspective without having to take a full orbital flight.



Figure 1.6: >24-hour loitering of Strattolite balloon[4]

1.3 Objectives and Scope of the Thesis

The aim of this work is to explore the potential of stratospheric balloons as platforms for a wide range of applications, taking advantage of the ability to change flight altitude, thereby encountering different wind directions and indirectly controlling the flight trajectory. These balloons can have a significant impact on research areas such as payload testing for space missions and research into energetic atmospheric phenomena such as auroral X-ray emission and terrestrial gamma rays or Earth observation. The main focus will be on investigating and comparing different methods of altering the flight level of these balloons, evaluating aspects such as energy and power requirements, balloon lifetime, carrier gas leakage and the balance between operational mass and payload capacity, along with other operational constraints.

Different methods for altitude modification will be investigated, including the use of physical ballast, carrier gas volume manipulation, and mass modification by atmospheric gas compression, applicable to both zero and super-pressure balloons and combinations thereof. In addition, the efficiency, power-to-weight ratio and drag effects of different photovoltaic panel and battery configurations will be compared.

The evaluation of stratospheric behaviour will provide insight into the optimal atmospheric conditions for trajectory control through altitude changes and outline the limits of operation in such an environment. The work will also address the performance of ECMWF or NOAA forecast models in the

stratosphere, and the selection and discussion of critical parameters affecting balloon flight and thermal dynamics.

A significant part of this work will be devoted to the design and development of a software tool that will be used to optimize the design of a system of controlled stratospheric balloons and to simulate their flight trajectories. This tool will incorporate various inputs such as payloads, flight mission characteristics, material properties and technology choices (solar panels, batteries, altitude change technology) to design an integrated flight system. It will also include a simulation environment using real meteorological data to predict balloon behaviour and trajectory, including energy management, gas leakage and control options.



Part II

Theoretical Foundations and Design Aspects

Chapter 2

Overview of Altitude and Trajectory Control Methods

2.1 Day and Night Cycle

For most scientific experiments, maintaining a constant flight altitude is crucial for accurate data collection. While the sun is visible 24 hours a day in the polar regions in summer, ensuring stable thermal conditions, balloons in mid-latitudes face challenges due to daily fluctuations in solar radiation. These thermal fluctuations have a direct effect on the volume of the gas - it expands when it heats up and contracts when it cools down. [1] Such fluctuations in altitude can greatly affect the reliability and accuracy of scientific measurements. Furthermore a zero-pressure balloon is inherently unstable and any change in the thermal conditions of the gas will result in an unlimited change in altitude.[5] Two main strategies are used to mitigate altitude fluctuations ballast and venting and super-pressure balloons.

1. **Ballast and gas venting:** With this method, additional buoyancy gas and ballast are carried to stabilise the altitude. The gas is vented during the day and the ballast is dropped at night when the gas contracts, which nominally amounts to about 8% per day. This method usually limits flights up to 6 daily cycles in mid latitudes and much longer at the poles. [1]
2. **Super pressure balloons:** These balloons contain gas in a fixed volume, which prevents volume expansion and minimises altitude changes. This

design allows potentially unlimited flights at a stable altitude if the gas leakage is controlled, requiring a stronger envelope than unpressurised balloons. [1]

2.2 Options for Controlling Altitude and Trajectory

Altitude control mechanism were studied by Voss and Riddle (2005)[23] and Hall et al. (2019) [5] There are several possibilities to control the trajectory of the balloon, such as active propulsion or sailing, where a controllable wing is suspended at a distance of several km below the carrier balloon, which pulls the wing along the desired trajectory[24], or controlling the sailing of the balloon utilizing different flight altitudes with different wind directions, which is the focus of this work, mainly due to the cost-effectiveness and low complexity of such a system. For such a system to work effectively, the most efficient, lightweight and reliable flight level control system must be found. Possible methods of flight level control include the following:

1. **Ballast and gas venting:** When a ballast (usually sand) is released, the total weight of the balloon is reduced and the balloon can rise to its maximum altitude, which is limited by the maximum volume of the balloon. To lower the flight level, the lift gas must be vented. It is more commonly used to maintain a constant flight level in uncontrolled scientific balloons to compensate for gas release between day and night cycles, which limits their mission up to several days[1] or to control carrier gas release in super-pressure balloons. The disadvantage is the very limited amount of ballast that can only be removed, which greatly reduces the ability to regulate, and also takes away the payload carrying capacity of the balloon. For steerable balloon, it is used more as a supplementary method for trimming when the weight is negligible.
2. **Air Ballast:** It works on the same principle as the ballast, but thanks to the possibility to compress and deflate repeatedly, regulation in both directions is possible and is limited only by the capacity of the gas compression container and the maximum power of the air compressor.[5] Altitude regulation is accomplished by compressing or releasing air into and out of the pressurised vessel, where the vessel is a super-pressure balloon rather than a solid structure. There are two possible arrangements of the super-pressure balloon with the lifting balloon. The first option is when the super-pressure balloon is outside the zero-pressure lifting balloon, which is the method used for the Stratollite controlled balloon [4], the second option is a single super-pressure balloon where the

ballast and lift gas are separated by a diaphragm, which is the method used for the Project Loon balloons.[2]

- 3. **Lift gas compression:** Buoyancy can also be controlled by compressing the lift gas into a pressurised container, thus reducing the volume of the lift balloon and thereby reducing the balloon’s flight level. The advantage is that a super-pressure balloon with compressed gas still functions as a carrier balloon unless it is compressed so that the density of the lift gas exceeds that of the ambient gas. There are two possible configurations where either the super-pressure balloon is inside the zero-pressure balloon and forms a single lifting volume, or where the super-pressure balloon is outside the zero-pressure lifting balloon.[5]

There are other options for flight level changes, including heating/cooling of the carrier gas or mechanical compression of the balloons. These methods are not ideal primarily because of the high energy requirements for temperature control or the complexity and balloon loads involved in mechanical compression. In figure 2.1 you can see the 4 altitude control options using either pumped helium or air to control buoyancy.

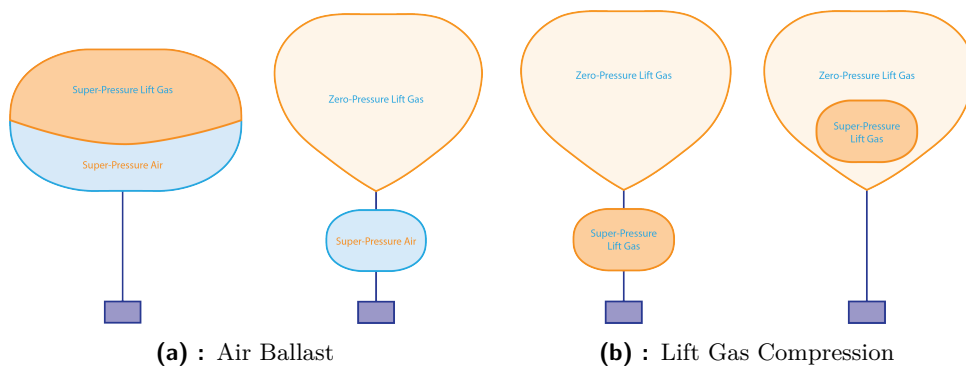


Figure 2.1: Altitude control methods[5]

2.3 Role of Super-Pressure balloon

2.3.1 Differences in energy demand

High-pressure balloons, whether using helium or compressed air as ballast, always require a pump to descend to lower altitudes and maintain a balance of forces. Conversely, the energy requirement during ascent is negligible, as only a valve needs to be opened to allow the gas to reach a lower pressure region

naturally. This discrepancy in energy requirements means that balloons ascend much faster than they descend. Another factor that influences the energy requirement when changing altitude is the overpressure in the balloon, as this affects the amount of energy that needs to be used to pump more gas into the balloon. The higher the overpressure, the higher the energy requirement.

■ 2.3.2 Balloon Stability

At zero overpressure, a balloon reaches neutral stability. Any deviation from this state can cause an unlimited vertical displacement, which does not require any energy. However, this can lead to uncontrolled ascents until the balloon has reached its maximum volume. At this point, it can no longer expand and further vertical movement is prevented either by venting the gas via a valve or, as with weather balloons, by bursting. For these reasons, a type of pressurised balloon that limits uncontrolled vertical movement is almost a necessity.[5] In balloons with compressed helium, transferring gas from a balloon with excess pressure to a balloon with ambient pressure causes the balloon with ambient pressure to expand, which increases the lift and the balloon rises until the forces equalise again. In the case of balloons with air ballast, releasing the compressed air leads to a reduction in mass and thus to the same result. High-pressure balloons not only enable height regulation, but also provide stabilisation due to their constant volume. Excessive downward movement can be prevented through the release of gas from the high-pressure balloon and undesirable upward movement through the compression of the gas at a sufficiently rapid rate. However, this approach necessitates a considerable amount of energy, rendering it impracticable, particularly for stratospheric balloons, which are only capable of utilising a limited energy supply. Consequently, the high-pressure balloon plays an essential role in passive stabilisation due to its constant volume. Unfortunately, the overpressure cannot simply be a free variable, as its value at other altitudes depends on the prevailing ambient conditions. Consequently, it is not feasible to increase the overpressure at extreme altitudes with the intention of improving stability, nor to decrease it at intermediate altitudes with the objective of reducing the energy per altitude change.

This passive stability is illustrated in Figure 2.2, in which a tandem helium balloon lifts a payload of 1000N to a float altitude of 29500m. While the buoyancy of the zero-pressure balloon does not change, the buoyancy of the super-pressure balloon changes with altitude due to its constant volume and the changing density of the surrounding air. If the balloon deviates from its float altitude, it automatically returns to this altitude without the need for active gas release or compression, as the balloon is only in force equilibrium at this altitude. If an external vertical force acts on the balloon, it merely

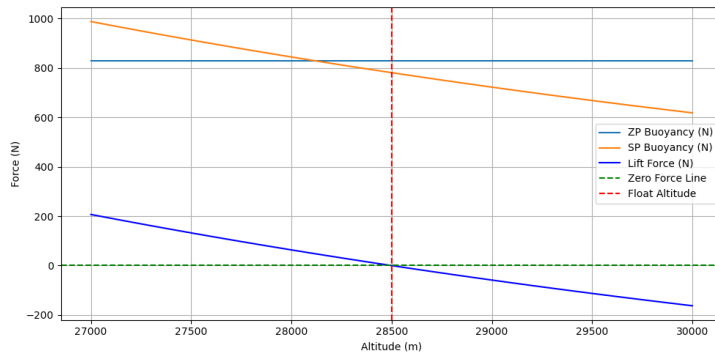


Figure 2.2: Passive stability of tandem ZP and SP helium balloons lifting 1000 N payload

shifts the stable float altitude but remains stable. However, this must be taken into account, as although the balloon can reach its maximum altitude, any upward vertical force will cause it to move further up towards a stable altitude and exceed the maximum designed altitude, which may result in the loss of lift gas from the zero-pressure balloon or its bursting. For this reason, a balloon with zero pressure will never float close to its maximum altitude.

Chapter 3

Atmospheric Behavior and Flight Conditions

3.1 Characteristics of the Atmosphere

Understanding atmospheric conditions at different altitudes and latitudes is essential for the operation of high-altitude balloons, both steerable and non-steerable. The Earth's atmosphere is stratified into several layers, each characterised by different temperature gradients, air pressures and wind conditions. These layers include the troposphere, the stratosphere, the mesosphere and the thermosphere, with the stratosphere being the most important for high-altitude balloon operations due to its relative stability and lower incidence of turbulent weather events, as well as due to the maximum altitude achievable by stratospheric balloons.

3.1.1 Stratosphere

The stratosphere, which extends approximately 10 to 50 km above the Earth's surface, is crucial for balloons at high altitudes because of its stability. This stability is mainly due to the temperature inversion that occurs in the stratosphere, where the temperature increases with altitude, unlike in the troposphere. This temperature gradient prevents the turbulent updrafts that characterise weather in the lower atmosphere, making the stratosphere a calmer environment for balloon flights. The temperature gradient is shown in the figure:3.1. The stratosphere includes several circulations, the main

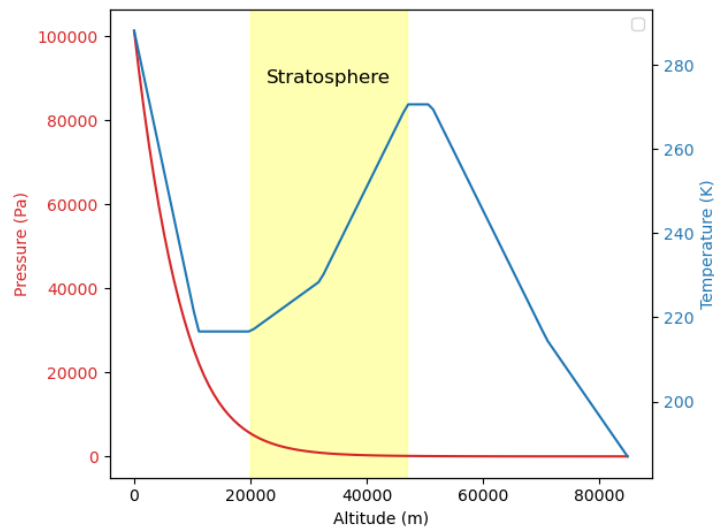


Figure 3.1: Atmospheric pressure and temperature in relation to altitude with highlighted stratosphere based on the US Standard Atmosphere 1976 model [6]

one being the Brewer-Dobson circulation. This is a large-scale atmospheric circulation system in the stratosphere, characterised by upward movement of air from the tropics into the stratosphere and subsequent movement towards the poles and down to higher latitudes. The resulting winds have both horizontal (poleward) and vertical components, with the vertical motions being particularly important in the upward transport from the tropics and the downward motion towards the poles. [25]

At the same time, large planetary waves can break in the stratosphere, especially in the "surf zone" of the winter hemisphere, leading to intense quasi-horizontal mixing. This mixing is much faster than the slower vertical motions. There are also other phenomena in the stratosphere such as the quasi-biennial oscillation (QBO) and sudden stratospheric warming. These phenomena can influence the global weather pattern. [25]

Another phenomenon occurring in the polar regions is the polar vortex, a large area of low pressure and cold air surrounding the Earth's poles. It is characterised by a belt of strong winds in the upper atmosphere that keeps colder air near the poles. This polar phenomenon is used extensively for scientific missions where balloon movement around the poles is assured. [25]

All of these events have a large effect on the weather and temperature conditions around the balloon and are thus very crucial to flight. Their prediction is therefore very important for the correct planning of a balloon mission.

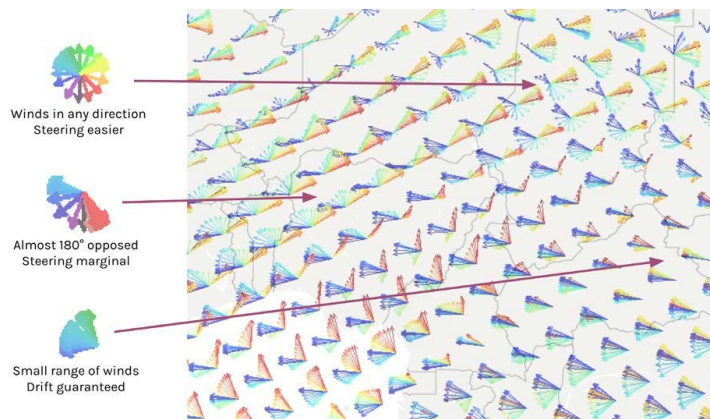


Figure 3.2: Wind cone illustrating the winds over the entire altitude range [2]

3.2 Optimal Flight Conditions

Uncontrollable balloons have quite different requirements for optimal flight conditions. Conditions such as minimal wind shear, stable temperature profiles and predictable atmospheric pressure gradients contribute to safer and more efficient flight operations and balloons can achieve longer flight duration under these conditions. Strategies for exploiting these conditions include launching during periods of expected atmospheric stability, such as during local summer months at high latitudes where stratospheric winds are weaker and more predictable. However, such conditions are not ideal for trajectory control. If the goal is to control the trajectory using changes in flight altitudes, the greatest possible wind shear is required. Such that the minimum change in flight level has a large effect on the change in trajectory. The ideal is if the appropriate flight level is always found for any wind direction. While this is difficult to achieve in the troposphere, the stratosphere is more variable with wind directions at different altitudes due to low air densities and because of the mostly horizontal flow. Figure 3.2 shows a map with wind cones illustrating the direction and strengths of winds found at different flight altitudes, and hence provides a good indicator of directional control options.

If the goal is not to have the balloon pass directly over some area, but rather just the direction of its motion is specified, so that it is, for example, over some definite latitude, then steering it is much easier, as such a large range of different directions is not necessary.

■ 3.3 Forecast Models

The accuracy of the weather forecast model is critical to the accuracy of the flight path prediction. However, the primary concern of most forecast models is not the stratosphere, but the region directly above the ground. Therefore, forecast models often do not even provide data at balloon flight altitudes, or the data are very far from reality. Fortunately, some models do provide data for the stratosphere. The two largest models are the ECMWF [26] and the NOAA GFS model[27].

■ 3.3.1 Important Parameters for Flight Simulation

There are numerous parameters that affect the trajectory of a balloon. However, those that affect flight very substantially are fewer and include ambient temperature, pressure, wind speed and direction, and solar radiation levels at various altitudes. At a minimum, accurate simulations must account for these variables to accurately predict balloon behavior from ascent through mission duration and descent. Additional parameters that thermally affect the balloon environment and the balloon itself would be useful for refinement. These may include earths and clouds albedo, cloud cover, etc.

■ 3.3.2 ECMWF Model

The European Centre for Medium-Range Weather Forecasting (ECMWF) HRES model is considered the most accurate forecast model. The latest high resolution version contains 137 vertical levels with a horizontal resolution of 9km. It produces an hourly forecast for the first 90 hours and then uses a 3 hour forecast up to 10 days. [28]

■ 3.3.3 GFS Model

The National Oceanic and Atmospheric Administration's (NOAA) Globe Forecast System (GFS) model is another important tool for predicting the trajectories of high-altitude balloons. In its updated 2019 version, it contains

127 vertical layers up to 80km high with a resolution of around 13km. It produces an hourly forecast for the first 120 hours and then a 3 hour forecast within 16 days. [27]

■ 3.3.4 Selection and Use of Forecast Model

In terms of model accuracy, the ECMWF HRES model is still the main winner, providing both higher vertical resolution and more layers in the stratosphere, as well as higher horizontal resolution. The strengths of this model are described in the annual "Forecast performance YEAR" report, where its strengths can be seen in the latest 2023 report [29]. The choice of a suitable model depends not only on its accuracy but also on its availability. In this respect, it is preferable to use the GFS model, whose data are freely available for download. The ECMWF HRES model data are hidden behind a paywall and the open access data, have a lower resolution and a very low coverage of balloon flight levels.

Chapter 4

Balloon Shape and Structure

4.1 Shape of Balloon

There are several possible balloon shapes, each with a specific application.

Spherical Balloons

This is one of the most common and most used shapes, having the shape of a near perfect sphere. They are simple to manufacture and are mainly used for very small load weights in the range of several grams. Examples of such balloons include latex weather balloons or the so-called pico balloons most commonly made from mylar foil.[30] The spherical shape is the shape with the smallest possible weight, with zero load, and resists internal pressures very well[31], but when a larger load is suspended from the bottom of the balloon, the forces from internal pressure and load combine and the shape is no longer ideal.[7]

■ Pear-shaped Balloons

These balloons are wider at the top and gradually narrow downwards, resembling the shape of an upside-down pear. The proposed shape is optimised for zero internal pressure and for the load at the bottom of the balloon and is the result of a calculation for a natural-shape balloon without circumferential stress.[31] Its main advantages include lower stress in the envelope and hence the ability to carry higher loads to higher altitudes.

■ Pumpkin-shaped Balloons

These are balloons optimized for both internal overpressure and payload at the bottom of the balloon and are the result of the same balloon shape calculation as pear-shaped balloons. In flight they retain their shape and volume, making them ideal for long duration flights at constant altitude.

■ Cylindrical-shaped Balloons

The cylindrical shape of the balloon is very similar to the shape of an airship. Their advantage is good directional stability and reduced air resistance. At the same time, compared to expensive airships, which are built from very complex fabric envelopes consisting of several layers, balloons are built from cheap foils and have much better mass efficiency, so they can reach higher altitudes. Their advantage is mainly in conjunction with active propulsion. In the last phase of development, the Loon project tried to optimize this design and while the first design was essentially an elongated pressurized balloon with many bulges. The last design was very similar to the airship design with their very aerodynamic shape and was entirely covered in aeroshell to improve airflow around the envelope. These improvements provided very greatly reduced drag, but still not as low as fabric based envelope designs.[2] The evolution of the iterations of the designed cylindrical shapes is shown in Figure 4.1.

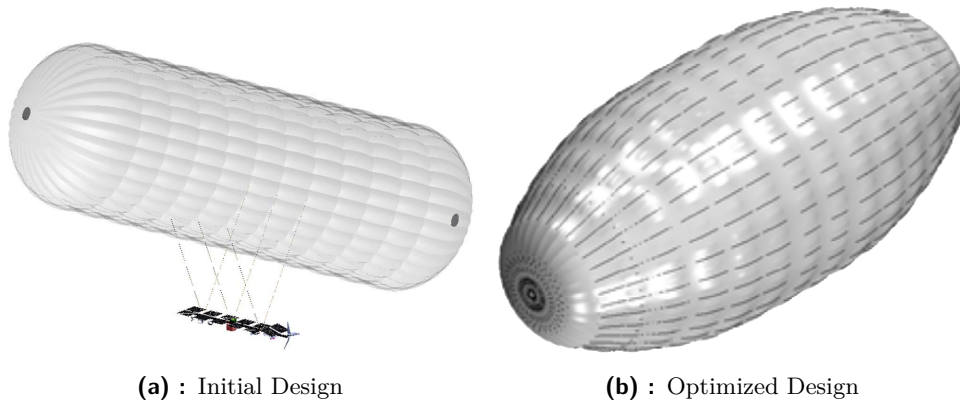


Figure 4.1: Cylindrical-shaped Balloons designed by Project Loon[2]

4.2 Balloon Elements

4.2.1 Gores

A balloon cannot be made from one piece of film. It must therefore be assembled from individual panels called gores, which when combined form the envelope of the entire balloon. The gores are usually made out of extremely thin films, for example the balloon material from Raven Aerostar for super-pressure balloons is polyethylene film only $75 \mu\text{m}$ thick [1], this is the material used for loon balloons. On the other hand NASA used for their zero pressure balloon called the "Big 60" a three-layer co-extruded film out of polyethylene with thickness of $10.2 \mu\text{m}$ for the shell and $13.2 \mu\text{m}$ for each of the two caps. This balloon climbed to altitude of 49.4 km with 690 kg cosmic ray measuring instruments and had volume of 1.7 million cubic meter. The production of the balloon took places on so called stable tables illustrated in Figure 4.2, which had to accommodate almost 230 meter long gores. [32] Particularly with pressurised balloons, the elasticity of the balloon envelope often meant that the balloon did not open fully and evenly due to excess material and also due to the 180degree radius between the load tapes used on the first super-pressure balloons. To eliminate this buckling phenomenon, Calladine and Robinson(1980) [33] contributed through an analysis of this phenomena and figured out that for a lobed balloon with constant lobe angle, there is a limiting angle for a given number of gores. This geometry is shown in Figure 4.3, where α is the half lobe angle, c is the tendon to tendon distance, r is the lobe radius, and s is the manufactured gores width. The semiempirical formula derived by Calladine is then as follows[7]:

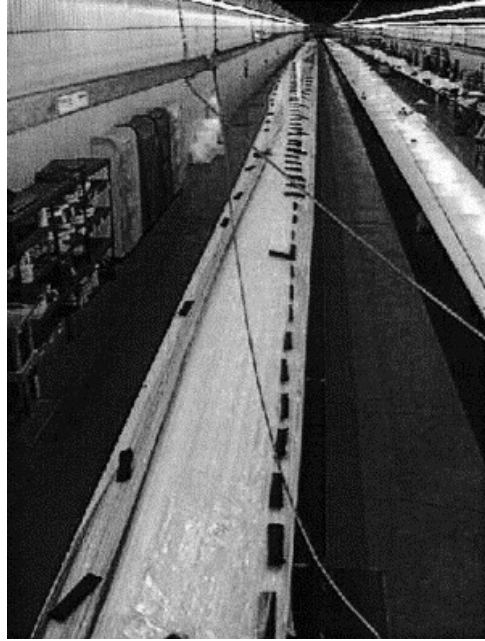


Figure 4.2: The production of the Big 60 balloon

$$\alpha_{\max} = \left(\frac{47}{n}\right)^2 \quad (4.1)$$

$$s/c_{\max} = \frac{\alpha_{\max}}{\sin \alpha_{\max}} \quad (4.2)$$

,where:

α_{\max} : maximal lobe angle

s/c_{\max} : maximal ratio between gore width and tendon distance

n : number of gores

The shape of the tape can be designed to be either constant α or s/c . Project Loon, for example, designed the shape of the gores by taking advantage of the flexibility of the film and assembling the balloon from diamond shapes to simplify overall production but also to improve stress distribution. See Figure 4.4. It's also worth saying that the number of gores in a balloon is mostly dependent on production capabilities. Therefore, usually the number of gores is calculated based on the maximum production width and the thickness of tendons is determined based on that.

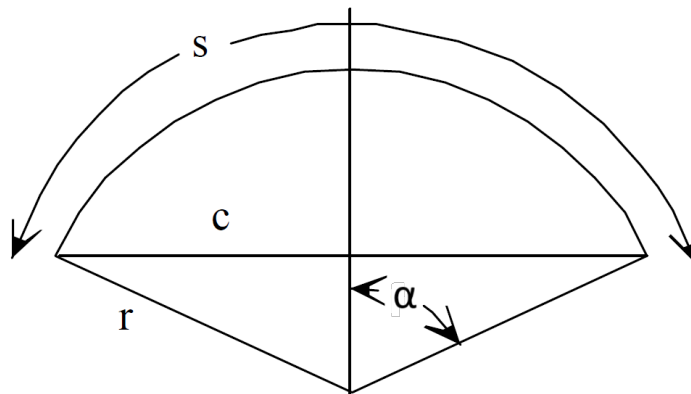


Figure 4.3: Lobed Gore Geometry [7]

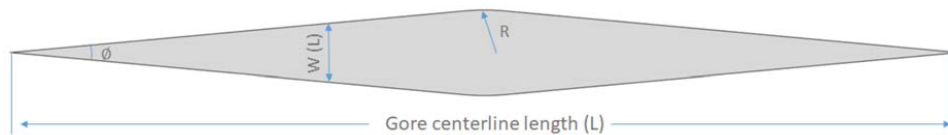


Figure 4.4: Diamond shaped gore of project Loon Super-pressure Balloon

4.2.2 Tapes and Tendons

The tapes used to form the gores of high pressure balloons are an important ingredient in the structure and performance of these devices. It is the use of these support elements as longitudinal force transfer elements that is critical. Particularly at the balloon poles where stress concentrations occur that the balloon film itself is unable to support. This is amplified in the case of pressurized balloons where the demands on strength are noticeably higher. In zero-pressure balloons the demands are lower and often only tapes are used to connect the two gores. These tapes therefore serve not only as a load-bearing element but also as a bond. They are therefore required to be peel-proof and resistant to UV and ozone radiation, which could cause degradation. Although the ideal shape for large pressurised balloons has been known since the early 20th century. Until the late 1960s, there was no fibre technology that could withstand such large longitudinal forces in a balloon. Thus, the first reinforcements used were glass fibres. [7] As time progressed, high strength fibres such as Zylon, Kevlar or Dyneema were adopted.[34] In the first pressurized balloons, the fibers were not tightly attached to the balloon envelope and so the fibers would slip and large amounts of material would bulge out, hence the use of tendons sealed in place on each seam. [7] Figure 4.5 shows the dyneema ropes of the Loon balloon and their connections at the poles, which serve as the supporting element and form the so-called balloon cage.



Figure 4.5: Braided Dyneema tendon attached to the apex assembly load ring on Loon super-pressure Balloon [2]

■ 4.2.3 Caps

Caps are used primarily in straight balloons where, when passing through the troposphere, when the balloon is not fully inflated, the carrier gas is concentrated in the upper part of the balloon and stresses accumulate. As a solution to this problem, so-called caps have come into use. which are reinforcements at the top of the balloon. At first they were placed on the inside of the balloon but after several catastrophic balloon failures it became apparent that the inner caps, when the balloon is fully inflated, are freely hanging from the gores seams and serve as additional localized ballast, at the same time several video recordings have shown the flutter of these inner caps. For this reason, caps began to be installed on the outside of the balloon and sometimes in multiple layers. [35]

Chapter 5

Balloon Aerodynamics and Thermodynamics

5.1 Aerodynamics

5.1.1 Introduction

The dynamics of balloon motion in the atmosphere is affected by the drag or air pressure exerted on the balloon due to the interaction of the moving balloon with the surrounding air. Due to the lower density of air at high altitudes and the small relative air velocities with respect to the balloon, the resulting forces per unit area are relatively small. However, the considerable size of stratospheric balloons compared to most other air vehicles amplifies these forces. This force, referred to as F_d , is essential to enable a steerable balloon to manoeuvre and adjust its course by exploiting changes in wind direction at different flight altitudes and is defined as[36]:

$$F_d = \frac{1}{2}\rho v^2 C_d A \quad (5.1)$$

where:

ρ : air density at altitude (kg/m^3)

v : velocity of the balloon relative to the air (m/s)

C_d : drag coefficient

A : front area of the balloon (m^2)

Other important parameters

Reynolds Number. The Reynolds number (Re) is a dimensionless quantity in fluid mechanics used to predict flow patterns in different fluid flow situations. It is defined as[36]:

$$\text{Re} = \frac{\rho v D}{\mu} \quad (5.2)$$

where:

- D : characteristic linear dimension (typically diameter for balloons approximated by sphere) (m)
- μ : dynamic viscosity of air (Pa·s)

Dynamic viscosity. To calculate dynamic viscosity of air at a specified temperature Sutherland's Law can be used[36]:

$$\mu = \mu_0 \left(\frac{T + C}{T_0 + C} \right) \left(\frac{T_0}{T} \right)^{1.5}$$

where:

- μ : dynamic viscosity of air at temperature T in Kelvin (Pa·s)
- μ_0 : reference viscosity (1.716×10^{-5} Pa·s) at the reference temperature T_0 (273.15 K, or 0°C)
- C : Sutherland's constant (110.4 K)

5.1.2 Zero and Super pressure balloons differences

Zero-pressure balloons exhibit variability in volume and shape due to not being pressurized relative to their ambient environment. This variability may affect their aerodynamic stability. Volume and shape changes can alter the airflow around the balloon, which can lead to increased drag and oscillations in the flight path. This is particularly noticeable at higher airflow velocities relative to the balloon or at very low flight altitudes relative to the maximum flight level, when the carrier helium is only in the upper part of the balloon and the rest of the envelope is hangs of the balloon. Furthermore, the non-uniform shape of zero-pressure balloons can create lift, either positive or negative, and generate a pitching moment that further affects the aerodynamic behaviour of the balloon.[37]

In contrast, pressurised balloons, which maintain a constant volume and shape due to the sealed envelope, generally exhibit a more stable flight path. The shape of pressurised balloons is lobed (pumpkin-shaped) and is designed to distribute stresses, but also affects their aerodynamic properties. This pumpkin shape design can lead to smoother airflow and less turbulent flow compared to a zero-pressure balloon, which can take on a more irregular shape, especially when not fully inflated. Smoother airflow around the super-pressure balloon increases aerodynamic efficiency and can contribute to a more stable and controlled climb and descent through the atmosphere.

Overall, the design and operational characteristics of a super-pressure balloon provide aerodynamic advantages over a zero-pressure balloon, which generally gives them advantages and better predisposes them to the successful execution of long-term and sensitive science missions in the stratosphere.

■ 5.1.3 Simplification

The precise calculation of the aerodynamic behavior of a balloon is very complex, and since a balloon is a body that deforms under the influence of the wind, it must take these factors into account. Therefore, certain simplifications are often made in balloon simulation.

A common approach to simplify the analysis of the aerodynamics of a balloon is to model it as a sphere.[38] This approximation makes it easier to calculate the aerodynamic forces, in particular the air resistance. The assumption of a spherical shape is reasonably accurate if the balloon is fully inflated and under uniform pressure conditions, which is often the case for balloons with zero pressure at maximum altitude. [39]

■ 5.1.4 Estimation of Drag Coefficient

A proper understanding of the air drag characteristics C_d of high-altitude balloons is essential to accurately predict their rate of ascent and their trajectories. During flight, a balloon typically encounters a range of Reynolds numbers from 3×10^5 to 3×10^6 . [39] Traditional data on smooth spheres suggest that the drag coefficient varies considerably in this range, with the lowest rank of drag in the wind being approximately 0.1, but empirical data from balloon flights suggest a constant coefficient at values of approximately

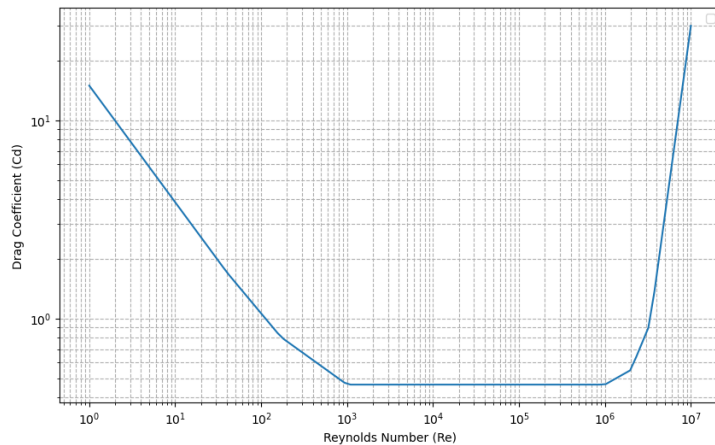


Figure 5.1: Estimated Drag Coefficient of a Balloon as a Function of Reynolds Number

0.47 to 0.5 over a wide range of Reynolds numbers. [39] This consistency represents a laminar flow separation with no reattachment, reflecting the behaviour observed in high altitude balloon flights.

In this paper, a simplification of the calculation of Cd is adopted which depends only on the Reynolds number and is based on the estimates of the Carlson and Horn, 1983 [39]. This simplification is illustrated in Figure 5.1. However, it should be noted that it would be preferable to modify the estimates of Cd to be more accurate and to account for the specific balloon shapes and behavior, adjusting it not only based on Re but dynamically based on the phase of ascent or descent and also on, for example, the thermal state of the gas in the balloon and its quantity.

5.2 Heat Environment

5.2.1 Introduction

High altitude balloons and their flight trajectories are strongly influenced by the thermal environment, both the thermal environment around the balloon and the thermal conditions inside the balloon. To correctly predict trajectories, it is necessary to calculate both the temperature of the envelope and the gas inside, which has a large influence on the volume or overpressure of the balloon. The internal temperature depends on several factors. The gas heats up slightly when the gas is compressed and cools down when it is

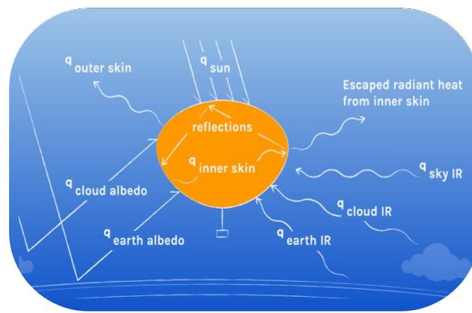


Figure 5.2: Thermal Environment of High Altitude Balloon [2]

vented. At the same time, the ambient air temperature varies with different flight altitudes and current solar conditions. In addition, direct and reflected solar radiation together with infrared radiation from the ground or clouds, or internal reflection of radiation in the balloon together with heat exchange with the envelope affect the internal temperature.

■ 5.2.2 Heat Transfer Mechanisms

The heating of the gas within the balloon and the envelope is governed by three basic heat transfer mechanisms:[38]

- **Conductive heat transfer:** takes place between materials that are in direct contact, with temperatures moving from a warmer region to a colder one. This heat transfer mechanism is weakest in balloons because of the very thin envelope of the balloon.
- **Radiative Heat Transfer:** heat is radiated or absorbed in the form of electromagnetic radiation, which can traverse the vacuum of space. For Balloon the most dominant radiative source is the solar radiation.
- **Convective Heat Transfer:** Heat is transferred through fluid motion, driven by the temperature difference in the fluid. In the case of a balloon, it takes place both outside the balloon between the envelope and the surrounding flowing air, but also inside the balloon due to internal temperature gradients.

All the thermal exchanges taking place that affect the thermal conditions of the balloon are shown in Figure 5.2.

■ 5.2.3 Modelling Thermal Environment

The following thermal model was first introduced by Carlson and Horn, 1983[39], for the purpose of accurately predicting balloon flight trajectories. The model was developed for zero-pressure balloons with no flight altitude control, while allowing for the simplification that the gas and film temperatures of the balloon are spatial averaged values, additionally all gases are taken as ideal.

■ Heat Balance Equations

Heat Balance for Balloon Film. The heat transfer for the balloon film is represented by the equation:

$$\dot{q}_f = m_f c_f \frac{dT_f}{dt}$$

where:

- \dot{q}_f : Net heat flux to/from the balloon film
- m_f : Mass of the balloon film
- c_f : Specific heat capacity of the balloon film
- $\frac{dT_f}{dt}$: Rate of temperature change of the film

Heat Balance for Balloon Lifting Gas. The heat transfer for the lifting gas is described by:

$$\dot{q}_g = m_g c_g \frac{dT_g}{dt} + \frac{g M_a m_g T_g}{T_a M_g} \frac{dz}{dt}$$

where:

- m_g : Mass of the balloon gas
- c_g : Specific heat capacity of the balloon gas
- T_g, T_a : Temperatures of the balloon gas and atmospheric air, respectively
- \dot{q}_g : Net heat flux to/from the balloon gas

- M_a, M_g : Molecular weights of the atmospheric and balloon gas, respectively
- g : Acceleration due to gravity
- $\frac{dz}{dt}$: Rate of altitude change

■ Heat Flux Equations

Heat Flux to Balloon Film. The comprehensive equation for the heat flux to the balloon film is:

$$\dot{q}_f = [G\alpha_f \left(\frac{1}{4} + \frac{1}{2}r \right) + \epsilon_{int}\sigma(T_g^4 - T_f^4) + h_{c_{fg}}(T_g - T_f) + h_{c_{fa}}(T_a - T_f) - \epsilon_{if}\sigma T_f^4 + \epsilon_{if}\sigma T_{bb}^4]S \quad (5.3)$$

where:

- G : Solar constant
- α_f : Solar absorptivity of the balloon film
- r : Planet's reflectivity
- ϵ_{int} : Effective interchange IR emissivity
- ϵ_{if} : IR emissivity of the balloon's film
- σ : Stefan-Boltzmann constant
- $h_{c_{fg}}, h_{c_{fa}}$: Convective heat transfer coefficients for gas-to-film and atmosphere-to-film heat transfer, respectively
- T_{bb} : Black body temperature
- S : Surface area of the balloon

Heat Flux to Balloon Gas. The heat flux to the balloon gas is given by:

$$\dot{q}_g = [G\alpha_g(1+r) - \epsilon_{int}\sigma(T_g^4 - T_f^4) - h_{c_{fg}}(T_g - T_f) - \epsilon_{ig}\sigma T_f^4 + \epsilon_{ig}\sigma T_{bb}^4]S \quad (5.4)$$

where:

- α_g, ϵ_{ig} : Solar absorptivity and IR emissivity of the balloon gas

Since the balloon film is semi-transparent, any radiation to or from the balloon film is partially transmitted and then partially transmitted an infinite

number of times from the opposite wall. Therefore, equations 5.3 and 5.4, $\alpha_g, \alpha_f, \epsilon_{ig}, \epsilon_{if}, \epsilon_{int}$ are effective coefficients that account for this multiple passage phenomenon. For more details, please refer to the original article by Carlson and Horn [39].

■ Use of derived equations for complex balloon systems

It should be noted that the equations are derived for a single equal-pressure balloon that does not have a variable gas quantity and does not share gas with other balloons or surroundings or have a balloonette. Therefore, such an unmodified model does not directly correspond to reality. For simplicity, one can assume each balloon separately for a tandem balloon arrangement and ensure that the enthalpy of the gas in the balloon is affected during compression or deflation. For a balloon-in-balloon arrangement, this is much more complicated and such a simplification is not directly possible. Since the temperature of the gas in the outer balloon affects the temperature of the gas and the envelope of the inner balloon, at the same time all the envelopes collect the radiation that passes from one side to the other and at the same time, radiate between them. To solve an accurate model for both types of balloon would be a difficult work in itself and is beyond the scope of this thesis.

■ 5.2.4 Standard Atmosphere

In all calculations where standard atmosphere data are used, the USSA model [6] was employed. The USSA provides a model for changes in atmospheric properties as a function of altitude up to 84852 m above sea level. It is an essential reference to ensure consistency and accuracy in various analyses and simulations. The evolution of temperatures and pressures is shown in Figure 3.1. Density and other parameters are derived from the ideal gas equation 5.5, which for air can be expressed as follows[36]:

$$PV = mrT \quad (5.5)$$

where:

P is the absolute pressure (Pa)

V is the volume (m^3)

m is the mass of the air (kg)

r is the specific gas constant for dry air ($287.05 \text{ J}/(\text{kg} \cdot \text{K})$)

T is the absolute temperature (K)



Chapter 6

Energy Systems



6.1 Introduction

High altitude balloons equipped with trajectory control mechanisms are complex systems designed to perform specific tasks in the near-space environment. The power systems of these balloons are fundamental to their operation and include several components that ensure functionality and stability during flight. The overall configuration of these systems includes power sources such as solar panels, energy storage units such as batteries, and trajectory control units such as compressors and other electronic devices to ensure reliable and stable operation. These components are strategically integrated to efficiently manage the distribution of energy in various subsystems, including payloads, which often consist of energy-intensive scientific instruments or communications devices.



6.2 Batteries

Batteries in high-altitude balloons serve as the primary storage units of electrical energy. They are designed to withstand the extreme temperatures and pressures at high altitudes and have very similar requirements to batteries used in space missions. These batteries must be lightweight and at the same time have a high energy density to enable longer missions. They are

usually lithium-ion or lithium-polymer batteries, which are characterized by a high energy density and low weight. The battery management systems, which ensure safety and optimum performance through charge regulation and temperature control, are also of crucial importance.

Today, batteries are manufactured in two forms: in pouch form, where the battery is enclosed in a flexible casing, and in cylinder form, where the battery is housed in a metal casing. Although pouch cells generally have a higher energy density, cylindrical cells offer many advantages.[2] They are more robust and ultimately enable a lighter construction. In addition, the large-scale commercialization of the standard 18650 or 21700 cells leads to excellent consistency and uniformity in production due to advanced automation processes. This attribute is highlighted in the work of F.C. Krause et al. (2021) reporting on the frequent use of these commercial cells in space missions [40].

Furthermore, the Loon project concluded that using standard cells with a normal temperature range is more suitable than using cells that can operate at lower temperatures. This is because these cells have a lower energy and power density, so it is ultimately less energy intensive to thermally insulate the batteries along with other avionics equipment and keep them at an optimal temperature through active heating. [2]

6.3 Solar Panels

Solar panels are the most feasible energy source and are essential, especially for long-term missions.[2] While there are often more efficient and lighter technologies available, choosing the right solar panel technology usually involves balancing cost efficiency, mass efficiency and area efficiency. In addition, the durability of the panels is important. However, with most technologies, there is no risk of significant degradation of the cells even during long-term missions lasting up to few months[41].

Among the most efficient and lightweight are multi-junction cells, but these are rarely used in balloon systems due to their high cost. GaAs cells are also generally avoided for cost reasons. Consequently, the most commonly used cells are either monocrystalline or multicrystalline silicon cells, which offer a more cost-effective solution despite their lower area efficiency.[2] More recently, the development of ultra-thin cells has been subject of research. These can be applied directly to the upper part of the balloon envelope,



Figure 6.1: GUSTO observatory at the NASA Columbia Scientific Balloon Facility[8]

where they are not shaded by the balloon film and do not create additional air resistance. Although these cells generally have a shorter lifetime [41], it is usually sufficient for the duration of the balloon mission, which is usually lasting between few days up to few months. Their effect on thermal performance has explored by Zhu et al.(2018)[42], who demonstrated increase of balloons internal temperature and pressure. By integrating these cells into the upper part of the balloon and possibly thickening the material, a similar effect to the use of balloon caps can be achieved for structural integrity when flying through low altitudes.

In addition to the technology of the cells themselves, the configuration of the panels and their ability to track the sun has a significant impact on their effectiveness. Some large scientific balloons, use a fixed angle of tilt of the panels, either without any possibility of rotation, where the panels are then on all sides of the nacelle, or allowing for a single-axis tracking, such as in a project Gusto, shown in Figure 6.1. Another option is a panel ladder suspended directly under the balloon and allowing only single-axis control, this system is used by Stratollite balloons [4], visible in Figure 1.5. The advantage is the possibility of using a large panel area and not being limited to the size of the gondola. However, for controlled balloon flight, two-axis control systems are a significant advantage as they allow near-perfect alignment of the panels perpendicular to the sun, greatly improving power generation. A particular advantage is the possibility of large solar gains at sunrise, when the batteries are often at their lowest state of charge.

6.4 Compressor

Compressors play a crucial role in altitude manipulation in trajectory-controlled balloons. They either regulate the volume of the lift gas, usually helium, to change the balloon's buoyancy, or they pressurize the ambient air as ballast. These compressors must be highly efficient and be able to operate under low pressure conditions and cold temperatures without any loss of performance. The design of the compressor must ensure reliable operation throughout the flight and maintain integrity to prevent leakage of compressed gas.[2] Figure

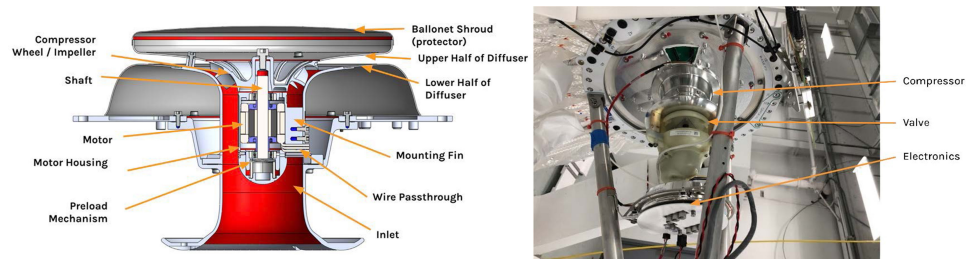


Figure 6.2: Altitude Control Compressor of Project Loon [2]

6.2 shows an altitude control compressor from the Loon project, showing the basic components in a schematic cross-section along with an example of the final integration into the balloon and its support structure. By using more effective control algorithms based on reinforcement learning, it was found that higher cycle rates correspond to improved navigation. Therefore, over 6000 compressor actuations, over 12000 valve actuations and more than 1000 hours of compressor runtime are expected for a typical vehicle with 300 days lifetime.[2]

This high number of cycles results in vibrations on the impeller, failures of the preload mechanism and failures in the valve sealing mechanism due to deposits caused by both wear and compressor-induced vibrations. [2]

For this reason, the last unrealized proposal in the Loon project was the design of a dual redundant system where the failure of one of the compressors would not lead to an early and sometimes catastrophic termination of the mission. This is a very crucial aspect especially for scientific missions carrying highly expensive equipment.

6.5 Payload

The primary function of a balloon's payload is the very reason for its deployment, so a consistent, reliable and adequate power supply must be ensured for its operation. Balloons can host a variety of instruments, each of which has its own power requirements. Optical earth observation instruments, for example, are mainly operated during daylight hours and do not usually require extensive power storage for night operations. Conversely, space-based optical telescopes are primarily active at night to avoid interference from solar radiation and therefore require significant battery capacity to operate after dark.

In addition, other payloads such as telecommunication devices, atmospheric sensors or X-ray telescopes require continuous operation day and night. This requires not only sufficient battery storage for night-time operation, but also sufficiently large solar cells that can generate and store excess power during the day to enable uninterrupted operation around the clock.

6.6 Thermal Management Systems

High altitude balloons must be equipped with thermal management systems that maintain the optimum temperature of the on-board systems and the payload. The stratosphere presents a particular challenge due to the very low temperatures and low pressure, which significantly limit the ability to exchange heat by convection. Temperatures can fluctuate greatly, with sun-exposed devices experiencing a significant rise in temperature during the day due to solar radiation and a sharp drop at night. It is therefore important to develop an efficient heating and cooling solution that protects the balloon's sensitive systems and instruments. Temperature measurement is also an important component and must be carried out at several points, as the temperature gradients can be higher than on the ground due to the limited heat transfer. Passive thermal control strategies, such as insulation combined with reflective materials that deflect solar radiation, are commonly used alongside active systems that regulate internal temperatures in response to external conditions. Among these active methods, direct electrical heating is widely used to maintain higher temperatures within the insulated envelope. Alternatively, high emissivity panels facing the ground can emit heat to the environment during the day and absorb infrared radiation from the ground at night, reducing the need for active heating. One such device, known as a 'photon harvester', was used in the Loon project to moderate temperatures

during the day and provide heat at night to prevent damage to the maximum power point trackers. [2] It is also important not to underestimate the effect of very low temperatures on the moving parts of the equipment. It is often the case that lubricants do not function optimally at low temperatures, so in some cases preheaters are used to raise the temperature to a sufficient level to ensure reliable operation before the system start-up. Although the energy requirements of these systems are often negligible, they should be considered, especially when planning long missions.



Part III

Flight Control System Design



Chapter 7

Selection of Design Approach and Configuration

As discussed in Chapter 2, there are many approaches to control the trajectory of altitude balloons. This work has chosen the altitude change trajectory control method by either compressing the ambient air as ballast or compressing the lift gas to reduce the total volume. This method has proven to be very effective [5], and a reliable control algorithm has already been developed through the long-term efforts of Project Loon, as described in Bellemare et al. (2020) [43]. This method is suitable for missions with small budgets and small balloons as well as for large scientific balloons with large budgets and expensive equipment. Recent iterations of the Loon balloon have shown that combining this method with an active propulsion system could further improve the balloon's controllability, although this would increase complexity and development costs.[2] In addition, the low air density at high altitudes necessitates the use of large diameter propellers.



7.1 Reasons for the choice of control methods

In chapter 2, four possible methods for changing altitude were presented, involving either tandem or balloon-in-balloon configurations and either helium compression for volume reduction or air compression as ballast. For reasons given below, only two of these four methods were selected:

- All methods are computationally similar, allowing the calculations for the two selected methods to be extended to the others if required.
- Implementing multiple methods in the code increases the potential for errors and bugs and makes debugging more complex. It is more efficient to perfect the code for a limited scope before extending it. However, the code is designed to accommodate all methods so that they can be added in the future once everything is fully implemented.
- By focusing on fewer methods, the scope is narrowed, allowing for more detailed analysis and testing of the selected methods.
- Initially, only one ideal method was to be selected. However, it became clear that each method has unique advantages. The two selected methods have different advantages, making them suitable for different tasks, and they have fewer disadvantages compared to the other two methods for the intended optimal task, moreover these two methods were the only studied methods together with mechanical compression by Voss and Riddle (2005)[23], see the next chapter for detailed discussion.

7.2 Selected methods

The first selected method is the tandem arrangement with buoyant gas compression, the second is the balloon-in-balloon arrangement with air compression. The tandem arrangement, which uses a lifting balloon with equal pressure and a pressurized balloon, is ideal for carrying heavy loads or reaching high altitudes, but has a narrow range of flight altitudes, which limits the controllability of the balloon. The balloon-in-balloon arrangement offers a wide range of altitudes, but is not suitable for very high altitudes or heavy loads due to the heavier construction of the super-pressure balloon envelope. The other two methods also use zero-pressure balloon as the main lifting balloon, so like the first selected method they are suitable for high altitudes. However, the balloon-in-balloon with lifting gas compression significantly limits the range of flight altitudes and requires a much larger balloon, as the super-pressure balloon does not contribute to the overall buoyancy. Furthermore, the placement of the super-pressure balloon inside the equal pressure balloon leads to internal stresses, which affects the optimal shape of the equal pressure balloon necessitating heavier materials. This method also lacks passive stability as the super-pressure balloon does not contribute to buoyancy. Nevertheless, the helium loss is limited as the gas only passes from the super-pressure balloon into the zero-pressure balloon and does not escape into the atmosphere, which could extend the mission duration. The second not selected method uses tandem layout with a lifting zero-pressure

balloon with suspended super-pressure balloon acting as air ballast. The main drawback is that the air ballast balloon does not contribute to buoyancy, but reduces the overall buoyancy of the balloon. As a result, the balloon must be significantly larger for the same load and altitude. This method also lacks passive stability and the flight altitude is similarly limited to the chosen first method, but the benefits is that only air is lost from the super-pressure balloon, which extends the deployment time.

Chapter 8

Stratospheric Balloon

The design of the stratospheric balloon is one of the foundation pieces of the entire system and is an essential part of the optimization calculation, while also being one of the most complex calculations. The balloon is both the load bearing and the control element and the largest element of the system. Its size, but especially its volume-to-weight ratio, determines the success of the design and maximizes the possible payload and flight level achieved.

Since the design of the optimal balloon shape is the most frequent and most challenging calculation in system optimization, the aim of this work was to simplify this calculation as much as possible while maintaining the corresponding accuracy of the calculation.

A balloon consists of an envelope, a payload and carrier gas and is kept in the air by Archimedes' law, which states that, if the balloon is in equilibrium, it must displace an amount of air equal to its mass[5]:

$$b \cdot V = w_s \cdot A + L \quad (8.1)$$

where:

- b : volume specific buoyancy (kg/m^3)
- V : volume of balloon (m^3)
- w_s : areal density (kg/m^3)
- A : balloon's envelope surface area (m^2)
- L : payload (kg)

Volume specific buoyancy is calculated using ideal gas law based on difference in densities between the lifting gas (Helium) and surrounding gas (air)[5]:

$$b = \rho_{\text{air}} - \rho_{\text{He}} = \frac{p}{T} \cdot \frac{1}{r_{\text{air}} \cdot r_{\text{He}}} \quad (8.2)$$

The equation shows that the mass of the balloon surface has an impact and therefore it is necessary to predict a suitable balloon shape that has a large volume to surface ratio while being able to support the payload. To do this, a set of nonlinear equations must be solved along with appropriate boundary conditions, which will be presented in the next section. To solve these equations, *Baginski et al.* [44] used the so-called "parallel shooting method". Which was found to be an accurate method to determine the natural shape of an axisymmetric balloon, where the base is a cone with a prescribed base angle θ_0 and assuming only meridional forces.

However, this calculation is computationally intensive and although accurate is not the most suitable for optimization. Hence, Wen and Dorrington came up with a approximate numerical solution and developed a method called the "Tangential increment method" [9]. This method is not computationally demanding, however, after analyzing the method, it was found to be unstable, where for given input parameters, a suitable solution was not found despite its existence. The instability occurs mainly in the calculation of super-pressure balloons, which were not in the scope of investigation when this method was proposed. Thus, it was necessary to develop a custom method that is based on the tangential incremental method, but is capable of designing super-pressure balloons and is more stable due to the use of damping. The actual numerical method of shape design is described in the forthcoming subsection.

8.1 Derivation of the Equations

To simplify the calculation, it is necessary to start with the assumptions that were used for the initial derivation of the equilibrium equations for a small section by Smalley [31].

Assumptions:

- The balloon is assumed to be rotationally symmetric about a vertical

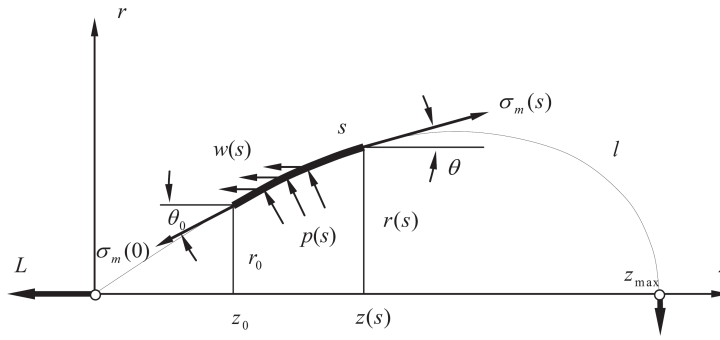


Figure 8.1: Small section of balloons envelope for derivation of the equations[9]

axis.

- Meridional and circumferential stresses are assumed to be constant at all points on the circle lying in a plane normal to the axis of symmetry, precluding the possibility of shear stresses within the balloon.
- The densities of the inflation gas and surrounding air are constant.
- The balloon material is inextensible, thin, and incapable of supporting any bending or compressive loads.

By applying these assumptions to the section shown in 8.1, we derive the following equilibrium equations[44]:

Meridional Stress Balance:

$$r(s)\sigma_m(s) \cos \theta - r(0)\sigma_m(0) \cos \theta_0 = \int_0^s r(s)p(s) \sin \theta ds + \int_0^s w(s)r(s) ds \quad (8.3)$$

Circumferential Stress Balance:

$$r(s)\sigma_m(s) \sin \theta - r(0)\sigma_m(0) \sin \theta_0 = \int_0^s \sigma_c ds - \int_0^s r(s)p(s) \cos \theta ds \quad (8.4)$$

The two equations correspond to the differential equations below, for which Baginski et al.[44] developed a numerical solution using the parallel shooting

method:

$$\frac{d}{ds}(r\sigma_m \cos \theta) = rp \sin \theta + wr \quad (8.5)$$

$$\frac{d}{ds}(r\sigma_m \sin \theta) = \sigma_c - rp \cos \theta \quad (8.6)$$

$$\frac{dr}{ds} = \sin \theta \quad (8.7)$$

$$\frac{dz}{ds} = \cos \theta \quad (8.8)$$

Definitions and Additional Parameters:

- $w(s)$: effective film weight per unit area.
- σ_m : meridional (longitudinal) stress.
- σ_c : circumferential (latitudinal) stress.
- p : aerostatic pressure due to the density difference between the lifting gas and ambient air and overpressure Δp , calculated as [44]

$$p = b(z - a) + \Delta p \quad (8.9)$$

where:

z : distance from the base of the balloon (m)

a : effective distance from the zero-pressure level to the base of the balloon (m)

The effective film weight, $w(s)$, includes the constant film weight per unit area w_f together with the weight of the reinforcing tapes. Assuming a constant weight per unit length, w_t , it is given by [44]:

$$w(s) = w_f + \frac{w_t}{2\pi r(s)} \quad (8.10)$$

Boundary Conditions: At the base of the balloon [44]:

$$2\pi r(0)\sigma_m(0) \cos \theta_0 = L \quad (8.11)$$

Modified Equilibrium Equation: The tangent of the angle θ is formulated as [44]:

$$\tan \theta = \frac{dr}{dz} = \frac{L \tan \theta_0 + 2\pi (\int_0^s \sigma_c ds - \int_0^s rp \cos \theta ds)}{L + 2\pi (\int_0^s rp \sin \theta ds + \int_0^s rw ds)} \quad (8.12)$$

Total Film Load: The total film load, T , is defined as [44]:

$$\frac{T}{2\pi} = r\sigma_m = \sqrt{\left(\frac{L}{2\pi} \tan \theta_0 + \int_0^s \sigma_c ds - \int_0^s rp \cos \theta ds\right)^2 + \left(\frac{L}{2\pi} + \int_0^s rp \sin \theta ds + \int_0^s rw ds\right)^2} \quad (8.13)$$

In this model, θ_0 represents one-half the 'cone-angle' at the base of the balloon.

Geometry and Boundary Conditions for Shape Prediction: The geometry of any balloon shape must satisfy the nonlinear equation provided, with the condition that at the uppermost point of the balloon, if there is no point load at the apex, the radius r reduces to zero, and the angle θ_{end} , reaches $\frac{\pi}{2}$. This represents tangential alignment at the end of the balloon, as would occur at its apex.. For the given design parameters, two unknowns θ_0 and l can be determined based on these boundary conditions. In the natural shape of the balloon where $\sigma_c = 0$, equation 8.12 simplifies to [44]:

$$\tan \theta = \frac{dr}{dz} = \frac{L \tan \theta_0 - 2\pi \int_0^s rp \cos \theta ds}{L + 2\pi (\int_0^s rp \sin \theta ds + \int_0^s rw ds)} \quad (8.14)$$

8.2 Simplified numerical calculation algorithm

The presented optimization calculations are based on the approximation method introduced by Wen and Dorrington, which serves as a simple approach to estimate the shape of stratospheric balloons. [9] This method makes use of the equations discussed in the previous section, in particular the equation 8.12. It simplifies the process by using numerical approximations and optimization steps, thus avoiding the need to solve complex differential equations. The calculation is derived from the approximation method proposed by Wen and Dorrington [9] as a simple method to estimate the shape of a stratospheric balloon. The method is based on the equations illustrated in the previous section, mainly equation 8.12. However, the computation is a numerical approximation that proceeds in several optimization steps, which greatly accelerates the computation in question and thus bypasses the complex system of differential equations altogether.

In this section, a revised version of the tangential incremental method for balloon design at float altitude will be presented. The modified version is more robust, especially for the calculation of pressurized balloons.

First the approximation strategy used needs to be introduced. To determine the position of the envelope in the step $n + 1$, the tangent angle can be approximated from the equation 8.12 as follows:

$$\tan \theta_{n+1} \approx \frac{L \tan \theta_0 + 2\pi \int_0^s \sigma_c ds - 2\pi \int_0^{s_n} rp \cos \theta ds}{L + 2\pi \int_0^{s_n} rp \sin \theta ds + 2\pi \int_0^{s_n} rw ds} \quad (8.15)$$

where $n = 0, 1, \dots, N$.

Another equivalent form is given by:

$$\tan \theta_{n+1} = \frac{L \tan \theta_0 + 2\pi \sigma_c s_n - 2\pi I_r}{L + 2\pi I_z + I_s} \quad (8.16)$$

where parameters are defined as follow:

$$\begin{aligned} s_n &= \sum_{i=1}^n \Delta s, \\ I_r &= \sum_{i=1}^n (r_i(z_i - a) + \Delta p) \cos \theta_i \Delta s, \\ I_z &= \sum_{i=1}^n (r_i(z_i - a) + \Delta p) \sin \theta_i \Delta s, \\ I_s &= \sum_{i=1}^n 2\pi r_i w_f \Delta s + n_t w_t \Delta s, \\ r_n &= \sum_{i=1}^n \sin \theta_i \Delta s, \\ z_n &= \sum_{i=1}^n \cos \theta_i \Delta s. \end{aligned} \quad (8.17)$$

Definitions and Additional Parameters:

- w_f : Film weight per unit area [N/m²]
- n_t : Number of tapes

- w_t : Tape linear density [N/m]
- a : Pressure head at bottom of balloon [m]

■ Natural shape:

When considering the natural balloon shape at floating altitude, the tangent equation in step $n + 1$, simplifies 8.16 to:

$$\tan \theta_{n+1} = \frac{L \tan \theta_0 - 2\pi I_r}{L + 2\pi I_z + I_s} \quad (8.18)$$

with $a = 0$. The incremental technique is applied over the entire length l of the generating curve, with detailed steps outlined for each iteration from the base angle at step k to the length of curve at $n + 1$ as follows:

1. Input the base angle θ_0^k .
2. If $n^k = 1$, then $r_1 = z_1 = I_{r1} = I_{z1} = I_{s1} = 0$;
3. Calculate the base angle θ_{n+1}^k using equation 8.18;
4. Calculate $s_{n+1}^k, r_{n+1}^k, z_{n+1}^k, I_{r,n+1}^k, I_{s,n+1}^k, I_{r,n+1}^k$ using equations 8.17;
5. If $r_{n+1}^k > 0$, then $n^k = n^k + 1$, return to step 3; else if $|\theta_{n+1}^k + (\pi/2)| < \epsilon$, then proceed to last step 8; otherwise continue to step 6
6. If $k < 10$, then calculate new starting angle using following equation (bisection method) and return to step 2, otherwise continue to step 7.

$$\theta_0^{k+1} = \theta_0^k - \frac{\theta_0^k - \theta_0^{k-1}}{\theta_N^k - \theta_N^{k-1}} \left(\theta_N^k + \frac{\pi}{2} \right) \quad (8.19)$$

7. If the method is not converging after 10 steps, the calculation needs to be dampened. Calculate new starting angle using following equation (dampened bisection method) and return to step 2.

$$\theta_0^{k+1} = \theta_0^k - D \frac{\theta_0^k - \theta_0^{k-1}}{\theta_N^k - \theta_N^{k-1}} \left(\theta_N^k + \frac{\pi}{2} \right) \quad (8.20)$$

D is damping factor with selected value 0.6

8. Print $\theta_0^k, l = s_N^k$ and the curve $[r_n^{k+1}, z_n^{k+1}]$, $n_k = 1, 2, \dots, N^k$, where N^k is the maximum number corresponding to the base angle θ_0^k .

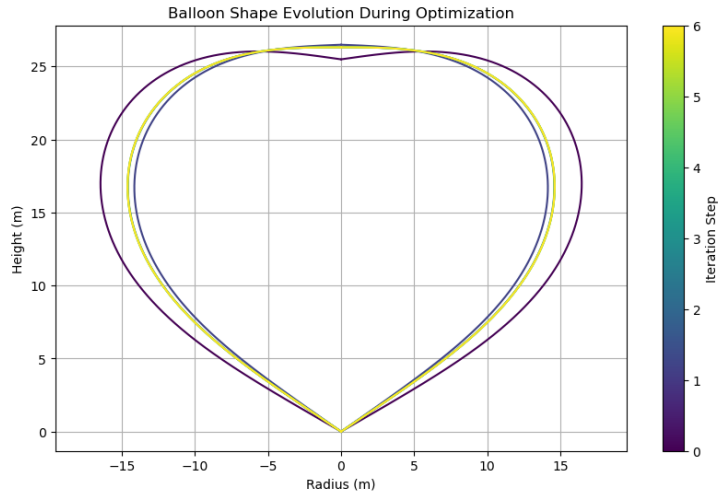


Figure 8.2: Shape optimization of zero-pressure balloon

Figure 8.2 shows optimization steps of zero-pressure balloon with following input parameters:

$$\begin{aligned}
 L &= 500 \text{ N}, \\
 h &= 35000 \text{ m}, \\
 \theta_0^1 &= 65^\circ, \\
 \epsilon &= 10^{-6}, \\
 \Delta_s &= 1, \\
 w_f &= 0.1 \text{ N/m}^2, \\
 w_t &= 0.1 \text{ N/m}, \\
 n_t &= 30
 \end{aligned}$$

■ Further Insights:

- The tangent of $\frac{\pi}{2}$ is undefined, and as θ_0 approaches $\frac{\pi}{2}$ in super-pressure balloons, a method was required to manage this issue. Accordingly, a transformation has been developed to adjust the angle θ_0 to approach zero as it nears $\frac{\pi}{2}$.
- For the computation of $\sin(\theta)$ and $\cos(\theta)$, θ is typically obtained from the arc-tangent function in accordance with Equation 8.18. It is advantageous to directly calculate the sine and cosine from Equations 8.17, which facilitate reaching the terminal angle near $-\frac{\pi}{2}$. Without this method,

optimization would be constrained, as the angle θ_N^k would not surpass this threshold.

$$\sin(\theta) = \frac{\text{numerator}}{\sqrt{\text{denominator}^2 + \text{numerator}^2}}, \quad (8.21)$$

$$\cos(\theta) = \frac{\text{denominator}}{\sqrt{\text{denominator}^2 + \text{numerator}^2}} \quad (8.22)$$

- Particularly in super-pressure balloons, the lift generated does not always match its weight, largely due to the approximation method and the errors arising at angles close to $\frac{\pi}{2}$. Thus, a scaling method has been introduced, as detailed in the subsequent section, to ensure that the error between the lift and pressure is minimized.
- During the computation of incremental parameters in equation 8.17, the incremental section length of the balloon envelope, Δs , is used, which is an input parameter provided by the user. Ideally, this parameter should be parameterized so that it corresponds to a smaller value for smaller balloons and a larger value for larger balloons. Therefore, the parameterization of this input parameter has been implemented according to the following equation and with behaviour presented in 8.3:

$$k = 0.0002, \quad (8.23)$$

$$\lambda = \sqrt[3]{\frac{L}{b}}, \quad (8.24)$$

$$\Delta s_{\text{new}} = k\Delta s\lambda \quad (8.25)$$

■ Lift/Load balance:

As previously stated, there are frequently issues with inadequate or excessive buoyancy in balloon design, particularly in the case of pressurised balloons. Even if the shape is correct, an inappropriate size can disrupt the equilibrium of forces. Consequently, it is crucial to establish a scaling factor to adjust the dimensions of the balloon and achieve equilibrium. However, determining this scaling factor is not a straightforward process. Overcoming these challenges necessitates the development of a method employing two distinct optimisation algorithms based on the initial scaling factor: 8.26, the Nelder-Mead simplex algorithm and the dual annealing technique.

$$\text{initialscalefactor} = \left| \frac{L}{\text{lift balance} + L} \right| \quad (8.26)$$

The Nelder-Mead algorithm is employed when the square of the initial scaling factor is less than 4, which is well-suited to scenarios requiring minor adjustments. In contrast, the dual annealing method is employed when the square of

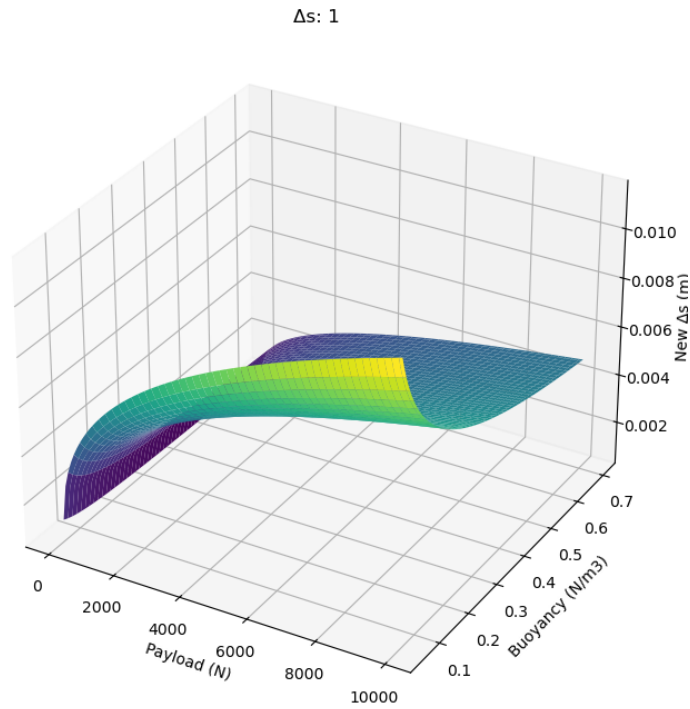


Figure 8.3: Graph showing behaviour of Δs_{new} parametrization function for $\Delta s = 1$

the initial scaling factor is equal to or greater than 4, which indicates a more complex optimisation scenario. This robust technique combines the principles of simulated annealing and local search, thereby exploring a broader search space and mitigating the risk of local minima that may not be adequately addressed by the Nelder-Mead algorithm.

This strategic choice of optimisation algorithms optimises the allocation of computational resources and increases the likelihood of achieving an optimal balance between lift and load in balloon design by systematically considering both simple adjustments and more complex scenarios.

Chapter 9

System for Changing Flight Levels

9.1 Tandem pumped helium balloon

Introduction

The balloon system with a tandem arrangement of helium-filled balloons consists of two balloons, both of which ascend. The first is a zero-pressure balloon and the second is a super-pressure balloon. To lower the flight altitude, helium must be pumped from the zero-pressure balloon into the super-pressure balloon, which reduces the total volume and the balloon begins to descend. The super-pressure balloon maintains a constant volume and therefore a constant buoyancy, while the buoyancy of the zero-pressure balloon changes. To design an ideal system, it is primarily necessary to determine the size ratio between the two balloons. The larger the super-pressure balloon, the more the system resists external disturbances such as temperature fluctuations or vertical air currents. However, a larger super-pressure balloon reduces the range of flight altitudes.[23]

Another important factor is the maximum flight altitude. If the system exceeds the maximum flight altitude, the zero-pressure balloon has no room to expand and to prevent the envelope from bursting due to overpressure, some of the helium must be released, which is highly undesirable and should be prevented. It is therefore necessary to select a so-called hover altitude. This is the maximum flight altitude at which the balloon can withstand external

conditions and does not exceed the maximum flight altitude in the event of a disturbance.

The calculations presented are based on the model proposed by Hall et al. (2019) [5] and Voss and Riddle (2005) [23].

■ Constants

As the balloon does not exchange gas with its surroundings due to its operating principle, the total mass of the gas in the first and second balloon is always constant.

$$m_{\text{HeSP}} + m_{\text{HeZP}} = m_{\text{He}_{\text{total}}} = \text{constant} \quad (9.1)$$

Assuming that the balloon envelope is not flexible, the volume of the super-pressure balloon does not change with altitude.

$$V_{\text{SP}} = \text{constant} \quad (9.2)$$

Naturally, the weights of the balloon components (W_{ZP} and W_{SP}) do not change during the flight, as they are determined by the physical materials and the construction of the balloons, which remain constant.

■ Equilibrium equation

The basic equation is the equilibrium equation, which indicates when the balloon is in equilibrium of forces. This is represented for this particular balloon by the following equation:

$$B_{\text{ZP}} + B_{\text{SP}} = L + W_{\text{ZP}} + W_{\text{SP}} + m_{\text{HeZP}} + m_{\text{HeSP}} \quad (9.3)$$

Where:

B_{ZP}, B_{SP} : weights of the displaced air by the zero-pressure and super-pressure balloons, respectively

W : weight of the corresponding balloon

m_{He} : mass of the helium filling of the corresponding balloon

The weights of the displaced air are following this equation:

$$B_{\text{balloon}} = V_{\text{balloon}} \times \rho_{\text{Air}} \quad (9.4)$$

The amount of helium in the super-pressure balloon can be derived using the ideal gas law:

$$m_{\text{HeSP}} = V_{\text{SP}} \times \frac{p + \Delta p}{T \times r_{\text{He}}} \quad (9.5)$$

Similarly, the following applies to the zero-pressure balloon

$$m_{\text{HeZP}} = V_{\text{ZP}} \times \frac{p}{T \times r_{\text{He}}} \quad (9.6)$$

■ Calculation for Maximum Flight Level and Recalculation for Other Flight Levels

In this setup, the calculation at maximum altitude is quite simple. First, the payload must be divided between the two balloons based on the initial size ratio, and then each balloon is calculated individually according to the procedure described in section 8.2. It is important to calculate the shape of the super-pressure balloon at the maximum pressure, but then adjust the overpressure to the nominal overpressure in order to correctly calculate the shape and the helium mass in each balloon. From the calculation of the balloon shape, we determine both the mass of each balloon and its volume, from which the mass of the helium mass can be calculated according to the equations 9.5 and 9.6.

To set the balloon to a different altitude, the temperature and pressure of the ambient air must first be determined, from which the density of the

air is then calculated according to the ideal gas law. The volume of the zero-pressure balloon must subsequently be calculated, which is determined from the equilibrium equation 9.3 and the equation for the displaced air 9.4 as follows:

$$V_{ZP} = \frac{L + W_{ZP} + W_{SP} + m_{He_{total}} - B_{SP}}{\rho_{Air}} \quad (9.7)$$

The next step is to determine the mass of the helium in the zero-pressure balloon, which is calculated using the equation 9.6 by using the temperature and pressure corresponding to the given altitude. The mass of helium in the super-pressure balloon can then simply be calculated as the difference between the total mass of helium and the amount of helium in the zero-pressure balloon, as follows:

$$m_{He_{SP}} = m_{He_{total}} - m_{He_{ZP}} \quad (9.8)$$

It is also possible to determine the overpressure in the balloon, which - perhaps surprisingly - is almost constant and only changes with the ambient temperature. The overpressure can be determined using equation 9.5.

■ Minimal flight altitude

The type of balloon discussed cannot descend indefinitely, as helium must be transferred from a zero-pressure balloon to a super-pressure balloon. This transfer continues until the helium in the zero-pressure balloon is completely depleted at a certain altitude, a condition that must be avoided to prevent the balloon from collapsing. It is therefore important to find an altitude at which the helium filling of the zero-pressure balloon is sufficient to sustain itself and not collapse onto the super-pressure balloon below. This effect is illustrated in the following figure 9.1, which shows a tandem balloon with a total payload of 100 kg, with each balloon carrying half the weight at the maximum design altitude 30,000 meters. The diagrams start at 0 meters. The first graph shows the helium levels in each balloon with a calculated minimum flight altitude. The next graph shows the overpressure in the balloon at different flight altitudes and confirms that the overpressure of the balloon is only affected by the ambient temperature when no external forces or temperature gradients are acting on it. The last graph illustrates the development of the balloons volume.

It should be pointed out that the balloon cannot be in any region with negative values of volume or amount of helium. It also shows that the minimum flight level is not directly at 0 but shifted a bit to balance the buoyancy of an equal pressure balloon with its mass.

To determine the minimum flight altitude, the Secant algorithm is used,

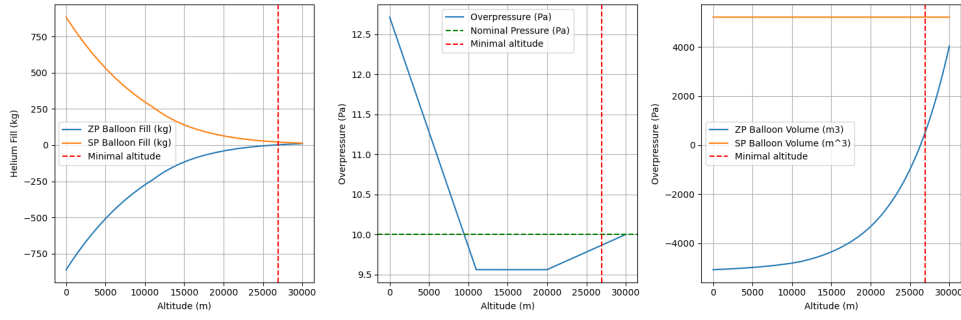


Figure 9.1: Variation of tandem helium system parameters across the entire altitude range

which attempts to find the root at which the buoyancy of a zero-pressure balloon is in equilibrium with its weight. The following applies to the minimum flight altitude for a zero-pressure balloon:

$$B_{ZP} - W_{ZP} - m_{He_{ZP}} = 0 \quad (9.9)$$

■ Maximal stabilizing force

The maximum stabilizing force corresponds to the force exerted by a balloon that is moved from its hovering altitude to another altitude without changing the helium mass in the individual balloons and without exceeding the maximum pressure or the maximum altitude of the balloon. This force is primarily necessary to counteract the force created by vertically rising air at a certain speed or to compensate for the temperature difference between the gas in the balloon and the ambient air.

Calculation Procedure:

1. **Recalculation of the balloon at hovering altitude:** It is necessary to recalculate the balloon to the flight altitude which corresponds to the hover altitude. The procedure is the same as described earlier. First, the volume is calculated according to equation 9.7. Then the mass of the helium in a zero-pressure balloon is calculated using the equation 9.6. Finally, the mass of the gas in the super-pressure balloon is calculated using the equation 9.8.
2. **Determining the altitude at maximum overpressure:** Before finding the force at the maximum permissible overpressure, an optimization

algorithm is used to find the flight altitude at which the overpressure is equal to the maximum permissible overpressure. For the optimization the overpressure of the balloon at a certain altitude must be determined, which can be calculated from the ideal gas law using the following equation

$$\Delta p = \frac{m_{\text{HeSP}} r_{\text{He}} (T + \Delta T_{\text{max}})}{V_{\text{SP}}} - p \quad (9.10)$$

3. **Selecting the limiting altitude:** After finding the corresponding flight altitude at which the pressure of the super-pressure balloon is equal to the maximum pressure, it is necessary to compare if the found altitude is lower than the maximum flight altitude, if not, the limiting flight altitude is the maximum flight altitude and not the one with the highest over-pressure.
4. **Determining the max force:** After the limiting flight altitude is set, the corresponding pressure, temperature and density of the ambient air are calculated, from which the volume of the zero-pressure balloon is calculated using the following equation 9.11.

$$V_{\text{ZP}} = \frac{m_{\text{HeZP}} r_{\text{He}} (T + \Delta T_{\text{max}})}{p} \quad (9.11)$$

Then the masses of the displaced air for both balloons are calculated using the equation 9.4 and finally the force is calculated using the following modified equation for the equilibrium of forces:

$$F = L + W_{\text{ZP}} + W_{\text{SP}} + m_{\text{HeZP}} + m_{\text{HeSP}} - B_{\text{ZP}} - B_{\text{SP}} \quad (9.12)$$

■ Effect of helium temperature increase

The increase in the internal helium temperature due to solar heating affects both zero- and high-pressure balloons in different ways. In zero-pressure balloons, the expansion of helium increases the buoyancy, while in super-pressure balloons it increases the overpressure. This double effect is reflected in the equations 9.10 and 9.11, where the calculated values are supplemented by the temperature increase, represented by the temperature difference ΔT_{max} .

■ Effect of Up Wind

In addition to the thermal effects on balloon stability, vertical updrafts have a significant influence on balloon behavior. As the wind can be gusty and

far more variable than the thermal effects on a balloon, it is a critical factor. It is also difficult to counteract due to the limited power of the compressor. For this reason, it is important to ensure sufficient passive stability against disturbances in order to prevent the maximum flight altitude from being exceeded.

Calculation Procedure:

1. **Recalculation of the balloon at hovering altitude:** The calculation is exactly the same as when recalculating altitude, except that only the volume of the zero-pressure balloon is of interest, according to equation 9.7. The volume of the super-pressure balloon remains unchanged and corresponds to the calculated volume for the maximum flight altitude.
2. **Calculation of the required parameters:** As mentioned in chapter 5.1.3, the balloon is approximated by a sphere. Therefore, it is necessary to convert the volumes of the balloons into spheres with a certain radius r . We then use equation 5.2 to calculate the Reynolds number, which we use to determine the drag coefficient for both balloons. After that, it remains to calculate the drag area, which corresponds to the area of a circle A with radius r .
3. **Drag Force:** The last step of the calculation is to determine the drag force, which in the case of a vertical air flow is approximately equal to the drag of the larger balloon plus half the drag of the smaller balloon. In this simplification, it is assumed that the second balloon is in the slipstream of the first and that its drag is therefore lower.[5] The resulting force is calculated based on equation 5.1 as :

$$F = \frac{1}{2} \rho_{\text{air}} \times v_{\text{max}}^2 \times (A_{\text{bigger}} \times C_{d_{\text{bigger}}} + 0.5 A_{\text{smaller}} \times C_{d_{\text{smaller}}}) \quad (9.13)$$

■ Optimization

The final step is optimization, which seeks to find an arrangement that will not exceed the maximum flight altitude during the hovering altitude flight, despite the thermal heating of the balloon and the effects of the vertical updraft, while achieving the lowest possible flight altitude. The lowest possible altitude is achieved precisely when the stabilising force is in balance with the drag force and balloon heating, and at the same time when the maximum stabilising force, limited by the maximum pressure in the super-pressure balloon, is directly at the maximum flight level. Although

the super-pressure balloon provides stability, it also reduces the achievable flight altitude; therefore, a compromise must be found at the limit of the stabilising force. The optimization consists of two inputs, the first is the ratio between the buoyancy of the super-pressure and zero-pressure balloon and the second input is the float altitude. There are two outputs corresponding to these inputs, the first is the balance of forces after recalculating the balloons and the second is the difference between the altitude at which the maximum stabilizing force is located and the maximum altitude. The optimization is very sensitive to the inputs, and a poor procedure could cause one of the inputs to be shot out of realistic value. Therefore, optimization algorithms with multiple inputs were not used, but only a simple double secant algorithm where the optimization of the float flight level is performed within each optimization step looking for the ratio of lift forces.

Max. Temperature Difference [°C]	45	10
Max. Up Draft [m/s]	20	10
Min. Altitude [m]	32 861	24 181
Float Altitude [m]	34 207	33 363
Balloon Lift Ratio	0.343	0.877
ZP Balloon Volume [m ³]	16 636	38 962
SP Balloon Volume [m ³]	30 137	6 928

Table 9.1: Optimization Outcomes for Tandem Helium System Across Temperature and Updraft Variations

Table 9.1 shows the optimization results for a tandem helium system with a 250 kg payload, a maximum flight altitude of 35,000 meters and a maximum overpressure of 200 Pa under two different environmental conditions. The table illustrates the significant role of the super-pressure balloon in stabilization and how it significantly lowers the minimum flight altitude. Unfortunately, the first scenario is more realistic, making the tandem arrangement more suitable for maintaining a stable altitude and reaching high altitudes rather than for controlled flight. However, within a very limited range of flight heights, slight trajectory adjustments are still possible. These adjustments serve less to keep the balloon stationary, which would require a very large range of altitudes, but rather as long-term corrections to the flight path, for example to recover the balloon's payload.

■ 9.2 Super pressure balloon with air ballast

■ Introduction

This balloon system consists of two balloons, one inside the other. The outer balloon is a super-pressure balloon that contains compressed air and serves as ballast. The inner balloon is filled with buoyant helium. To cause the balloon to descend, the ambient air is pressed into the outer balloon, increasing the weight of the balloon and causing it to sink. The weight of the displaced air remains constant at all altitudes due to the constant volume. The overpressure only exists between the outer balloon and the surroundings, so that no helium can leak out.

With this system, there is no risk of helium being released if the maximum flight altitude is exceeded, and the only limitation is the overpressure caused by the expansion of the gas inside the balloon. As a super pressure balloon, it is very stable and resistant to external disturbances and theoretically has no lower flight limit. However, its disadvantages include a higher energy requirement during descent and greater overpressure when heated.

The optimization of this balloon system is rather different and involves initially finding a volume at which both balloons are in equilibrium under nominal overpressure. This means that the amount of displaced air corresponds to the weight of the balloon envelopes, the compressed gases and the payload. The subsequent optimization is about finding the minimum overpressure required to withstand the external factors.

The calculations presented are based on the model proposed by Hall et al. (2019) [5] and Voss and Riddle (2005) [23].

■ Constants

Since the inner balloon does not exchange helium with any other balloon, the mass of helium remains constant at all flight levels.

$$m_{\text{He}} = \text{constant} \tag{9.14}$$

At the same time, assuming that the balloon envelope is not flexible, the outer envelope of the balloon does not change with altitude, therefore the volume of the outer balloon is constant. This results in a non-constant mass of displaced air, which is where the stabilising force of this balloon comes from.

$$V_{\text{outer}} = \text{constant} \quad (9.15)$$

Again, the weights of the balloon components (W_{outer} and W_{inner}) do not change during the flight.

■ Equilibrium equation

The basic equation is the equilibrium equation, which indicates when the balloon is in equilibrium of forces. This is represented for this particular balloon by the following equation:

$$B = L + W_{\text{outer}} + W_{\text{inner}} + m_{\text{He}} + m_{\text{air}} \quad (9.16)$$

Where:

- B : weight of the displaced air by the super-pressure balloon
- W : weight of the corresponding balloon envelopes
- m_{He} : mass of the helium in the inner balloon
- m_{air} : mass of the air in the outer balloon

■ Calculation for Maximum Flight Level and Recalculation for Other Flight Levels

Determining the shape at maximum altitude is not straightforward with this type of balloon system. It is an iterative calculation with the aim of determining the optimum volume of the outer balloon. The process is carried out in the following steps with the aim of achieving a balance of forces:

1. Calculate the inner and outer balloon according to the procedure described in section 8.2, where the inner balloon has the same shape and size as the outer balloon.

2. Calculate the volume of the inner balloon according to Boyle's law using the following formula:

$$V_{\text{inner}} = \frac{V_{\text{outer}} \times p}{p + \Delta p} \quad (9.17)$$

3. Calculate the mass of the helium in the inner balloon using the ideal gas law:

$$m_{\text{He}} = V_{\text{inner}} \times \frac{p + \Delta p}{T \times r_{\text{He}}} \quad (9.18)$$

4. Calculate the mass of the air in the outer balloon:

$$m_{\text{air}} = (V_{\text{outer}} - V_{\text{inner}}) \times \frac{p + \Delta p}{T \times r_{\text{air}}} \quad (9.19)$$

5. Finally, calculate the equilibrium of the forces from the equilibrium equation 9.16. If the forces are not in equilibrium, the input parameters for calculating the balloon shape must be adjusted, which is done using a root-finding algorithm.

To bring the balloon to a different altitude, the air density must first be determined, which is calculated from the standard atmosphere and the ideal gas law. The next step is to calculate the air mass in the outer balloon, which can be determined using the equilibrium equation 9.16. To calculate the volume of the inner balloon, the total pressure inside the balloon must be known, which can be calculated by applying Dalton's law for partial pressures in the following steps:

1. *Density calculation:* The density of the gas mixture inside the balloon is computed using the formula:

$$\rho = \frac{m_{\text{air}} + m_{\text{He}}}{V_{\text{outer}}} \quad (9.20)$$

2. *Mean Specific Gas Constants for the Mixture:* This calculation uses a weighted average based on the mass fractions of the individual gases in the mixture, with each gas having its specific gas constant (r_{air} for air and r_{He} for helium). This indirectly applies Dalton's law, whereby it is assumed that each gas behaves independently and contributes to the total pressure according to its partial pressure, which depends on its quantity (in this case mass) and its specific properties. The average specific gas constant for the mixture is calculated as follows:

$$r_{\text{mixture}} = \frac{r_{\text{air}} \times m_{\text{air}} + r_{\text{He}} \times m_{\text{He}}}{m_{\text{air}} + m_{\text{He}}} \quad (9.21)$$

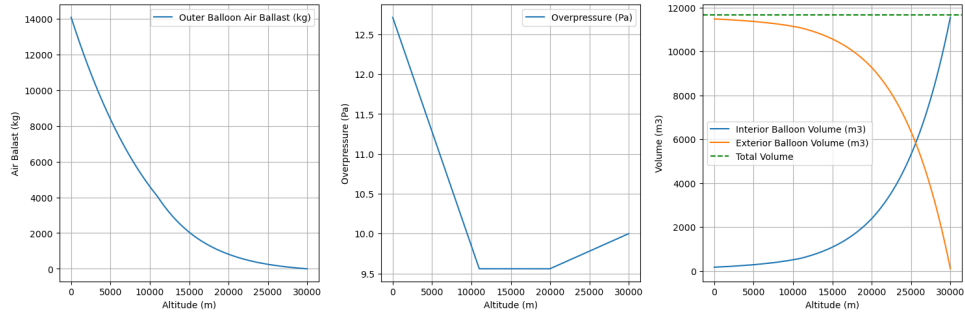


Figure 9.2: Variation of BinB air ballast system parameters across the entire altitude range

3. *Calculation of the total pressure:* Next, the total pressure of the gas mixture in the balloon is calculated using the ideal gas law:

$$p_{\text{total}} = \rho \times r_{\text{mixture}} \times T = \frac{(r_{\text{air}} \times m_{\text{air}} + r_{\text{He}} \times m_{\text{He}}) \times T}{V_{\text{outer}}} \quad (9.22)$$

4. *Calculation of internal balloon volume:* Finally the internal balloon can be determined using again ideal gas law:

$$V_{\text{inner}} = \frac{m_{\text{He}} \times r_{\text{He}} \times T}{p_{\text{total}}} \quad (9.23)$$

The following figure 9.2 shows a balloon with this arrangement at various flight altitudes with a total payload of 100 kg with a maximum design altitude of 30 000 metres and a nominal overpressure of 10 Pa. The first graph shows the weight evolution of the compressed air used as ballast. The next graph shows the balloon overpressure at different flight altitudes and confirms, even for this arrangement, that the balloon overpressure is only affected by the ambient temperature if no external forces or temperature gradients act on it. The last graph shows the evolution of the individual balloon volumes. When the volume of the outer balloon is taken as the volume taken up by the compressed air in the balloon. The graph also shows that the balloon theoretically has no minimum flight level.

■ Maximal stabilizing force

The maximum stabilization force is calculated in a similar way to the tandem balloon system, with the following differences. The overpressure of the balloon is calculated based on the total pressure p_{total} . Nevertheless, it is important

to take into consideration the increased temperature of the gases inside the balloon. The overpressure is then given by:

$$\Delta p = \frac{(r_{\text{air}} \times m_{\text{air}} + r_{\text{He}} \times m_{\text{He}}) \times (T + \Delta T)}{V_{\text{outer}}} - p \quad (9.24)$$

The mass of the air is calculated according to equation 9.19. The resulting stabilizing force is then calculated as follows:

$$F = L + W_{\text{outer}} + W_{\text{inner}} + m_{\text{He}} + m_{\text{air}} - B \quad (9.25)$$

■ Effect of helium temperature increase

In this system, the increase in temperature of the internal gases has only one effect, namely the increase in overpressure inside the balloon. The increase in temperature has no effect on the volume of the balloon, which remains constant and therefore the balloon is absolutely temperature resistant. The effect of the temperature on the increase in pressure can be seen from equation 9.24.

■ Effect of Up Wind

With this type of balloon, vertical winds also act on the balloon. However, as opposed to zero-pressure balloons, this type of balloon cannot exceed the flight altitude necessitating the release of helium; the only consequence is an increase in overpressure in the balloon. It must therefore be ensured that the balloon can withstand maximum vertical wind forces without the risk of exceeding the maximum pressure. An advantage of this balloon is not only its resilience of exceeding the maximum altitude, but also the reduction of the drag force acting on the balloon due to the single envelope. The calculation procedure follows the same steps as for the tandem system, with the difference that the final drag force only acts on one balloon and is therefore defined as in the single body drag equation 5.1.

■ Optimization

The final step is once again optimization. In this type of system, the process is simplified and focuses exclusively on finding the optimum overpressure to withstand external influences. At lower altitudes in particular, the overpressure increases significantly during the day due to the rise in internal temperature. At night, when temperatures drop considerably, the balloon must maintain a minimum overpressure to prevent a reduction in volume and the balloon from sinking. At the same time, it must withstand the heating of the gas inside the balloon during the day to prevent the maximum overpressure from being exceeded.

Chapter 10

Energy Systems

10.1 Energy Requirements

10.1.1 Energy for altitude change

Introduction. With super-pressure balloons, work must be done to compress the gas when it moves from a higher altitude to a lower one. No work is required in the reverse direction, as the compressed gas only needs to be released. This work can be calculated using the basic laws of thermodynamics as the work required to compress a certain amount of air or helium in a pressurized container.

Derivation of equations.

General equation for work done. The general equation for the work done by a pump is based on the change in enthalpy and mass flow rate of the gas:

$$\dot{W}_{\text{pump}} = \dot{m}_{\text{gas}}(h_{\text{out}} - h_{\text{in}})$$

where:

- \dot{W}_{pump} : rate of work done by the pump
- \dot{m}_{gas} : mass flow rate of the gas through the pump
- h_{out} : enthalpy of the gas at the pump outlet
- h_{in} : enthalpy of the gas at the pump inlet

Work for Isentropic Compression. For an ideal gas, the enthalpy h can be expressed as a function of temperature:

$$h = C_p T$$

where C_p is the specific heat at constant pressure. The isentropic temperature relationship is given by:

$$\frac{T_{\text{out}}}{T_{\text{in}}} = \left(\frac{P_{\text{out}}}{P_{\text{in}}} \right)^{\frac{\gamma-1}{\gamma}}$$

where γ is the ratio of specific heats.

Substituting the expressions for the enthalpy into the working equation yields the following result:

$$\dot{W}_{\text{pump}} = \dot{m}_{\text{gas}} C_p (T_{\text{out}} - T_{\text{in}})$$

$$\dot{W}_{\text{pump}} = \dot{m}_{\text{gas}} C_p T_{\text{in}} \left(\left(\frac{P_{\text{out}}}{P_{\text{in}}} \right)^{\frac{\gamma-1}{\gamma}} - 1 \right)$$

Total Energy. To find the total energy required for a given time change, the rate of work is integrated over the time:

$$\Delta E_{\text{pump}} = \int \dot{W}_{\text{pump}} dt$$

$$\Delta E_{\text{pump}} = \int \dot{m}_{\text{gas}} C_p T_{\text{in}} \left(\left(\frac{P_{\text{out}}}{P_{\text{in}}} \right)^{\frac{\gamma-1}{\gamma}} - 1 \right) dt$$

Considering $\dot{m}_{\text{gas}} = \frac{dm_{\text{gas}}}{dt}$, results in the final equation for the total energy required to pump gas into a pressurized container for a given change in mass.

$$\Delta E_{\text{pump}} = \int_{m_1}^{m_2} C_p T_{\text{in}} \left(\left(\frac{P_{\text{out}}}{P_{\text{in}}} \right)^{\frac{\gamma-1}{\gamma}} - 1 \right) dm_{\text{gas}}$$

Final Formulation. Thus, we arrive at the equation for the total energy required to pump gas into an overpressure reservoir:

$$\Delta E_{\text{pump}} = \int_{m_1}^{m_2} C_p T_{\text{in}} \left(\left(\frac{P_{\text{out}}}{P_{\text{in}}} \right)^{\frac{\gamma-1}{\gamma}} - 1 \right) dm_{\text{gas}} \quad (10.1)$$

The next step is to use equation 10.1 and, with the help of the calculations in chapter 9 showing the change in mass of compressed air or helium based on altitude, calculate the average amount of energy required to change the flight level by one meter both at night and during the day when the balloon is pressurized due to the increase in internal temperature relative to the surroundings.

These values are then used to calculate the energy required for the design of solar panel and battery.

■ 10.1.2 Energy for Payload

The payload energy requirement is an input defined by the user and is one of the basic parameters defining the design of the stratospheric balloon energetic system. This energy depends on the energy requirements based on the mission requirements. Some scientific devices, for example, which take measurements of the night sky, operate only at night when the sun is behind the horizon, while other devices only operate when the ground is illuminated and can be

observed optically. Other devices that are not affected by sunlight operate continuously.

The input for the calculation is therefore not only the required power for the payload, but also whether it operates at night, during the day or continuously. The required energy is then calculated as follows.

$$E_{\text{payload}_{\text{night}}} = P_{\text{payload}} \times t_{\text{night}}$$

$$E_{\text{payload}_{\text{day}}} = P_{\text{payload}} \times t_{\text{day}}$$

where:

$E_{\text{payload}_{\text{night}}}, E_{\text{payload}_{\text{day}}}$: night and day energy requirement of payload, respectively

P_{payload} : required power of the payload

$t_{\text{night}}, t_{\text{day}}$: time of operation during night and day, respectively

10.1.3 Other Energy Requirements

It is important to remember that the energy requirements are not only for payload and flight level change systems, but also normal operational equipment needs to have an assured power supply. These include, for example, the overnight temperature control system, GPS and flight computer and other electrical equipment. In the calculations this is provided by two types of power requirements, the first is the requirement for auxiliary power supply which needs to be provided continuously throughout the day, this power budget is used for example for the flight computer etc. The other is night heating, which only runs overnight.

The resulting energy for is calculated using the following equations:

$$E_{\text{auxiliaries}} = P_{\text{auxiliaries}} \times (t_{\text{night}} + t_{\text{day}})$$

$$E_{\text{heating}} = P_{\text{heating}} \times t_{\text{night}}$$

where:

$E_{\text{auxiliaries}}, E_{\text{heating}}$: energy requirement of auxiliary and heating systems, respectively

$P_{\text{auxiliaries}}, P_{\text{heating}}$: required power of the auxiliary and heating systems, respectively

■ 10.2 Solar Panels

■ 10.2.1 Introduction

The design of solar panels and their proper application is very important for high-altitude balloons because of the balance between needed energy supply and the weight of the solar system. This section discusses the fundamental aspects that affect the operation of solar panels and presents the basics of solar technology and the calculations used. The aim is to design a system that provides sufficient energy while minimizing the additional mass burden. The calculations consider a variety of input requirements, the energy required, different options for tracking the movement of the sun, and different technologies affecting panel efficiency and weight. The calculations also take into account a safety factor to ensure that the balloon never runs out of energy and becomes uncontrollable.

■ 10.2.2 Theoretical Background

Solar Time. All calculations will be performed in apparent solar time (AST), which differs from local standard time (LST), because it represents the time based on the apparent motion of the Sun in the sky with solar noon at the time the Sun crosses the observer's meridian.

To translate the local standard time, the date, time and longitude of the observer are needed and it is calculated as follows [11]:

$$\text{AST} = \text{LST} + ET + 4 \cdot (\text{SL} - \text{LL}) \quad (10.2)$$

where:

AST : apparent solar time

LST : local standard time

SL : longitude of the standard time meridian for the local
time zone (in degrees)

LL : local longitude (in degrees)

ET : equation of time (in minutes)

Factor 4 : converts the degree difference into minutes

(because the Earth rotates 15 degrees per hour,
which is equivalent to 4 minutes per degree)

Equation of time. Due to variations in the Earth's orbital speed around the Sun, which change throughout the year, the apparent solar time (AST) may deviate slightly from the mean time kept by a clock running at a constant frequency. This deviation, known as the equation of time (ET), is shown in Figure 10.1 and is calculated using the following equation [10]:

$$E = 229.2(0.0000075 + 0.001868 \cos(B) - 0.032077 \sin(B) - 0.014615 \cos(2B) - 0.04089 \sin(2B)) \quad (10.3)$$

, where B is the day-of-the-year angle computed as:

$$B = \frac{360}{365} \cdot (n - 1) \quad (10.4)$$

and:

- d is the day of the year, starting from January 1st as day 1.

Solar angles. In order to calculate the solar radiation incident on the surface of a solar panel, it is necessary to know the angle of the solar beam with respect to a certain point and inclined plane depending on the date, time and geographical position. This requires the calculation of key angles, which are illustrated in Figure 10.2.

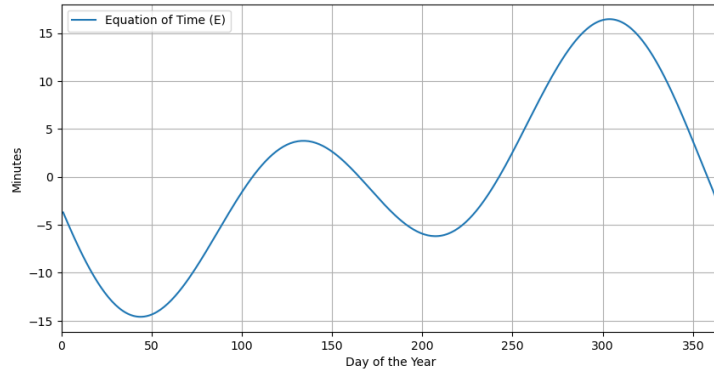


Figure 10.1: Equation of Time [10]

- **Declination:** (δ) is the angle between the plane of the equator and the line between the center of the earth and the sun. It varies seasonally due to the tilt of the earth on its axis in relation to its orbit around the sun and affects the intensity and duration of solar radiation at a particular latitude. The formula to calculate declination angle is as follows[10]:

$$\delta = 0.006918 - 0.399912 \cos(B) + 0.070257 \sin(B) - 0.006758 \cos(2B) + 0.000907 \sin(2B) - 0.002679 \cos(3B) + 0.00148 \sin(3B) \quad (10.5)$$

, where B is the day-of-the-year angle.

- **Hour Angle:** represents the angular displacement of the sun rays from the local meridian. It simply indicates how far the sun is from the highest point in the sky and is expressed [11]:

$$H = 15^\circ \times (\text{AST} - 12) \quad (10.6)$$

- **Zenith Angle:** (θ_z) is the angle between the direction of the sun rays and the vertical direction directly overhead (the zenith). Specifically, the zenith angle measures how far away the sun is from the direct overhead direction at a particular place and time and can be determined as follows[11]:

$$\theta_z = \cos^{-1} (\sin \delta \sin \phi + \cos \delta \cos \phi \cos H) \quad (10.7)$$

, where ϕ is latitude.

- **Solar Altitude Angle:** (α) measures the height of the sun rays above the horizon and is complementary to the zenith angle, i.e. it can be calculated as follows[11]:

$$\alpha = 90^\circ - \theta_z \quad (10.8)$$

- **Solar Azimuth Angle:** (γ) is the angle between the projection of the sun's rays onto a horizontal plane and a line due south or north and is calculated as follows[45]:

$$\gamma = \tan^{-1} \left(\frac{\sin H}{\cos H \sin \phi - \tan \delta \cos \phi} \right) \quad (10.9)$$

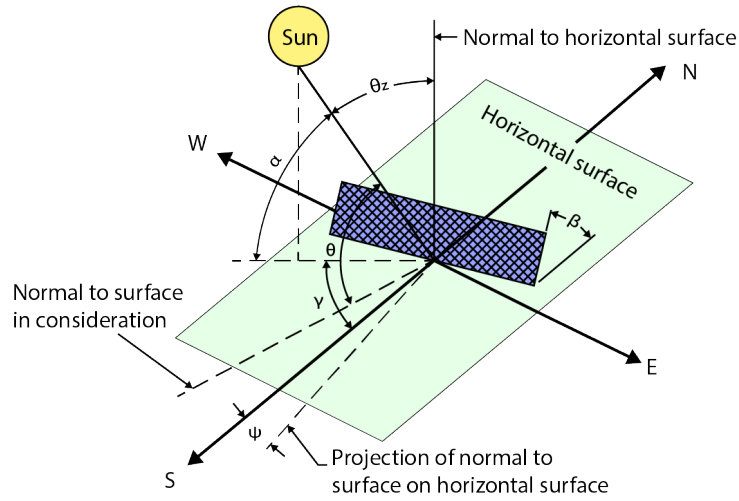


Figure 10.2: Solar angles[11]

Extraterrestrial solar radiation. Extraterrestrial solar radiation, G_0 , refers to the solar energy received outside the Earth's atmosphere, which is influenced by the distance between the Earth and the Sun. This varies slightly due to the Earth's elliptical orbit and is calculated as follows [10]:

$$G_0 = G_{sc} \left(1.00011 + 0.034221 \cos(B) + 0.00128 \sin(B) + 0.000719 \cos(2B) + 0.000077 \sin(2B) \right) \quad (10.10)$$

where:

$$G_{sc}: \text{solar constant and is equal to } 1366.1 \text{ (W/m}^2\text{) [11]}$$

Passage Through the Atmosphere. As solar radiation passes through the Earth's atmosphere, it is attenuated as a result of scattering and absorption by air molecules, water vapour, dust and other atmospheric constituents. The degree of attenuation is quantified by the mass of air, which is a measure of the length of the path that solar rays travel through the atmosphere compared to the length of the path when the Sun is directly overhead (zenith). The attenuation of solar radiation can be modelled using the Beer-Lambert law, which describes the absorption and scattering of light as it passes through the environment and is described as follows[46]:

$$G = G_0 \cdot e^{-\tau \cdot m \cdot \frac{p}{p_0}} \quad (10.11)$$

where:

τ : attenuation coefficient

m : air mass

$\frac{p}{p_0}$: fraction representing the ratio of the atmospheric pressure

at the altitude of interest (p) to the sea-level atmospheric pressure (p_0)

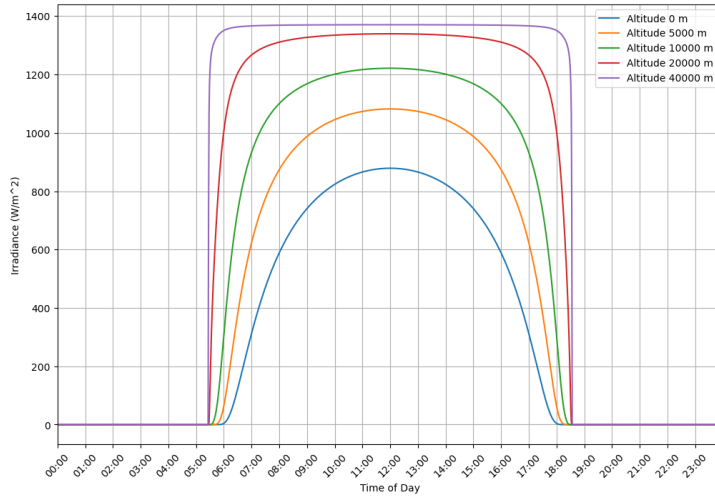


Figure 10.3: Solar Irradiance Over the Day for Different Altitudes in Prague on March 26, 2024

The attenuation coefficient is not constant and depends on several variables such as the composition of the atmosphere, aerosol and particulate matter, water vapour or the ozone layer. However, since balloons often pop up at high altitudes there is absolutely no need for such a complex calculation, since most of the atmosphere is below them and therefore a constant value of 0.3 was chosen.

The mass of air plays a critical role in determining the length of the path over which the decay occurs. The Young model is used for the calculation, which refines a simple model for calculating air mass with respect to ground curvature and refraction is defined as follows [47]:

$$m = \frac{1.002432 \cdot (\cos(\theta))^2 + 0.148386 \cdot \cos(\theta) + 0.0096467}{(\cos(\theta))^3 + 0.149864 \cdot (\cos(\theta))^2 + 0.0102963 \cdot \cos(\theta) + 0.000303978} \quad (10.12)$$

For the same reason that constant value was used for the attenuation coefficient, the air mass has almost no effect at high altitudes and solar radiation can be considered almost unattenuated by the atmosphere. The solar irradiation as a function of altitude using the calculation presented for Prague on March 26 is shown in Figure 10.3.

Radiation on tilted surface. The effectiveness of a solar panel also depends on its orientation in relation to the sun rays. The irradiance received by an inclined surface can be calculated as follows:

$$G_\theta = G \cdot \cos \theta \quad (10.13)$$

, where θ is the incident angle.

■ 10.2.3 Calculation of Solar Panel Design Parameters

The design process for solar panels involves determining the area required to meet the energy needs of the balloon system without excessively increasing the weight. Using the formulas and environmental information that has been presented earlier, the panel can be modelled to ensure maximum efficiency and energy production throughout the duration of the mission.

The input parameters are the technical parameters of the panel such as efficiency, areal density and sun tracking capabilities, with additional parameters such as the position of the balloon expressed in latitude and longitude, the lowest flight altitude and the departure date with the expected mission duration.

Day with lowest solar radiation: The first step is to design the system for the most unfavourable conditions, i.e. to fly at the lowest altitude during the day with the least solar radiation.

The steps to determine the day with the lowest solar radiation are summarised as follows:

- For a given set of dates D and latitude λ calculate the solar declination δ for each day d in D .
- If $\lambda > 0$ (Northern Hemisphere), find the day d_{\min} with the least amount of sunlight by selecting:

$$d_{\min} = \arg \min_{d \in D} \delta(d)$$

- If $\lambda \leq 0$ (Southern Hemisphere), find the day d_{\max} with the least amount of sunlight by selecting:

$$d_{\max} = \arg \max_{d \in D} \delta(d)$$

Here, d_{\min} is the day with the lowest solar radiation in the Northern Hemisphere, and d_{\max} is the day with the the lowest solar radiation in the Southern Hemisphere.

Power Curve: The next step is to determine the performance curve of an ideal solar panel based on its tracking capability. Three tracking options are considered in the calculations:

1. *No tracking:* the panel cannot track the sun and is only set as a horizontal plane. While on the ground it can be fixed at an angle to increase solar gains, this would not work for a balloon as the balloon can rotate around a vertical axis. Often the panels are therefore set at angles to all sides to increase solar gains. However, here for the purpose of calculation the panel is set as a horizontal plane. The resulting angle of incidence of solar radiation at a given time corresponds to the angle of the zenith.
2. *1 axis tracking:* the panel can be tilted along a single axis. In the case of a balloon, this axis is vertical, where the panel can be rotated most easily. This maximises solar yields compared to the no tracking option. The angle of incidence is calculated as:

$$\theta = \alpha - \beta \tag{10.14}$$

, where β is tilt angle of the solar panel and is calculated based on the hemisphere:

$$\begin{aligned} \text{For Northern Hemisphere: } & \beta = (90 - \lambda) + \delta, \\ \text{For Southern Hemisphere: } & \beta = (90 + \lambda) - \delta. \end{aligned}$$

3. *2 axis tracking:* the panel can be tilted and also rotated around the vertical axis. This guarantees optimum settings at all times and the irradiation of the panel is the same as for an ideal panel, i.e. the angle of incidence is 0.

Based on the altitude, the date with the lowest solar radiation, the latitude and the tracking method, the solar radiation on an ideal panel during the entire day is then calculated using the equation 10.13. This calculation provides the power profile of an ideal tilted panel with an area of 1 m². The amount of energy gained from this panel during the day is then calculated by integrating from 0h to 24h:

$$E_{id} = \int_0^{24} P_{id}(t) dt \tag{10.15}$$

where $P_{id}(t)$ represents the power output of the ideal panel at time t . The area of a non-ideal plate that takes losses into account is then calculated as follows

$$A_{real} = \frac{E_{req} \times k_{panel}}{E_{id} \times \eta_{panel}} \tag{10.16}$$

- **Maximum Depth of Discharge (DOD):** This defines the maximum proportion of the battery capacity that can be utilised.
- **Safety Coefficient:** Ensures that the battery is operated below its maximum capacity to ensure safety during critical operations.

Battery pack weight calculation. To determine the total weight of the battery system required for a particular application, both the required energy capacity and the maximum power output must be taken into account.

- Weight based on capacity:

$$W_C = \frac{C_{\text{req}} \times \frac{k_{\text{battery}}}{1-\text{DOD}}}{\text{Specific Energy}}$$

- Weight based on power:

$$W_P = \frac{P_{\text{req}} \times \frac{k_{\text{battery}}}{1-\text{DOD}}}{\text{Power Density}}$$

- Total weight is the maximum of the two weights:

$$W_{\text{total}} = \max(W_C, W_P)$$

This calculation ensures that the battery fulfils both the energy and power requirements without exceeding the battery's capabilities.

Chapter 11

Simulation Environment Setup

11.1 GFS Forecast Parameters Retrieval

An important part for the trajectory prediction model is the download of weather forecast data from the GFS model mentioned in Chapter 3.3. This is done by automated downloading of the data from National Oceanic and Atmospheric Administration GrADS Data Server[13] and then selecting the parameters relevant to the simulation and compressing them, another important factor is the 4d interpolation between data points so that the individual parameters match in time, pressure altitude, latitude and longitudinal position. The GFS data retrieval is based on following projects: EarthSHAB [48] and CUSF [49]

11.1.1 GFS Data Structure

The data set from the Global Forecast System (GFS) with a resolution of 0.25 degrees covers a global grid from 0°E to 359.75°E (comprising 1440 points) and from -90°N to 90°N (comprising 721 points). It extends vertically from 1000 hPa to 0.01 hPa over 41 levels, with an 3 hours temporal resolution of 129 time points starting at 0:00 on the first day of the dataset.

This dataset includes a comprehensive range of 215 meteorological variables.

These variables include surface conditions such as temperature, precipitation and cloud cover as well as upper atmospheric phenomena such as vorticity, altitude-specific wind speeds and atmospheric water content. The variables are either specified for specific atmospheric levels or averaged over specific layers or the entire atmosphere. For example, detailed wind speeds are available over several pressure levels, and different precipitation types and cloud cover are given for the surface and different atmospheric layers. In addition, this file contains characteristic measurements such as soil moisture at different depths, ice growth rates, vegetation cover, relative helicity of the storm and convective available potential energy in different atmospheric layers.

■ 11.1.2 Data compression

For flight path prediction application, it is crucial to select only the necessary parameters to avoid excessive data sizes. The selected key parameters include:

- `dzdtp`: Vertical speed (geometric) [m/s]
- `ugrdp`: U-component of the wind [m/s]
- `vgrdp`: V-component of the wind [m/s]
- `hgtpr`: Geopotential height [gpm]
- `tmppr`: Temperature [K]

To further reduce the file size, only the area that was covered during the balloon flight and within the specified time period is selected. These restrictions have a significant impact on the subsequent loading of the data from the file. The resulting meteorological data is saved in NetCDF4 format and compressed with zlib, which further reduces the file size considerably.

Downloading the data can be quite slow. For example, downloading an area with a latitude and longitude of 20 degrees at 5 different time points covering a 15-hour interval takes about 1 minute. The resulting file size is about 24.8 MB.

11.1.3 Positional indices

When selecting position indices within a specific range, it is important to consider the scenarios in which the range exceeds the maximum or minimum longitude or latitude position. For example, if the starting position is near the prime meridian, it is very likely that areas on both the left and right side of the spectrum will be selected. This is because the indices start at prime meridian and extend eastwards. You must also be careful to select the correct areas when flying over the poles.

The Figure 11.1 shows the temperature of the selected area at a pressure of 10 Pa. The area starts at the prime meridian (longitude 0) with a latitude of 80 and extends 25 degrees in each direction. This results in a data overflow over the North Pole and over the prime meridian. The Panoply tool [12] was used to visualise the downloaded data from the developed script.

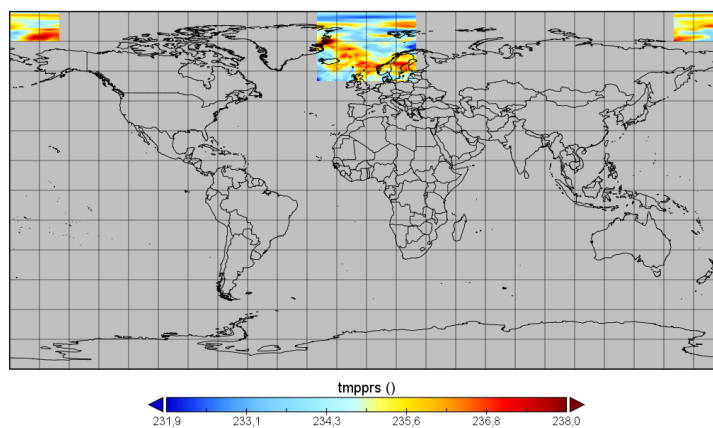


Figure 11.1: Temperature forecast data for area near south pole at 10 Pa pressure altitude visualised in Panoply[12] and downloaded using developed software from GFS GrADS Data Server[13]

11.1.4 Pressure levels

The downloaded GFS weather forecast model has a total of 41 pressure levels ranging from 1000 hPa to 0.01 hPa, of which a large part is in the high pressure range, which is not important for the balloon flight, only important for take-off or landing. Figure 11.2 shows the different pressure levels of the weather forecast model, while also indicating the flight range in which high altitude balloons may normally occur. The number of pressure levels used

for forecasting is higher, as mentioned in Chapter 3.3, but the data are then compressed to only these 41 levels.

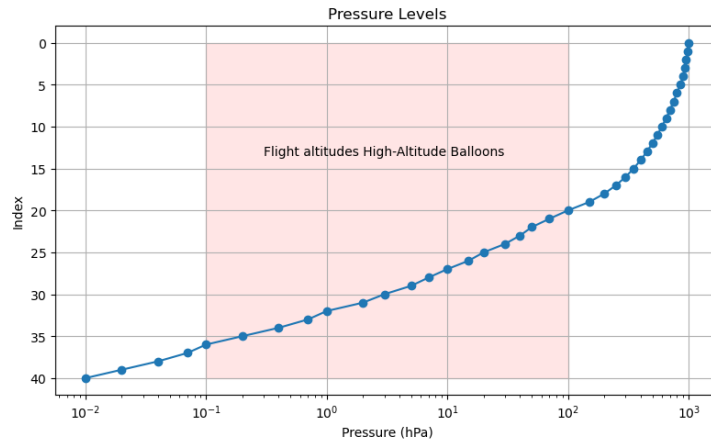


Figure 11.2: Pressure Levels of GFS model with indicated range of altitudes for high-altitude balloons

11.2 Simulation Modeling

Simulating the behaviour of the proposed balloon in an environment based on weather forecast data involves several parts. The first is the interpolation of the forecast model data for the current situation. The second part is the interaction of the wind direction and strength with the balloon and the kinematic model of the balloon, and the next part is the model of the thermal environment of the balloon and the change of parameters during compression and expansion of gas in and out of the balloon. Finally, it involves the possibility of balloon control and energy management.

11.2.1 Data interpolation

The downloaded data has a temporal resolution of 3 hours, 0.25 degree spatial resolution and variable resolution between pressure levels and its needed to get the data for each balloon state as quickly and efficiently as possible. So it is a 4d interpolation in time and space. Linear interpolation is adopted as the interpolation due to its simplicity and efficiency, however it would be useful to find a faster and more accurate solution.

11.2.2 Kinematic model

The presented kinematic model is based on Sobester et al. (2014) [50], Carlson and Horn (1983) [39] and Jeffery et al. (2019) [5]. It is convenient to divide the model into a horizontal plane defined by latitude and longitude and a vertical axis defined by altitude. The underlying equations are as follows:

Velocity Components The model is influenced by wind conditions which are a function of both position (pos): (altitude (z), longitude (v), latitude (w)) and time (t).

- $u_{wind}(u, v, z, t)$: Wind velocity component in the latitude direction .
- $v_{wind}(u, v, z, t)$: Wind velocity component in the longitude direction.
- $w_{wind}(u, v, z, t)$: Wind velocity component in the vertical direction.

The relative velocity between the balloon and the wind is:

$$\begin{aligned} u_{rel} &= \frac{du}{dt} - u_{wind}(pos, t) \\ v_{rel} &= \frac{dv}{dt} - v_{wind}(pos, t) \\ w_{rel} &= \frac{dz}{dt} - w_{wind}(pos, t) \end{aligned}$$

The drag force components act in the opposite direction to the relative velocity. The drag force in each direction can be expressed based on equation 5.1 for horizontal motion and the equation 9.13 for vertical motion for tandem balloon system.

Equations of Motion are defined as:

Vertical Motion: The equation for vertical movement for a given type of balloon system and includes the gravitational force, the buoyant force and the drag force and is given by:

$$m \frac{d^2 z}{dt^2} = \rho_{atm}(z) \cdot V \cdot g - m \cdot g - \frac{1}{2} \cdot C_d \cdot \rho_{atm}(z) \cdot A \cdot \left(\frac{dz}{dt} - w_{wind}(pos, t) \right) \cdot \left| \frac{dz}{dt} - w_{wind}(pos, t) \right| \quad (11.1)$$

Latitude Motion: The equation for latitudinal motion includes only the air drag effects.

$$m \frac{d^2 u}{dt^2} = -\frac{1}{2} \cdot C_d \cdot \rho_{atm}(z) \cdot A \cdot \left(\frac{du}{dt} - u_{wind}(pos, t) \right) \cdot \left| \frac{du}{dt} - u_{wind}(pos, t) \right| \quad (11.2)$$

Longitude Motion: The equation for longitudinal motion includes only the air drag effects.

$$m \frac{d^2v}{dt^2} = -\frac{1}{2} \cdot C_d \cdot \rho_{\text{atm}}(z) \cdot A \cdot \left(\frac{dv}{dt} - v_{\text{wind}}(\text{pos}, t) \right) \cdot \left| \frac{dv}{dt} - v_{\text{wind}}(\text{pos}, t) \right| \quad (11.3)$$

, where:

- z : Altitude above sea level (m)
- u : Latitudinal position (m)
- v : Longitudinal position (m)
- m : Total mass of the balloon system, includes also virtual mass of air ballast
- V : Volume of the balloon, can be constant or variable depending on system type
- A : Cross-sectional area of the balloon sphere
- C_d : Drag coefficient
- $\rho_{\text{atm}}(z)$: Atmospheric density at altitude z
- g : Gravitational acceleration taken as constant
- $\frac{dz}{dt}$: Balloon vertical velocity
- $\frac{du}{dt}$: Balloon latitude velocity component
- $\frac{dv}{dt}$: Balloon longitude velocity component
- $u_{\text{wind}}(z, t)$: Wind velocity component in the latitude direction as a function of altitude and time
- $v_{\text{wind}}(z, t)$: Wind velocity component in the longitude direction as a function of altitude and time
- $w_{\text{wind}}(z, t)$: Wind velocity component in the vertical direction as a function of altitude and time

All the parameters were already discussed in previous chapters. Notably the drag force for vertical movement is calculated differently than for horizontal movement for tandem balloon system type, in shown equations are simplified for general balloon system. Also note that Coriolis effect was not taken into account. Due to negligible effect. It will show in every instance in the air movements, that effect the balloons trajectory.

■ 11.2.3 Thermal model

The thermal environment has been extensively discussed in the chapter 5.2. That chapter already identifies problems with current models that focus solely on the thermal dynamics of a zero-pressure balloon and explicitly do not consider gas exchange with the surrounding environment and between balloons. These issues have emerged as quite serious when attempted to be implemented and the implementation thus wasn't successful. The failed implementation of these models can be attributed to their respective inability to integrate complex interactions such as heat and compressed air exchange with the environment and carrier gas exchange between multiple balloons; integrating gas leakage dynamics, compressor operation and its influence of thermal states. Retrieving thermal data from weather prediction models adds further complexity. In addition, factors such as the shadowing characteristics of individual balloons and the effect of relative velocity on internal temperatures are critical but other important neglected aspects by the current thermal models.

■ 11.3 Gas Leakage

■ 11.3.1 Introduction

In high-altitude balloon applications, especially for long-duration flights, the leakage of lifting gas through the balloon envelope is of significant importance. Lifting gas leaks more in super-pressure balloons, however, even zero-pressure balloons slowly lose carrier gas. It is therefore necessary to compensate for this loss. While in a super-pressure balloon the leakage is compensated passively by reducing the overpressure in an zero-pressure balloon, due to the leakage of gas, the volume is reduced and hence other compensation is needed, for example by releasing ballast to compensate for the reduction in buoyant force. This chapter discusses the main mechanisms of gas leakage in such balloons, including diffusion through the balloon material, permeation and losses through microholes, and presents the calculations used, which are based on [51] and [52].

11.3.2 Mechanisms

1. **Permeation:** Permeation refers to the movement of gas molecules through the balloon material itself. This process consists of three steps: Adsorption of gas molecules on the inner surface, diffusion of these molecules through the material and desorption on the outer surface. The driving force for permeation is the concentration gradient of the gas through the balloon material, from a higher concentration inside the balloon to a lower concentration outside.
2. **Leakage Through Micro Holes:** Micro-holes are small perforations in the balloon material that can be caused by manufacturing defects, environmental damage such as UV radiation or low temperatures, or wear and tear. The lifting gas passes through them due to the pressure difference.

11.3.3 Calculations

Pressure Difference: The first step is to calculate the Helium overpressure in the balloon between the envelope and the outside environment. For an equal pressure balloon, where the pressure inside the balloon is equal to the pressure outside, it would seem that there is no overpressure. However, this is not the case, there is only zero overpressure at the bottom of the balloon at float altitude, but as we go up the balloon, the overpressure increases due to the difference in density between the lifting gas and the ambient air. Using the equation 8.9, we can derive the aerostatic pressure as a function of height from the bottom of the balloon. From the equation, it can also be derived that for a pressurized balloon, one can simply add the overpressure.

To simplify the calculation, the overpressure is taken as the average overpressure at the center of the balloon.

Permeation: The permeation rate can be simplified to a simple equation using Fick's first law. Taking into account that the helium concentration in the air is close to 0, that the main driving force is pressure difference and that the permeation coefficient is measured for the given film and its thickness and its dependence on temperature is not taken into account, the permeation rate is given by the following equation:

$$\Delta m_{\text{permeation}} = -P \times A \times \Delta p \times \Delta t \quad (11.4)$$

, where:

P : permeability coefficient

(kg/m² · s · Pa)

A : balloon envelope surface area

Δp : average pressure difference between balloon gas and ambient air

Δt : time step

Microholes: In order to simulate the leakage of carrier gas through a defect in the envelope, it is first necessary to simulate how quickly these micro holes form in the first place. For the sake of simplicity, it is assumed that the defects form linearly over time, with the balloon already showing some defects at launch due to manufacturing imperfections and also due to wear during transportation and handling. The equation that represents the number of cracks in the balloon is therefore as follows:

$$A_H = A_{H_0} + r_{\text{formation}} \times t_{\text{launch}} \quad (11.5)$$

, where:

A_H : total area of holes at given time

A_{H_0} : initial micro-holes area at launch

$r_{\text{formation}}$: rate of formation of micro-holes

(m²/s)

t_{launch} : time since launch

The gas leakage due to cracks in the envelope can then be calculated as the flow through orifice as follows:

$$\Delta m_{\text{microholes}} = -D \times A_H \sqrt{2 \times \Delta p \times \rho_{\text{He}}} \times \Delta t \quad (11.6)$$

, where:

D : discharge coefficient

ρ_{He} : density of Helium inside the balloon

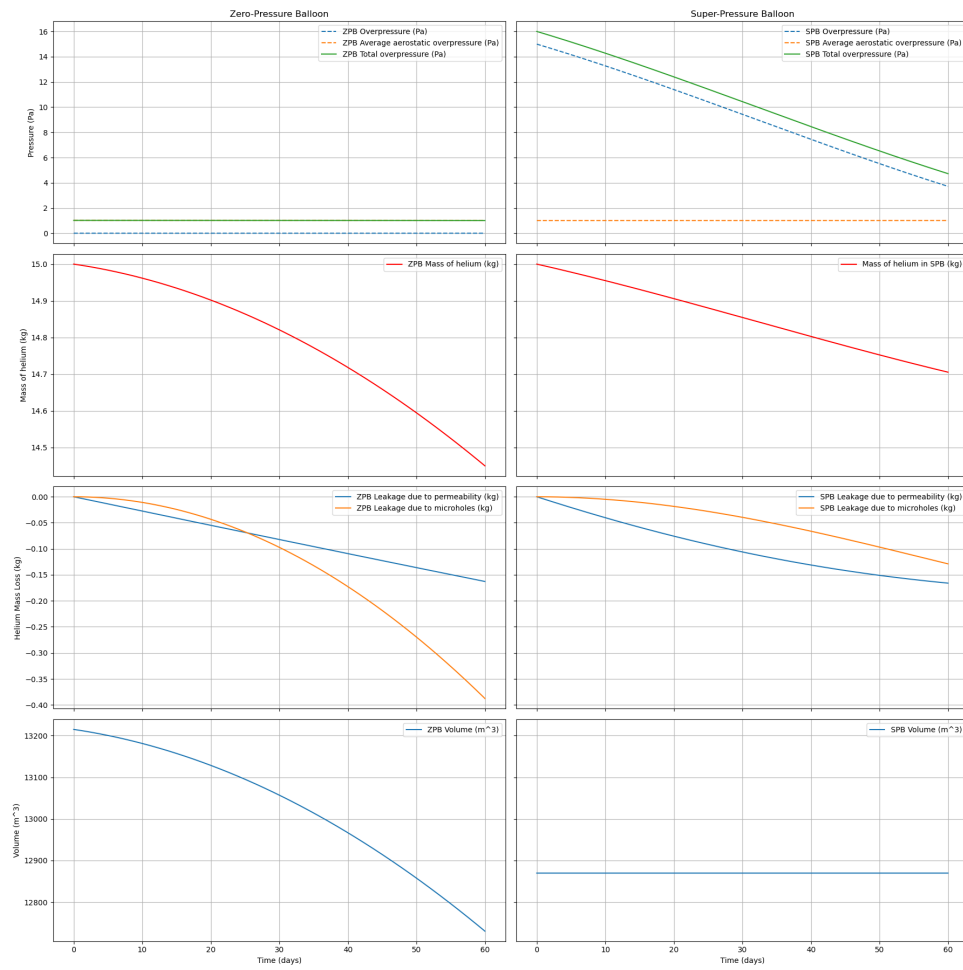


Figure 11.3: Comparison of gas leak in SP and ZP balloons over 60 days period

Plots: The figure 11.3 shows two balloons and how they are affected by the loss of carrier gas over 60 days. The first is a zero-pressure balloon, which has a noticeable drop in volume that must be compensated by ballast release. The second is the super-pressure balloon, which exhibits a decrease in overpressure. The graphs are idealized for illustration, so that the change in balloon overpressure during the day and night is not taken into account. Note that the material used in SP balloon is usually thicker and more resistant to gas permeation and micro-holes formation.

Part IV

Software Tool Development and Testing

Chapter 12

Development of Software Tool

12.1 Requirement Specifications

Programming language selection

Choosing the right language is an important aspect. Because the proposed software must have a user-friendly environment that makes it very easy to enter parameters and visualize the results. In addition, it must also be able to store and retrieve project data, validate input parameters and provide detailed descriptions of the inputs. Initially, Matlab was considered for software development because of its robust computational and simulation capabilities. However, due to expensive licensing, limited availability outside of academic settings, as well as other limitations, it was eventually abandoned. The original software designs shown in Figure 12.1, designed as a coursework during master's degree, was developed in Matlab and was able to design single balloon shape and its flight path in given wind vector field. However the original software, encountered significant limitations, including limited GUI capabilities and long load times or instabilities in balloon shape design. Python was therefore chosen as an alternative programming language because it is available as an open source program, supports extensive libraries, and provides a user-friendly environment.

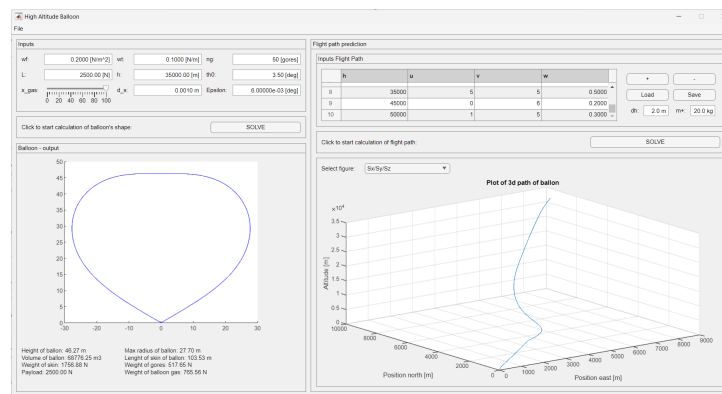


Figure 12.1: Original Software in Matlab

Structure of the software:

The software is divided into two main sections: one for the design and optimization of the stratospheric balloon system and another for the simulation of its flight.

Design and optimization: This component addresses all relevant factors required for the design of an optimal stratospheric balloon system. These include payload specifics, mission characteristics such as duration and launch date, desired flight altitudes, control options and resistance to external disturbances. Other important parameters are the materials used for the balloon and the technologies for batteries and solar cells. The design process aims to strike a balance between computational speed and accuracy to ensure timely yet precise results for the system and its components.

Simulation environment: In this part the behavior of the balloon is simulated and its trajectory is shown. The calculations take into account air resistance, heat exchange with the environment and use meteorological data from ECMWF or NOAA. The simulation also calculates the available energy in the batteries and enables the simulation of gas leakage from the balloon envelope. Manual controls via user commands or integration with a control algorithm are also possible to enable dynamic test scenarios.

■ Testing and validation

The final critical aspect of the software involves rigorous testing of the software, including limit and ad hoc testing. These tests are essential to verify the robustness and reliability of the system under different operating conditions and to ensure that the software tool is both robust and effective for practical use in designing stratospheric balloons and their flights.

■ 12.2 Design of the Optimal Stratospheric Balloon System

The objective is a software-controlled design of a stratospheric balloon system that can operate efficiently under predefined conditions with an appropriately optimized combination of balloon physics, solar cells and batteries. In this approach, the system design is divided into three main parts, each of which is handled by specific classes and functions in the code:

1. Stratospheric Balloon Design
2. Balloon System Design
3. Overall Balloon System Design

The first part aims to design only the envelope of the balloon to suit the given requirements and loads. The second part aims to design the balloon system for the mission, but without panels and batteries. The last part aims to design a complete system with energy management.

Stratospheric Balloon Design. The *Balloon* class is the lowest class of balloon system calculation and one of the most important. It is used only to design a single balloon based on the inputs from the *OptimizeBalloon* class to ensure that the resulting balloon meets specific requirements. Its calculations are based on those in Chapter 8.2.

Balloon System Design. The *OptimizeBalloon* class is a computationally more complex class than the *Optimize* class. It is used to optimize different

types of balloon systems, but does not consider solar panels or batteries. When created, it creates an initial state of balloons, which it then optimizes based on an optimization strategy that is unique for each type to achieve the most optimal system. It includes calculations to find the minimum flight level, to find the air drag forces and the maximum stabilizing force or energy required to change the flight level. This class already contains more complex calculations based on Chapter 9.

Overall Balloon System Design. The *Optimize* class is the main class used for the overall design and is directly created in the *ParameterModel* from the MVP architecture, while inside the actual optimization it creates the *OptimizeBalloon*, *SolarPanel* and *Battery* classes. This main class contains the calculations for the amount of energy required, while receiving data from the other classes to optimize so that the energy required matches the energy supplied. These calculations are based on Chapter 10. This corresponds to the optimization function. The class also prepares data for some graphs. Thus, this class manages only one optimization calculation and is more for the overall management of the other classes.

Solar Panels and Batteries. The *SolarPanel* class is used to calculate the parameters associated with solar panels. These include, for example, the power curve, as well as its weight and area, based on parameters from the main *Optimize* class. The calculations are based on chapter 10.2. The *Battery* class is used to calculate battery parameters based on input parameters from the main *Optimize* class. The calculations are based on Chapter 10.3.

The optimization environment is illustrated in Figure 12.2. The screen is divided into input and output sections. On the left side are most of the input fields that need to be filled in. The user can begin the optimization by clicking on the calculate button, and if all fields are filled in and are within the given limits, the optimization process commences. Once the optimization is complete, the right side of the output is filled with all the output parameters, plots of the shape of each balloon, and many other plots along with a summary report and a picture of the balloon system type.

12.3 Design of Simulation Environment

The simulation environment is shown in Figure 12.3. The screen is divided into two parts. The left part contains the flight specification. Where it is

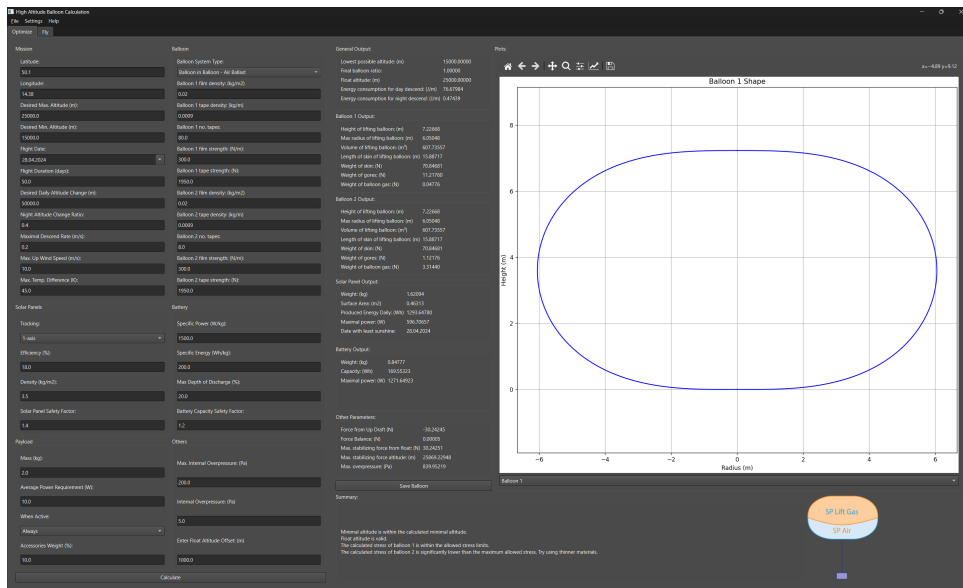


Figure 12.2: Optimization environment with input and output data

possible to enter all the necessary parameters to simulate the flight trajectory and balloon behavior. Below is the option to load an already generated and saved balloon system, along with the basic parameters of the loaded balloon system, allowing the user can check if this is indeed the balloon he wants to simulate. As with the optimize window, there is a simulate button at the very bottom. Right side is prepared for the simulation output graphs. Once the simulation is initiated, the inputs are checked first and then the simulation can proceed. The first step of the simulation is to check if a simulation has already been run in the same area and time period and if the meteorological data has already been downloaded. If not, the download and storage of the meteorological data starts. This can take up to several minutes for a longer flight. Once the data has been downloaded, the simulation starts. However, this has not been implemented for reasons already described in previous chapters. Nevertheless, large supporting parts, downloading and processing of simulation data are prepared and implemented for it. Simulation has also option to load control system, but this feature is for the same reason disabled for now.

12.4 User Interface and Software Usability

The user interface (UI) and usability of the stratospheric balloon simulation tool software are carefully designed to offer a user-friendly and intuitive environment for interaction. This is an important element that facilitates the

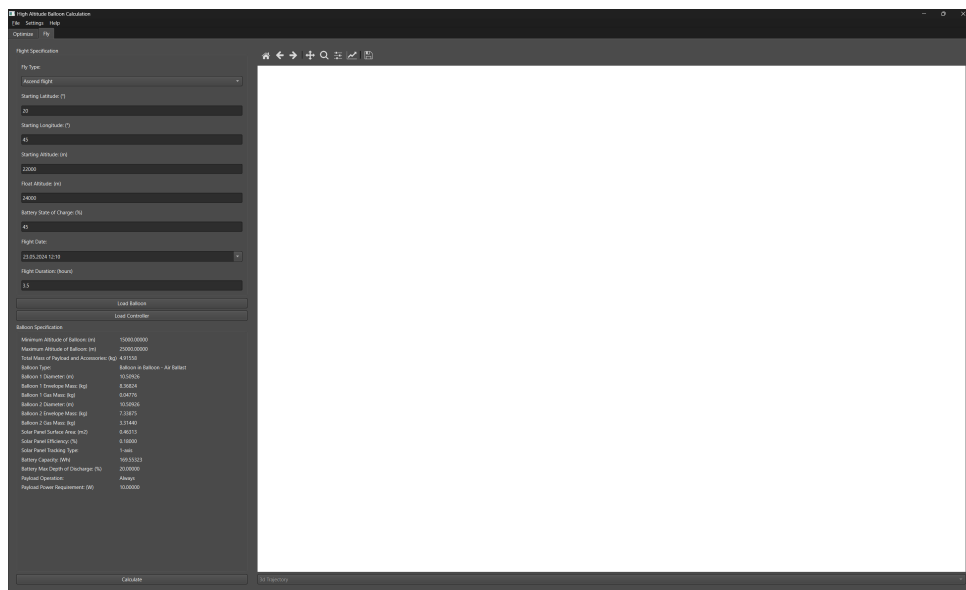


Figure 12.3: Simulation environment with loaded balloon data and input parameters

user friendliness of the designed software. This chapter discusses the implementation details, using the Model-View-Presenter (MVP) design pattern and PyQt6 to provide a robust and efficient user interface.

12.4.1 Model-View-Presenter architecture

The software tool features an MVP architectural pattern that enhances separation of concerns, which simplifies development and maintenance and improves user interaction. This model was recommended by Huber, 2023 [53], as a suitable model for use with PyQt and preferred over the MVC model. The MVP pattern is implemented through three main components:

- **Model** manages the logical structure and data of the application without a direct connection to the user interface. It manages the core functions such as the processing of simulation data, balloon optimization algorithms and environmental parameters. The model communicates with the presenter to reflect any changes to the underlying data or state of the application.
- **View** is created with help of PyQt6 and is responsible for the graphical and visual representation of the application. It displays the data provided by the presenter and sends user commands back to the presenter.

- **Presenter** acts as an intermediary layer between the model and the view. It responds to UI actions captured by the view, manipulates data using the model and manages the state of the UI. The presenter updates the view with new data, ensuring that the UI reflects the latest states without the view having to process any business logic.

■ 12.4.2 Implementation of PyQt6

PyQt6 was chosen for its comprehensive range of features, its ability to simplify the development of cross-platform GUI applications and for its wide distribution, making it easy to develop applications and to search for best practices on the Internet. It provides bindings to the Qt6 C++ library, which is widely recognized for its robust tools for creating complex user interfaces.

■ Main Windows and Dialogs

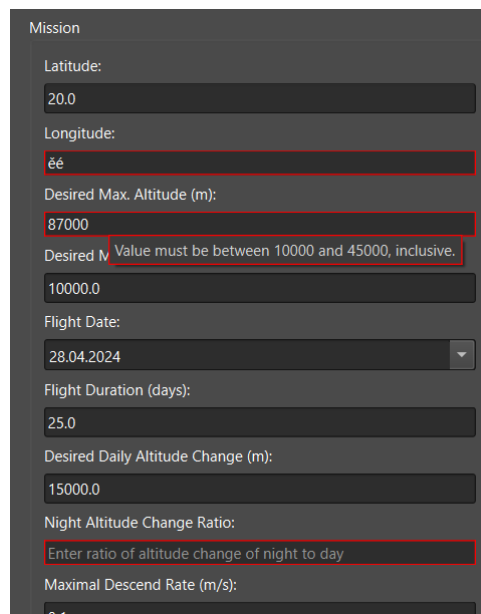
The main control panel, which is designed as a QMainWindow, serves as the central navigation hub. It contains a menu that provides access to various function modules such as simulation settings, save and load or help.

The two main subwindows, corresponding to optimization and simulation, are designed as separate classes OptimizeTabView(QWidget) and SimulationTabView(QWidget) and are selected via tab widget (QTabWidgets). Other windows such as settings, help or save and load are managed via QDialogs that focus user interactions on specific tasks and are only temporary.

■ Accessibility and Usability Enhancements

PyQt6 provides a number of widgets - including QComboBox, QDateEdit, QPushButton and QLineEdit - which are used extensively to enable effective user interactions within the simulation tool. These widgets allow users to enter and modify data seamlessly.

To assist users with correct data entry, tooltips are integrated into the QLineEdit fields to provide guidance on the expected input format and



The screenshot shows a 'Mission' configuration window with several input fields. The 'Longitude' field contains 'éé' and is highlighted with a red border. The 'Desired Max. Altitude (m):' field contains '87000' and is also highlighted with a red border. A tooltip is visible over this field, stating 'Value must be between 10000 and 45000, inclusive.' Other fields include 'Latitude:' (20.0), 'Desired Min. Altitude (m):' (10000.0), 'Flight Date:' (28.04.2024), 'Flight Duration (days):' (25.0), 'Desired Daily Altitude Change (m):' (15000.0), 'Night Altitude Change Ratio:' (with a tooltip 'Enter ratio of altitude change of night to day'), and 'Maximal Descend Rate (m/s):' (0.1).

Figure 12.4: Interactive Error Highlighting: Tooltip for Input Correction Upon Mouse Hover

content. To check the validity of the data entered, the application also performs comprehensive checks when the user starts a calculation. Any input that does not meet the required specification is clearly highlighted with messages explaining the errors. This feedback mechanism not only ensures data integrity, but is also the first step towards avoiding errors in subsequent calculations and also improves the user-friendliness of the application by helping users to correct their entries efficiently. Figure 12.4 illustrates the highlighting of a bad input with tooltip. A further improvement to the user-friendliness of the application is to restrict interaction with fields that should not be changed under certain conditions. For example, interaction with the entire output page is disabled until the calculation has been successfully completed. Similarly, input fields are disabled during the calculation.

■ 12.4.3 Saving and Loading Functionality

The software offers comprehensive storage and retrieval functions that improve user workflows. PyQt6's `QFileDialog` allows users to save the current project status in JSON format. This format captures all important parameters and settings and allows for easy data management and transparency, as JSON files can be edited directly in any text editor due to their text-based structure.

However, it is important to note that the JSON format is only used for

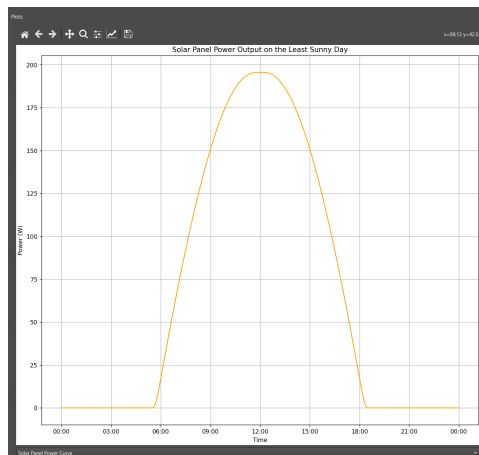


Figure 12.5: Optimize Tab Plot Layout Showing Solar Panel Power Output on the Least Sunny Day

saving input parameters. While this allows for easy changes outside of the application, the output data cannot be saved directly, so users will need to perform the calculations again after loading a project to regenerate the output data.

However, once a balloon design is optimized, it can be saved independently so that it can be used in future simulations. This functionality is particularly beneficial as it allows users to design multiple balloon configurations in advance - for example, creating five different balloon designs - and then test each one in the simulation environment. This pre-design and testing feature greatly simplifies the process of evaluating different balloon designs under simulated conditions.

■ 12.4.4 Plots

A key feature of the software's output functionality is not only textual data, but also comprehensive graphical representations. The software offers the possibility to switch between different plots via a drop-down menu. In addition, each plot is interactive and allows changes such as editing, scrolling, zooming and exporting via an integrated toolbar. An example of this functionality can be seen in Figure 12.5, which shows the layout of a solar panel power curve plot for optimization tab. Both the toolbar and the drop-down menu are clearly visible here. To display these plots, the software uses the PlotCanvas class, which is derived from the FigureCanvasQTA class from the matplotlib library.

Chapter 13

Testing and Validation

13.1 Testing

To ensure the reliability, accuracy and user-friendliness of the software, several test methods designed to test both the computational functionality and the UI were introduced. Testing this simulation software is not an easy task, since by the very nature of optimization, it is not always possible to find a solution and often it is hard to estimate in advance from the input parameters whether a solution exists. It is thus necessary to take this into account when designing the tests. The test selection and application were guided by the resource authored by Jorgensen and DeVries (2022) [54]

13.1.1 Selection of Test Methods

To ensure comprehensive software testing, several methods were selected based on their effectiveness in identifying bugs, verifying features, and assessing performance in different scenarios. For capacity reasons, it is not possible to test all functionality and all possible inputs. Therefore, it is necessary to test efficiently, and to test as many of the critical areas of the application as possible with as few tests as possible. For this reason, the following methods were selected:

- **Ad hoc testing:** This method was chosen for its flexibility and ability to quickly identify unexpected problems during the development process. It allowed to examine the software freely without predefined test cases and find unexpected bugs.
- **Limit testing:** This method was chosen to evaluate the performance and stability of the software under extreme conditions. It helps to identify the boundaries in which the software works properly and when the software is already less stable and it is better to avoid such computation.
- **Unit testing:** Unit tests have been written for specific functions to ensure that they produce correct outputs. This method was necessary to verify the correctness of individual critical components before integrating them into a larger system.

■ 13.1.2 Ad-Hoc Testing

Ad hoc testing is informal and random testing of software without predefined test plans or documentation. The main goal was to discover bugs that were not anticipated. At the same time, it is testing that has been ongoing throughout the development process. This testing was implemented on almost any functionality of the application and was performed with more or less random inputs, while revealing probably the largest number of bugs that could be fixed immediately and did not introduce error propagation into further calculations.

At the end of the development, Ad-Hoc testing was applied again, where the user interacted with the software by performing various tasks such as entering different data inputs, navigating through the interface and using different features. This method helped to identify UI issues, interface glitches and logic errors that would not have been caught in structured testing methods, mostly due to their very narrow testing scope.

Results. During the development process, a large number of bugs were discovered by applying this method. Some of these include, for example, incorrect data entry into the calculation class, which was resulting in unusual results. Or, for example, poor UI behavior, where when the start button was clicked, the entire software would get stuck when the calculation failed. It also revealed a problem with saving the data for a calculation if it was not valid. Therefore, data validation was set up for all input fields. If all the fields are not within the range and of the correct type, the calculation cannot continue and no data can be saved. At the end of development, Ad-Hoc testing was

performed again several times. And minor problems in the stability of the optimization were discovered, where no solution can be found when unique input parameters coincide. However, this is not a bug, as the user is notified of the wrong calculation and has the possibility to modify the inputs. All iterations have a maximum number of steps, which if exceeded will terminate the optimization and return a message that a solution has not been found, with short explanation. These maximal iteration values, can be set in the settings window.

■ 13.1.3 Limit Testing

Limit testing is used to push the software to its operational limit to determine robustness and stability. It is also used to see how the software behaves under completely unusual values and inputs. This method was implemented as follows:

- Extreme input of values and combinations of values into input fields
- Confusing input to form fields. Switching and saving in between. Switching between settings and other windows.
- Trying to cancel data loading so that input data is distorted.
- Modifying json data to be loaded to absolutely nonsensical or extreme values. Adding fields to json data.
- Trying to click buttons extremely fast and switch between screens. Using various standard and non-standard keyboard shortcuts.

Results. The robustness against extreme values is achieved by two main methods. Primarily, the user is prevented from entering extreme values in the input fields and it is ensured that non-validated inputs are not included in the calculation under any circumstances. The second method is to issue a warning if the combination of inputs does not lead to a realistic optimisation solution.

To prevent the input of extreme values, it was necessary to define what an extreme input is. Certain inputs were restricted due to their physical nature and inherent limitations, such as latitude, longitude and efficiency ranges. For other parameters, appropriate maximum and minimum values were estimated. For example, the desired maximum flight altitude was limited to 15 to 45

km. High flight altitudes can often lead to poor solutions due to other poorly chosen parameters. At high altitudes, the balloon requires a large volume due to the low density of the surrounding air, which increases the surface area and mass of the envelope. Consequently, a balloon may not be able to support itself if the input parameters, especially the material properties or the requirements for the energy system, are unrealistic. This problem becomes even more pronounced at higher altitudes. A steerable balloon is therefore not ideal for flight altitudes above 45 km. Instead, a simple balloon with the thinnest possible envelope is the optimum solution for high altitudes. Further limit values are given in Table C.2 for optimization calculation and in Table C.1 for flight simulation in Appendix C.

Problems in finding a solution also occurred when using a tandem system with helium for very low payloads and high altitudes or when using very heavy foils and tapes. Initially, it was assumed that these were calculation errors, but a more detailed evaluation revealed that the problems were due to physical limitations. At low loads, a balloon with the same pressure has an initial angle of almost 90 degrees according to the equation 8.11, similar to a balloon with overpressure. However, at zero overpressure, the balloon becomes much flatter following the equation 8.14. This increases the surface area and mass of the envelope. Therefore, a slight overpressure is preferable for small balloons, similar to meteorological balloons.

Often no solution is found for very heavy envelopes either, especially at high altitudes. It is therefore often a combination of parameters, not just individual values, that cause problems. Even if the optimisation starts with unrealistic parameter combinations, it may not find a solution and the user is warned accordingly.

No additional errors were found during further tests. When attempting to upload invalid data, the system either issues a warning or uploads the data but it does not pass the subsequent validation at initialisation. To avoid errors caused by user interactions during calculations, the input page is deactivated while a calculation is running so that no further interactions can result in additional calculations and potential errors.

■ 13.1.4 Unit Testing

An extensive suite of unit tests has been implemented to ensure the reliability and correctness of the software's core functions. A total of 17 unit tests were performed, covering a wide range of input values and scenarios. These tests

focused primarily on the classes involved in the balloon design and ensured that each component performed within the specified parameters.

Class 'Balloon'. was tested in three scenarios, with eight output parameters being verified for each scenario to ensure the accuracy and reliability of the balloon shape design calculations, both for zero-pressure and super-pressure balloons. The parameters checked include:

- Maximum radius
- Height
- Volume
- Lift force
- Tape weight
- Weight of envelope's skin
- Mean meridional tension
- Median total tension

To calculate the maximum stress of the material, a normalized value of maximum strength of 1 was used for ease of comparison. This approach was chosen because exact values are not as critical in this context.

Class 'OptimizeBalloon'. was thoroughly tested with two different scenarios, checking 14 parameters to ensure that they were within the specified ranges. The parameters tested include:

- General parameters:
 - Balloon ratio
 - Float altitude
 - Maximum stabilising force
 - Minimum height
 - Energy per meter during the day
 - Energy per metre at night

- Parameters specific to each balloon:
 - Maximum radius
 - Height
 - Volume
 - Weight of gas in balloon

Class 'Optimize'. was tested with only one scenario, as it is the most complex class, involving balloons, solar panels and battery calculations. A total of 8 output values are verified to ensure their correctness, and include:

- Battery weight
- Battery capacity
- Solar panel weight
- Solar panel area
- Total energy per day generated
- Total weight of accessories
- Volumes of both balloons

Due to the computational complexity of these classes, testing was limited to a few scenarios to maintain efficiency. Nevertheless, these tests were designed to cover a significant portion of the code base.

Utility Functions: In addition to the fundamental classes, utility functions were also extensively tested. These functions were tested using large datasets, with input and expected output values stored in NumPy array files located in the `tests/data` folder. This approach allowed thorough validation of the correctness and performance of the utility functions over a wide range and with a large amount of variation that could not be captured in the individual class tests. Thus, they help overall stability over a wider range.

Test Execution. All tests were executed using the `pytest` library, a powerful tool for executing and managing unit tests in Python. Currently, all 17 tests passed successfully and took approximately 12 seconds to complete. This demonstrates the efficiency and reliability of the testing framework and the

robustness of the software components. While the other tests tend to focus on the functionality of the UI and limiting elements, these tests focus on the functionality and core of the entire application and are particularly useful for verifying that new changes to the code do not negatively affect the accuracy of the computation. In particular, single class tests often failed during development because the data against which the software was compared were not accurate or used a different optimization method to optimize other parameters, or the range of input parameters for each class was expanded and the tests failed. Not always a badly run class test means that there is a bug somewhere. However, it is a good indicator that you need to look at the modification again to check that the result is indeed desired and find the reason why the test failed.

■ 13.2 Validation

■ 13.2.1 Balloons Envelope

The calculation of the balloon envelope is one of the most complex calculations and at the same time its functionality is of great importance for the accuracy of the whole optimization, because of its influence on both the buoyant force and the non-negligible weight of the balloon.

Validation of the calculation was done against the results in the paper by Wen and Dorrington [9], which compared their simpler method with the more accurate results of the parallel shooting method by Baginski [44]. The comparison was done only for equal-pressure balloons due to the lack of data for pressurized balloons. However, based on the approximate comparison with existing pressurized balloons, the shape and stress match and since the calculations are based on the same fundamentals as those validated for zero-pressure balloons, it can be argued that they are expected to be correct.

Payload (N)	10 684
Film Density (N/m ²)	0.17
Tape Density (N/m ²)	0.1045
No. of Tapes	159

Table 13.1: Inputs for Validation of Balloon Calculation

Shape. Figure 13.1 shows two balloon shapes designed with the same parameters listed in Table 13.1, for two variations of volume specific buoyancy, according to the equation 8.2, which corresponds to a flight level of 34099 m for $b = 0.08$ and 43370 m for $b = 0.02$ in a standard atmosphere according to USSA [6].

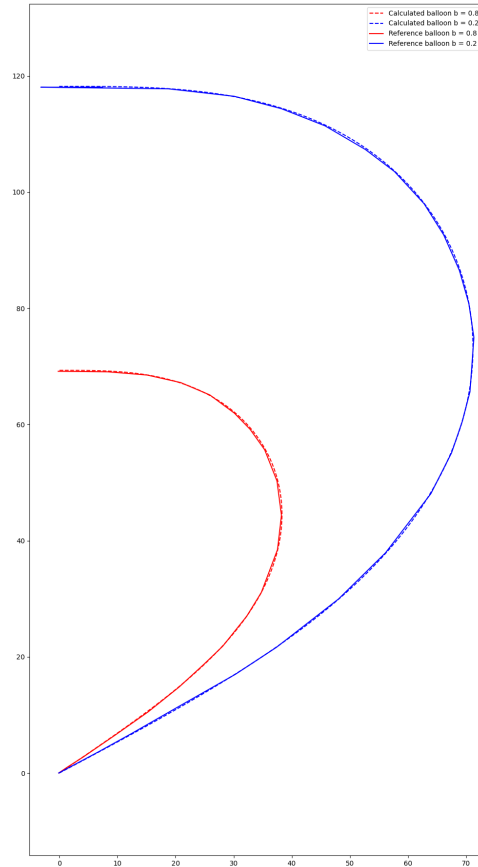


Figure 13.1: Validation of Envelope Shape for two specific buoyancy values

Stress. The stress in the envelope was compared for the two calculated balloon and is illustrated in the figure 13.2. The small difference in values is essentially negligible and most likely comes from a bad reading from the graph, as the values were very difficult to determine accurately. A comparison with measured data would have been ideal, unfortunately no measured data could be found to compare the calculation with.

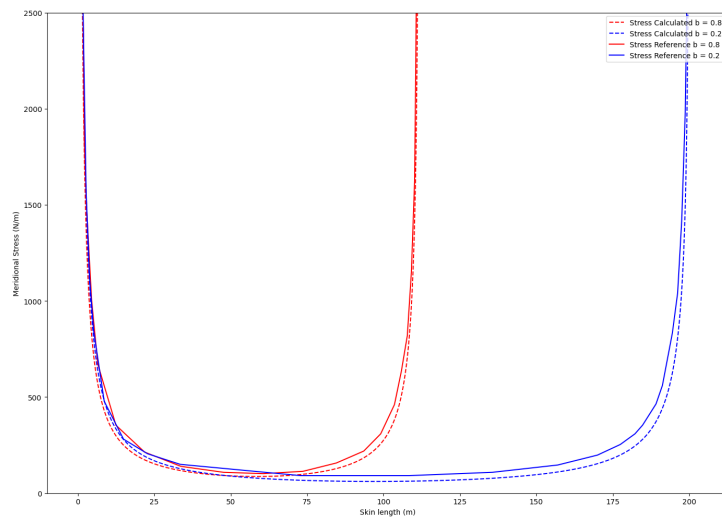


Figure 13.2: Validation of Envelope Stress for two specific buoyancy values



Part V

Conclusion

Chapter 14

Summary of Findings and Evaluation

14.1 Examples of Balloon Systems

The functionality of the software can best be demonstrated through the design configurations for various high-altitude balloon missions. This section presents two different missions wherein the software was utilized to develop the optimal balloon flight system.

14.1.1 Budget Example Mission

The first mission involves a high-altitude balloon flight reaching up to 25 km above the Earth's surface carrying a small payload comparable to Cubesat satellites. This relatively low altitude allows the payload to operate above most of the weight of the atmosphere (pressure of only 0.37 Pa [6]), while still keeping relatively compact size. The payload weighs 2 kg and the mission duration is about 50 days with a continuous power requirement of about 10 W. This mission requires precise trajectory control over a wide range of altitudes. Due to budget constraints, low-cost technologies are used, including single-axis solar panels with medium efficiency and low-cost batteries. Based on these parameters, a balloon-in-balloon design with air ballast was chosen. This configuration allows for high altitude control and minimizes carrier gas leakage. All the input parameters for this mission are presented in Appendix B in the table B.1. This mission may represent, for instance, a mission

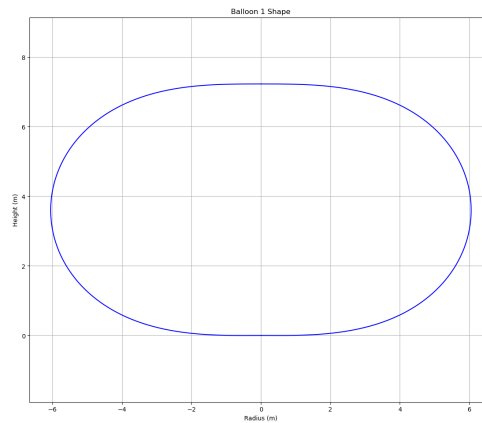


Figure 14.1: Outer Balloon Shape of Budget Example Mission

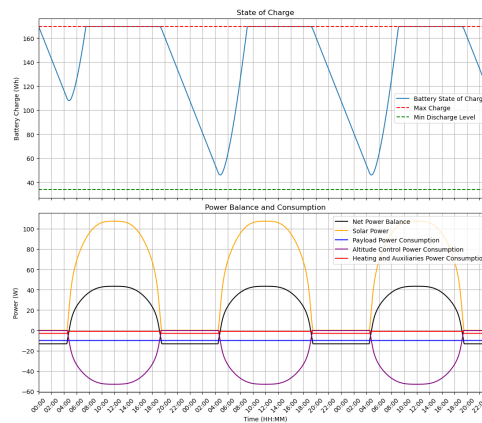


Figure 14.2: 3days Energy Balance of Budget Example Mission

organised by a university to test a particular technology and save the cost of testing in space. The balloon can be used to collect data on the composition of the atmosphere or could include sensors and cameras to monitor and capture images of the Earth’s surface. This can be useful for environmental monitoring, agricultural analysis, disaster prevention and urban planning. .

An important part was choosing the right materials. Due to the expected high pressure in the balloon, Kanirope Pro SK78 Dyneema ropes [55] were selected. These ropes are used in sailing and are UV-resistant. For the outer and inner balloon same ropes with a diameter of 1 mm, a breaking load of 1.95 kN and a weight of 0.9 g/m were selected. Both balloons envelopes are made from the same polyethylene film, with specific weight of 20 g/m². The use of same materials is for cost saving reasons. The resulting balloon has a total volume of 607.7 cubic meters and is 7.2 m high and 12.1 m wide. The maximum overpressure to compensate for destabilising conditions is 839.95 Pa. The outer balloon weighs 8.37 kg and the inner ballonet weighs 7.34 kg. The solar panel has an area of 0.46 square meters and on the day with

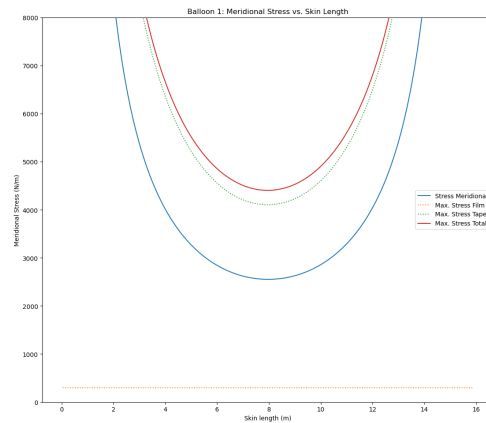
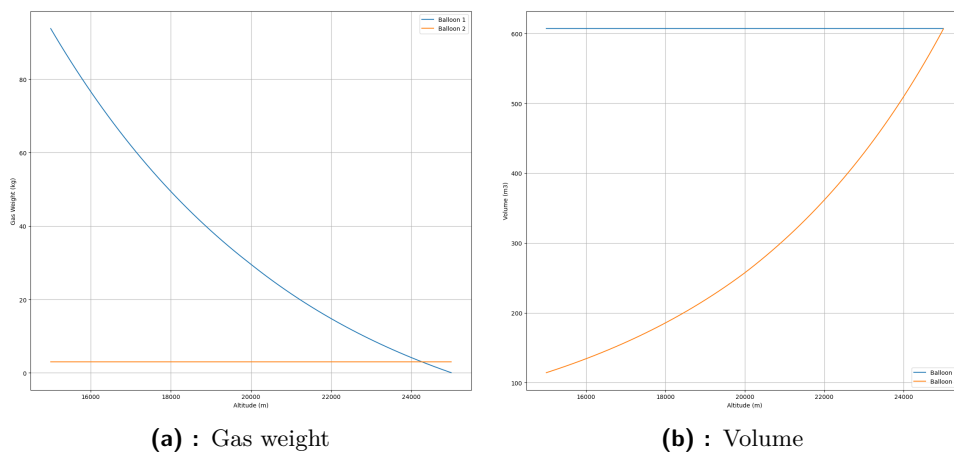


Figure 14.3: Stress in Outer Balloon of Budget Example Mission



(a) : Gas weight

(b) : Volume

Figure 14.4: Gas Weight and Volume of Balloons over altitude range of Budget Example Mission

the least solar radiation (28.04.2024) it produces 1394 Wh of energy and its weight is 1.62 kg. The battery weighs 0.85 kg and has a capacity of 167 Wh.

Figure 14.1 shows the shape of the resulting outer balloon. Figure 14.2 shows the energy balance during the 3-day run and Figure 14.3 shows the stress and limiting stress of the balloon at maximum overpressure. Figure 14.4 then shows the masses of the gases and volumes of the first and second balloons over altitude range.

14.1.2 Scientific Example Mission

The second mission involves a more advanced scientific payload for night sky observation that requires 100 W of power at night and weighs 100 kg launched

on 28.04.2024. The balloon flies at a maximal altitude of 38 km with limited control over the flight trajectory. The mission duration is approximately 60 days. Advanced battery and solar panel technologies with dual-axis sun tracking are used. Given these parameters, an tandem helium balloon design was chosen. This configuration allows to reach high altitudes and stay stable with limited control over trajectory. All the input parameters for this mission are shown in Appendix B in the table B.2.

Again, Kanirope Pro SK78 Dyneema ropes were selected. For the bottom super-pressure balloon ropes with a diameter of 4 mm, a breaking load of 13 kN and weigh 7 g/m were selected. For the top zero-pressure balloon, reinforcements made from the same type of ropes were selected, but with a diameter of 1 mm, a breaking load of 1.95 kN and a weight of 0.9 g/m. Both balloons envelopes are made from polyethylene film, with the super-pressure balloons film having specific weight of 25 g/m² and the zero-pressure balloons film 15 g/m². The resulting balloon system has a balloon ratio of 1.07351.

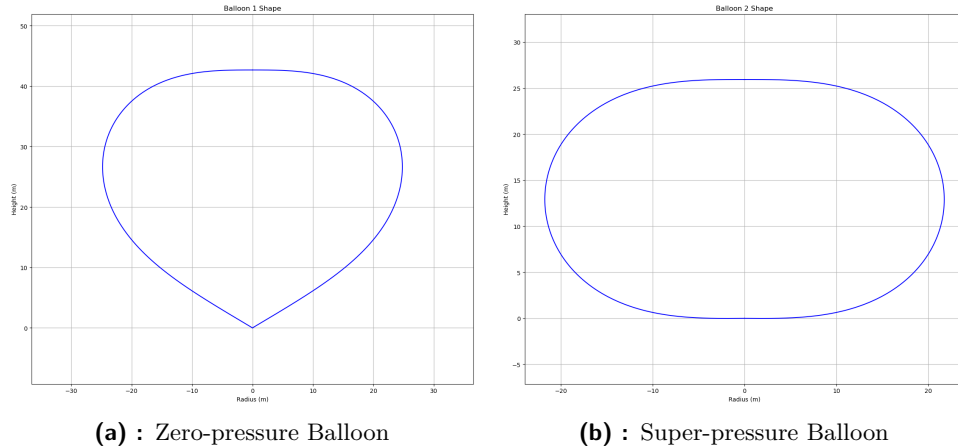


Figure 14.5: Shapes of ZP and SP Balloons of Scientific Example Mission

In a tandem helium balloon system, this ratio indicates how much payload the zero-pressure balloon carries compared to the super-pressure balloon. If the ratio is greater than 1, this shows that the super-pressure balloon is not carrying any payload. The float altitude is 36.305 meters, i.e. if the balloon rises above this altitude when subjected to maximum disturbance force, it would exceed the maximum altitude, which would lead to lift gas leak. The minimum possible altitude is 33,585 meters, which represents a narrow operating range, but is sufficient for limited steering.

The zero-pressure balloon has a volume of 50 429.2 cubic meters, is 42.7 meters high and 49.6 meters wide and weighs 102.07 kilograms. The nominal overpressure of the super-pressure balloon is 5 Pa, the maximum overpressure for external force equalization is 200 Pa. The super-pressure balloon weighs 134.2 kilograms, has a volume of 28 206.2 cubic meters, is 25.9 meters high

and 43.5 meters wide.

The solar panel with an area of 1.13 square meters produces 4 300 Wh of energy on the day with the lowest solar radiation (28 April 2024) and weighs 2.25 kilograms. The battery weighs 6.12 kilograms and has a capacity of 1 836 Wh. To resist the stress in the balloon envelope the zero-pressure balloon has 22 tapes and the super-pressure balloon has 44 tapes.

Figure 14.5 shows the shapes of the resulting balloons. Figure 14.6 shows the energy balance during the 3-day run and Figure 14.7 shows the stress and limiting stress of the two balloons balloon at maximum overpressure. Figure 14.8 then shows the masses of the gases in the first and second balloon and their volume over altitude range.

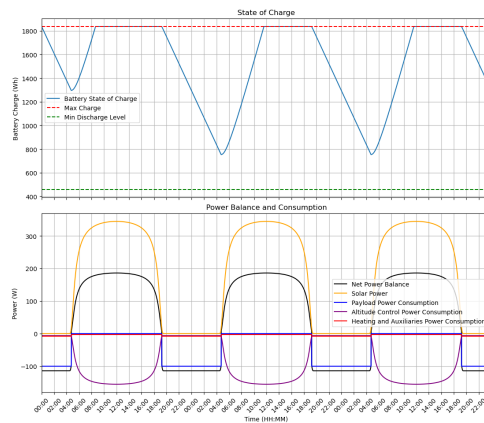
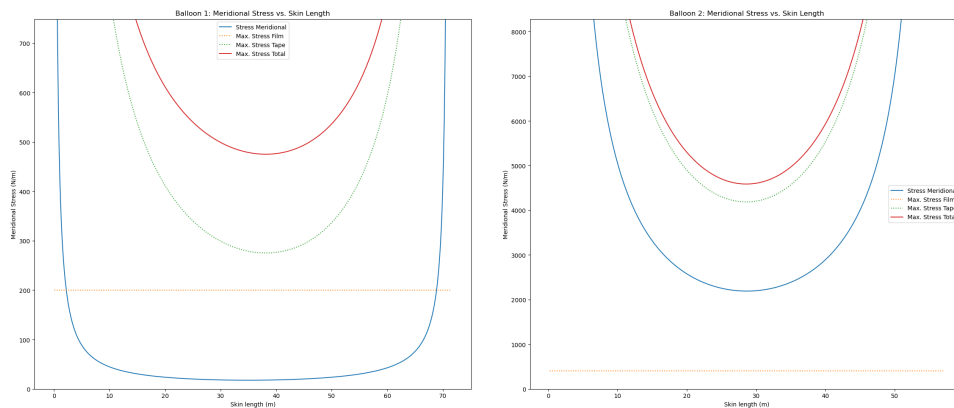


Figure 14.6: 3days Energy Balance of Scientific Example Mission



(a) : Zero-pressure Balloon

(b) : Super-pressure Balloon

Figure 14.7: Stresses in Balloons of Scientific Example Mission

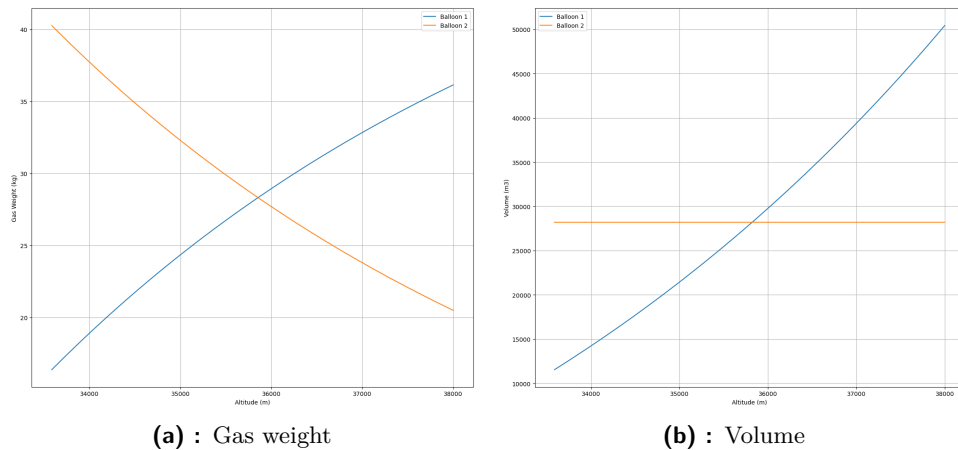


Figure 14.8: Gas Weight and Volume of Balloons over altitude range of Scientific Example Mission

14.2 Evaluation of the Proposed System and Results

14.2.1 Objectives

The two main objectives of the thesis were:

1. Introduction of a method to control the trajectory of stratospheric balloons by adjusting their altitude and a general overview of the field of stratospheric balloons.
2. Development of an optimization tool for the design of the entire flight system of a stratospheric balloon, with possibility to test the capabilities of the designed system in a flight simulator linked to weather forecasts.

14.2.2 Summary of the Study

The first part of this thesis introduces stratospheric balloons, their existing use and their current limitations. Subsequently, methods of balloon trajectory control options, theoretical foundations and design aspects were presented. Subsequently, methods of balloon trajectory control options, theoretical foundations and design aspects were presented. The atmospheric level in

which balloons occur and common types of circulation in the stratosphere were characterized, along with the optimal conditions for balloon trajectory control and a description of current forecast models and relevant parameters for balloons flight. At the same time, the stratospheric balloon, its types and design, together with the aerodynamic and thermal environment and external influences on the balloon were presented. An introduction to the individual energy components of the balloon is also given.

The next part of the work is focused on the individual calculations necessary to design the optimal system. It includes the design of the shape of the stratospheric balloon, its envelope and its stresses. The calculation is carried out for both zero-pressure and super-pressure balloons using the simplified numerical method. The next part is the design of the flight level change system. Two of the most suitable options for changing the flight path were selected from several options see Chapter 7, with one being more suitable for shorter missions with high loads and high flight altitude, but limited trajectory control capabilities. The second option is more suitable for longer missions at lower flight levels and allows greater balloon controllability. Governing equations characterizing the in-flight behavior have been presented for both methods. Further calculations are focused on power systems and investigate in depth the energy demands as well as the behaviour of solar panels or batteries. Finally, the calculations required for the simulation and the procedure for extracting data from the GFS prediction model are presented.

■ 14.2.3 Summary and Evaluation of the Software

■ Optimization and Simulation

Optimization software has been developed that can design the most ideal solution for a given configuration, based on mission requirements such as desired flight level, flight time and location, or payload weight and power requirements, material properties, selected battery and solar panel technologies, and solar tracking capabilities. The result is then several parameters describing the shape and mass of each balloon in the system, the overall size of the solar panels and the required battery capacity. At the same time, the system designs the balloon system to withstand external conditions such as vertical wind flow or temperature difference between the balloon and the environment, and proposes the minimum required passive stabilizing force, the float altitude at which the balloon can occur without risking reaching critical conditions.

Chapter 15

Recommendations and Future Perspectives

15.1 Further Software Development

This chapter outlines possible areas for improvement of the existing software tool used in the optimization and simulation of high-altitude balloons. The purpose of the proposed improvements is to refine the simulation accuracy, extend the functionality and improve the user experience. Key areas of development include thermal modelling, flight trajectory control, material selection, optimisation algorithms and more

Thermal Model Integration

Primarily a thermal model should be designed for the complex balloon system. Integrating the thermal model will improve the correctness of the flight simulations. This model would account for the thermal dynamics of the balloon, including solar heating, radiative heating, convective heat transfer along with helium exchange between balloons or compression and venting of ambient air. Incorporating these factors will allow more accurate predictions of changes in altitude and buoyancy during flight, particularly as a result of diurnal temperature cycles.

Adding more methods

To increase the versatility of the software, two additional flight path control methods that have not been added should be included. At the same time,

altitudes and Reynolds numbers. And based on the measurements, create a more comprehensive and accurate model, which would have a very significant effect on the accuracy of trajectory prediction.

■ Effects of solar panel shading

The current model does not account for the effects of solar panel shading caused by the balloon. Adding shading calculations will improve the accuracy of the power production estimates, which is essential for solar missions.

■ Optimised Design Modifications

Users should be able to manually edit the parameters of the optimized design. This flexibility will allow fine-tuning based on practical considerations or specific mission requirements.

■ Additional Reinforcing Elements

The current simulation assumes only the use of tapes as reinforcement elements. However, balloon caps are necessary to ensure safe ascent and reduce stress concentration. Incorporating the simulation of external caps will increase the accuracy and safety of the balloon design [35]. It would be ideal to include the calculation, for example, only in the user editing of the optimized design. In order not to burden the complexity of the optimization.

■ Simulation of flight and parachute landing

Including simulations of balloon landings with steerable and non-steerable parachutes allows for comprehensive planning of the entire mission. This feature will help evaluate landing safety and logistics. At the same time, it is the passage through low flight levels that is most critical due to air traffic movement and possible catastrophic collision.

■ Testing, logging and data transfer enhancements

The current software includes basic testing, but it would be useful to extend the testing especially if additional methods are implemented. At the same time, logging could be more detailed and accurate. Furthermore, the data transfer is not ideal and for example it is not possible to directly monitor the progress of the optimization or simulation. This could be improved to give the user a better overview of what is happening.

■ Incorporation of Weather Forecast Reanalysis

The current simulations are only planned for weather forecast models covering only a short period of time and which are not very accurate. Adding the

trajectory and thus have a very narrow launch window [22], the balloons with trajectory control can be launched from a variety of locations and at almost any time. Moreover, unlike weather balloons, they can remain in the air for days or months.

As mentioned, launching scientific balloons to high altitudes is largely dependent on specific conditions and is usually carried out in Antarctica.[1] These launches encounter a number of challenges including complex logistics, high costs and constrained infrastructure that can only support 2 balloon missions per year.[22] The ability to launch steerable balloons from different locations at any given time significantly reduces these constraints, making it easier and more cost-effective to conduct missions.

By cutting out the need for polar launches and specialized infrastructure, the overall cost of balloon missions can be significantly reduced. This financial flexibility allows for more frequent launches and wider participation by various research institutions and commercial entities or start-ups. Simultaneously, it is possible to launch balloons with smaller payloads or lower flight levels and lower overall production costs compared to large scientific balloons.

Balloons with trajectory control can be rapidly deployed in response to new scientific opportunities or urgent needs. They can be deployed almost from day to day and no complex infrastructure is required. Their trajectory can be adjusted in real time, offering unparalleled flexibility in mission planning and execution. This capability increases their utility for a wide range of applications, from environmental monitoring to emergency response.

The controlled flight paths of these balloons simplify recovery of deployed equipment. This capability not only reduces costs, but also ensures that valuable scientific instruments and data can be recovered and used for future missions.

■ 15.2.2 Scientific Research Applications

The improved capabilities of controllable balloons significantly expand the range of scientific research that can be undertaken at high altitudes.

Atmospheric research: such balloons can be used to conduct thorough atmospheric experiments that provide important data on weather patterns,

■ 15.2.4 Security and military applications

These balloons also have promising potential in security and military contexts, providing distinct advantages for surveillance, communications and tactical operations.

Surveillance and reconnaissance: High altitude balloons can carry advanced imaging and sensor payloads for surveillance and reconnaissance missions. Their ability to float over certain areas allows for continuous tracking and data collection, providing critical intelligence for military and security operations.

Communication relay: In military operations, stratospheric balloons can act as communication relays at high altitudes and provide reliable communication links over long distances. This capability is particularly valuable in remote or contested areas where ground communications infrastructure may be compromised or unavailable.

Monitoring and early warning systems: these balloons can be equipped with sensors to monitor environmental conditions and detect potential threats such as chemical or biological agents. They can also serve as platforms to detect hostile objects in the airspace. Their ability to transmit data in real time enables rapid response to emerging security threats.



Chapter 16

General Conclusion

The aim of this thesis was to explore the potential of stratospheric balloons with the possibility of trajectory control by changing the flight altitude and to develop a comprehensive optimization software for the design of the entire flight system.

The work began with an introduction to stratospheric balloons, describing their current capabilities and limitations. A thorough overview of trajectory control methods was given, along with the theoretical foundations and the design and physical aspects of steerable balloons. In addition, the optimal atmospheric conditions for trajectory control were described and the behavior of the stratosphere and current weather forecast models were presented. Detailed design calculations for zero and super-pressure balloons were presented, calculating the shape as well as the envelope stresses and energy requirements for flight attitude changes. This work also evaluated different methods for changing the flight altitude and their suitability for different mission profiles. In addition, calculations were carried out on the energy balance of the entire balloon system.

A major achievement of this work is the development of Python optimization software to design the most efficient balloon system based on mission-specific parameters. It also includes not fully implemented simulation environment for predicting balloon behavior and trajectory using real meteorological data and has a user-friendly graphical interface for parameter input and visualization of results.

Future development of the software will focus on improving the optimization

algorithms, finalizing the simulation environment, developing accurate thermal model and other aspects that increase the accuracy and usability of the software tool. Finally, two optimization results were presented for two different missions. These advances have the potential to significantly expand the availability and range of applications of stratospheric balloons with trajectory control.

In summary, this work has successfully fulfilled the objectives of the thesis, paving the way for a more versatile and efficient use of stratospheric balloons in various scientific and commercial fields.



Appendices

Appendix A

Bibliography

- [1] Manfred “Dutch” von Ehrenfried. *Stratospheric Balloons: Science and Commerce at the Edge of Space*. Springer Nature, 1 edition, 2021.
- [2] Loon LLC. Loon library: Lessons from building loon’s stratospheric communications service. <https://x.company/projects/loon/>, 2021. Accessed: 2024-02-23.
- [3] University of Arizona. Mt. lemmon sky center sees the stratollite balloon. <https://www.as.arizona.edu/mt-lemmon-sky-center-sees-stratollite-balloon>. Accessed: 2024-02-23.
- [4] Alexander D Miller, Iain Beveridge, Andrew Antonio, and Tom Pirrone. World view enterprises altitude controlled balloons: a new stratospheric platform for persistent earth and space imaging campaigns. In *Ground-based and Airborne Telescopes VII*, volume 10700, pages 1427–1435. SPIE, 2018.
- [5] Jeffery L. Hall et al. Altitude-controlled light gas balloons for venus and titan exploration. In *AIAA Aviation 2019 Forum*, page 3194, 2019.
- [6] National Oceanic, Atmospheric Administration, National Aeronautics, Space Administration, and United States Air Force. U.s. standard atmosphere, 1976. Technical report, U.S. Government Printing Office, Washington, D.C., 1976.
- [7] M.S. Smith and E.L. Rainwater. Optimum designs for superpressure balloons. *Advances in Space Research*, 33(10):1688–1693, 2004.
- [8] SRON Netherlands Institute for Space Research. Gusto mission image. <https://www.sron.nl/gusto/>, 2024. Accessed: 2024-05-07.

- [9] PH Wen and GE Dorrington. Simple method to predict balloon shape. *Proceedings of the Institution of Mechanical Engineers, Part G: Journal of Aerospace Engineering*, 224(8):897–904, 2010.
- [10] JW Spencer. Fourier series representation of the position of the sun. *Search*, 2(5):172, 1971.
- [11] Soteris A Kalogirou. *Solar energy engineering: processes and systems*. Elsevier, 2023.
- [12] NASA Goddard Institute for Space Studies. Panoply 5.4.0 - netcdf, hdf and grib data viewer. <https://www.giss.nasa.gov/tools/panoply/>, 2024. Accessed: 2024-04-18.
- [13] NOAA NCEP. Nomads gfs 0.25 degree grads data server. https://nomads.ncep.noaa.gov/dods/gfs_0p25/, 2024. Accessed: 2024-04-20.
- [14] VANAM Technologies. Cpr-1000. <https://vanamtechnologies.com/product/cpr-1000/>. Accessed: 2024-02-01.
- [15] World View Enterprises. Space tourism with zero-pressure balloons. <https://www.worldview.space/space-tourism>. Accessed: 2024-02-01.
- [16] NASA. Nasa mission will study the cosmos with a stratospheric balloon. <https://www.nasa.gov/centers-and-facilities/jpl/nasa-mission-will-study-the-cosmos-with-a-stratospheric-balloon/>. Accessed: 2024-02-01.
- [17] NASA. Landsat 5 sets guinness world record for longest operating earth observation satellite. <https://landsat.gsfc.nasa.gov/article/landsat-5-sets-guinness-world-record-for-longest-operating-earth-observati>. Accessed: 2024-02-23.
- [18] National Aeronautics and Space Administration. Sounding rockets overview. <https://www.nasa.gov/soundingrockets/overview/>. Accessed: 2024-05-21.
- [19] NASA Jet Propulsion Laboratory. Asthros. <https://www.jpl.nasa.gov/missions/asthros>, 2024. Accessed: 2024-03-05.
- [20] NASA. Galactic/extragalactic uldb spectroscopic terahertz observatory (gusto). <https://science.nasa.gov/mission/gusto/>, 2024. Accessed: 2024-05-07.
- [21] Helene Cooper and Edward Wong. Downing of chinese spy balloon ends chapter in a diplomatic crisis. <https://www.nytimes.com/2023/02/04/us/politics/chinese-spy-balloon-shot-down.html>, Feb 2023. Accessed: 2024-02-23.

- [22] Jorge Pineda et al. Asthros-astrophysics stratospheric telescope for high spectral resolution observations at submillimeter-wavelengths. *NASA APRA Proposal*, page 136, 2022.
- [23] Paul B Voss, Emily E Riddle, and Michael S Smith. Altitude control of long-duration balloons. *Journal of aircraft*, 42(2):478–482, 2005.
- [24] K.M. Aaron, M.K. Heun, and K.T. Nock. A method for balloon trajectory control. *Advances in Space Research*, 30(5):1227–1232, 2002.
- [25] L M Polvani, A H Sobel, and D W Waugh, editors. *The Stratosphere: Dynamics, Transport, and Chemistry*. Geophysical monograph. American Geophysical Union, Washington, D.C., DC, 1 edition, January 2010.
- [26] ECMWF. Ecmwf integrated forecasting system. <https://www.ecmwf.int/en/forecasts/documentation-and-support>, 2024. Accessed: 2024-05-22.
- [27] NOAA. Noaa global forecast system (gfs). <https://www.ncei.noaa.gov/products/weather-climate-models/global-forecast>, 2024. Accessed: 2024-05-22.
- [28] European Centre for Medium-Range Weather Forecasts. Plans for high-resolution forecast (hres) and ensemble forecast (ens). <https://www.ecmwf.int/en/about/media-centre/focus/2024/plans-high-resolution-forecast-hres-and-ensemble-forecast-ens>, 2024. Accessed: 2024-05-07.
- [29] European Centre for Medium-Range Weather Forecasts. Forecast performance 2023. <https://www.ecmwf.int/en/newsletter/179/news/forecast-performance-2023>, 2024. Accessed: 2024-05-07.
- [30] Leonard David. Mystery object shot down over yukon may have been 'pico balloon'. <https://www.space.com/mystery-object-shot-down-yukon-amateur-ballloon>, 2023. Accessed: 2024-05-13.
- [31] Justin H Smalley. Determination of the shape of a free balloon. *General Mills, Inc., Electronics Division, Report*, 2421, 1964.
- [32] EL Rainwater and MS Smith. Ultra high altitude balloons for medium-to-large payloads. *Advances in Space Research*, 33(10):1648–1652, 2004.
- [33] CR Calladine and JM Robinson. A simplified approach to the buckling of thin elastic shells. *Theory of shells*, pages 173–196, 1980.
- [34] MA Said, Brenda Dingwall, A Gupta, AM Seyam, G Mock, and T Theyson. Investigation of ultra violet (uv) resistance for high strength fibers. *Advances in space research*, 37(11):2052–2058, 2006.
- [35] KH Hazlewood. External caps: An approach to stress reduction in balloons. *Advances in Space Research*, 5(1):21–22, 1985.

- [36] Frank M White. *Viscous Fluid Flow*. McGraw-Hill Professional, New York, NY, 3 edition, February 2005.
- [37] Paul A Sherburne and GOODYEAR AEROSPACE CORP AKRON OH. Wind tunnel tests of natural shape balloon model. In *Proceedings of the 5th AFCRL Scientific Balloon Symposium*, 1968.
- [38] Jan F. Kreider. Numerical prediction of the performance of high altitude balloons. Technical report, Atmospheric Technology Division, National Center for Atmospheric Research, 1974.
- [39] Leland A. Carlson and Walter J. Horn. New thermal and trajectory model for high-altitude balloons. *Journal of Aircraft*, 20(6):500–507, 1983.
- [40] FC Krause, John-Paul Ruiz, SC Jones, EJ Brandon, EC Darcy, CJ Iannello, and RV Bugga. Performance of commercial li-ion cells for future nasa missions and aerospace applications. *Journal of The Electrochemical Society*, 168(4):040504, 2021.
- [41] Inès Massiot, Andrea Cattoni, and Stéphane Collin. Progress and prospects for ultrathin solar cells. *Nature Energy*, 5(12):959–972, November 2020.
- [42] Weiyu Zhu, Yuanming Xu, Huafei Du, and Jun Li. Thermal performance of high-altitude solar powered scientific balloon. *Renewable Energy*, 135:1078–1096, 2019.
- [43] Marc G. Bellemare et al. Autonomous navigation of stratospheric balloons using reinforcement learning. *Nature*, 588(7836):77–82, 2020.
- [44] Frank Baginski, Tami Williams, and William Collier. A parallel shooting method for determining the natural shape of a large scientific balloon. *SIAM Journal on Applied Mathematics*, 58(3):961–974, 1998.
- [45] Ibrahim Reda and Afshin Andreas. Solar position algorithm for solar radiation applications. *Solar energy*, 76(5):577–589, 2004.
- [46] Donald F Swinehart. The beer-lambert law. *Journal of chemical education*, 39(7):333, 1962.
- [47] Andrew T Young. Air mass and refraction. *Applied optics*, 33(6):1108–1110, 1994.
- [48] T.K. Schuler. Earthshabs. <https://tkschuler.github.io/EarthSHAB/>, 2023. Accessed: April 13, 2024.
- [49] Sowman et al. Cusf standalone predictor. <https://github.com/jonsowman/cusf-standalone-predictor>, 2010. Accessed: April 10, 2024.

- [50] Andras Sobester, Helen Czerski, Niccolo Zapponi, and I. P. Castro. High-altitude gas balloon trajectory prediction: A monte carlo model. *AIAA Journal*, 52(4):832–842, 2014.
- [51] Ahmad Fauzi Ismail, Kailash Chandra Khulbe, and Takeshi Matsuura. *Gas Separation Membranes: Polymeric and Inorganic*. Springer International Publishing, 2015.
- [52] Jun Li, Linyu Ling, Jun Liao, Zheng Chen, and Shibin Luo. Effect of lifting gas diffusion on the station-keeping performance of a near-space aerostat. *Aerospace*, 9(6):328, June 2022.
- [53] Markus Huber. A clean architecture for a pyqt gui using the mvp pattern. https://medium.com/@mark_huber/a-clean-architecture-for-a-pyqt-gui-using-the-mvp-pattern-78ecbc8321c0, September 2023. Accessed: 2024-05-09.
- [54] Paul C. Jorgensen and Byron DeVries. *Software Testing: A Craftsman's Approach*. Auerbach Publications, fifth edition, 2022.
- [55] Kanirope. Kanirope dyneema rope pro sk78. <https://www.kanirope.com/kanirope-dyneema-rope-pro-sk78>, 2024. Accessed: 2024-05-14.
- [56] Katherine E Lukens, Kayo Ide, and Kevin Garrett. Investigation into the potential value of stratospheric balloon winds assimilated in noaa's finite-volume cubed-sphere global forecast system (fv3gfs). *Journal of Geophysical Research: Atmospheres*, 128(3), 2023.



Appendix B

Input tables for Example Missions

Geographical Data	
Latitude	50.1
Longitude	14.38
Flight Date	2024-04-28
Altitude and Flight Duration	
Desired Max Altitude (m)	25000.0
Desired Min Altitude (m)	15000.0
Flight Duration (days)	50.0
Desired Altitude Change (m)	50000.0
Night Altitude Change Ratio	0.4
Balloon and Material Specifications	
Balloon System Type	Balloon in Balloon - Air Ballast
Nominal Over-Pressure (Pa)	5.0
Balloon 1 Film Density (kg/m ²)	0.02
Balloon 1 Tape Density (kg/m ²)	0.0009
Balloon 1 No. of Tapes	80.0
Balloon 1 Film Strength (N/m)	300.0
Balloon 1 Tape Strength (N)	1950.0
Balloon 2 Film Density (kg/m ²)	0.02
Balloon 2 Tape Density (kg/m ²)	0.0009
Balloon 2 No. of Tapes	8.0
Balloon 2 Film Strength (N/m)	300.0
Balloon 2 Tape Strength (N)	1950.0
Balloon Ratio	0.5
Physical and Power Specifications	
Payload Mass (kg)	2.0
Average Power Requirement (W)	10.0
Power Auxiliaries (W)	1.0
Power Heater (W)	2.0
When Active	Always
Solar Panel Tracking	1-axis
Solar Panel Efficiency (%)	18.0
Solar Panel (kg/m ²)	3.5
Solar Panel Safety Factor	1.4
Battery Specific Power (W/kg)	1500.0
Battery Specific Energy (Wh/kg)	200.0
Max Depth of Discharge (%)	20.0
Battery Capacity Safety Factor	1.2
Accessories Weight (%)	10.0
Maximal Descend Rate (m/s)	0.2
Maximal Upwind Speed (m/s)	10.0
Maximal Temp Difference (°C)	45.0

Table B.1: Flight and Balloon Specifications for Budget Example Mission

Geographical Data	
Latitude	50.10
Longitude	14.38
Flight Date	2024-04-28
Altitude and Flight Duration	
Desired Max Altitude (m)	38000.0
Desired Min Altitude (m)	30000.0
Flight Duration (days)	60.0
Desired Altitude Change (m)	25000.0
Night Altitude Change Ratio	0.4
Balloon and Material Specifications	
Balloon System Type	Tandem Balloon - Compressed Helium
Nominal Over-Pressure (Pa)	5.0
Balloon 1 Film Density (kg/m ²)	0.015
Balloon 1 Tape Density (kg/m ²)	0.0009
Balloon 1 No. of Tapes	22.0
Balloon 1 Film Strength (N/m)	200.0
Balloon 1 Tape Strength (N)	1950.0
Balloon 2 Film Density (kg/m ²)	0.025
Balloon 2 Tape Density (kg/m ²)	0.007
Balloon 2 No. of Tapes	44.0
Balloon 2 Film Strength (N/m)	400.0
Balloon 2 Tape Strength (N)	13000.0
Balloon Ratio	0.5
Physical and Power Specifications	
Payload Mass (kg)	100.0
Average Power Requirement (W)	100.0
Power Auxiliaries (W)	3.0
Power Heater (W)	5.0
When Active	Night
Solar Panel Tracking	2-axis
Solar Panel Efficiency (%)	25.0
Solar Panel (kg/m ²)	2.0
Solar Panel Safety Factor	1.4
Battery Specific Power (W/kg)	2000.0
Battery Specific Energy (Wh/kg)	300.0
Max Depth of Discharge (%)	25.0
Battery Capacity Safety Factor	1.3
Accessories Weight (%)	6.0
Maximal Descend Rate (m/s)	0.1
Maximal Upwind Speed (m/s)	10.0
Maximal Temp Difference (°C)	45.0

Table B.2: Flight and Balloon Specifications for Scientific Example Mission

Appendix C

Validation tables

Input Field	Limits	Units
Fly Type	Ascend flight, Simulation flight	-
Starting Latitude	-90 to 90 (inclusive)	degrees
Starting Longitude	-180 to 180 (inclusive)	degrees
Starting Altitude	0 to <i>max_altitude</i> (inclusive)	m
Float Altitude Balance	<i>min_altitude</i> to <i>max_altitude</i> (inclusive)	m
Battery State of Charge	0 to 100 (inclusive)	%
Flight Date	Date format: %d.%m.%Y %H:%M	datetime
Flight Duration	1 to 72 (inclusive)	hours

Table C.1: Limits of Flight Input Fields

Input Field	Limits	Units
Latitude	-90 to 90 (inclusive)	degrees
Longitude	-180 to 180 (inclusive)	degrees
Desired Max. Altitude	10000 to 45000 (inclusive)	m
Desired Min. Altitude	10000 to 45000 (inclusive)	m
Flight Date	Date format: %d.%m.%Y	date
Flight Duration	1 to 365 (inclusive)	days
Desired Daily Altitude Change	50 to 100000 (inclusive)	m
Night Altitude Change Ratio	0 to 1 (inclusive)	ratio
Maximal Descend Rate	0 to 100 (exclusive)	m/s
Maximal Upwind Speed	0 to 100 (exclusive)	m/s
Max. Temp. Difference	0 to 100 (inclusive)	Kelvin
Balloon System Type	List of options	-
Balloon 1 Film Density	0 to 0.1 (exclusive)	kg/m ²
Balloon 1 Tape Density	0 to 0.1 (exclusive)	kg/m
Balloon 1 No. Tapes	0 to 1000 (inclusive)	-
Balloon 1 Film Strength	0 to 100000 (exclusive)	N/m
Balloon 1 Tape Strength	0 to 100000 (exclusive)	N
Balloon 2 Film Density	0 to 0.1 (exclusive)	kg/m ²
Balloon 2 Tape Density	0 to 0.1 (exclusive)	kg/m
Balloon 2 No. Tapes	0 to 1000 (inclusive)	-
Balloon 2 Film Strength	0 to 100000 (exclusive)	N/m
Balloon 2 Tape Strength	0 to 100000 (exclusive)	N
Mass	0.01 to 2500 (inclusive)	kg
Average Power Requirement	0.01 to 200000 (exclusive)	W
When Active	List of options	-
Accessories Weight	0 to 100 (inclusive)	%
Tracking	List of options	-
Efficiency	5 to 100 (inclusive)	%
Density	0.01 to 50 (inclusive)	kg/m ²
Solar Panel Safety Factor	0.25 to 10 (exclusive)	-
Specific Power	1 to 100000 (exclusive)	W/kg
Specific Energy	10 to 5000 (exclusive)	Wh/kg
Max Depth of Discharge	10 to 100 (inclusive)	%
Battery Capacity Safety Factor	0.25 to 10 (exclusive)	-
Max. Internal Overpressure	0 to 100000 (exclusive)	Pa
Internal Overpressure	0 to 100000 (exclusive)	Pa
Float Altitude Offset	0 to 15000 (exclusive)	m

Table C.2: Limits of Optimization Input Fields



Appendix D

Acronyms

- AST* : Apparent Solar Time
- ASTHROS* : Astrophysics Stratospheric Telescope for High-Spectral Resolution
Observations at Submillimeter-waves
- BEXUS* : Balloon Experiments for University Students
- BinB* : Balloon-in-Balloon
- DLR* : German Space Agency
- ECMWF* : European Centre for Medium-Range Weather Forecasts
- ESA* : European Space Agency
- ET* : Equation of Time
- GFS* : Global Forecast System
- GrADS* : Grid Analysis and Display System
- GUI* : Graphical User Interface
- GUSTO* : Galactic / Extragalactic ULDB Spectroscopic Terahertz Observatory
- LST* : Local Standard Time
- MVC* : Model-View-Controller Architecture
- MVP* : Model-View-Presenter Architecture
- NASA* : National Aeronautics and Space Administration
- NOAA* : National Oceanic and Atmospheric Administration
- SNSA* : Swedish National Space Agency
- SP* : Super-pressure
- UI* : User Interface
- USSA* : United States Standard Atmosphere
- ZP* : Zero-pressure

Appendix E

Attachment Contents

The thesis includes a single attachment: the software compressed into a 7zip archive. The directory structure of the software is as follows:

